

On an Achievable Rate of Large Rayleigh Block-Fading MIMO Channels with No CSI

Keigo Takeuchi, *Member, IEEE*, Ralf R. Müller, *Senior Member, IEEE*,
Mikko Vehkaperä, *Member, IEEE*, and Toshiyuki Tanaka, *Member, IEEE*,

Abstract

Training-based transmission over Rayleigh block-fading multiple-input multiple-output (MIMO) channels is investigated. As a training method a combination of a pilot-assisted scheme and a biased signaling scheme is considered. The achievable rates of successive decoding (SD) receivers based on the linear minimum mean-squared error (LMMSE) channel estimation are analyzed in the large-system limit, by using the replica method under the assumption of replica symmetry. It is shown that negligible pilot information is best in terms of the achievable rates of the SD receivers in the large-system limit. The obtained analytical formulas of the achievable rates can improve the existing lower bound on the capacity of the MIMO channel with no channel state information (CSI), derived by Hassibi and Hochwald, for all signal-to-noise ratios (SNRs). The comparison between the obtained bound and a high SNR approximation of the channel capacity, derived by Zheng and Tse, implies that the high SNR approximation is unreliable unless quite high SNR is considered. Energy efficiency in the low SNR regime is also investigated in terms of the power per information bit required for reliable communication. The required minimum power is shown to be achieved at a positive rate for the SD receiver with no CSI, whereas it is achieved in the zero-rate limit for the case of perfect CSI available at the receiver. Moreover, numerical simulations imply that the presented large-system analysis can provide a good approximation for not so large systems. The results in this paper imply that SD schemes can provide

Manuscript received August, 2011. The work of K. Takeuchi was in part supported by the Grant-in-Aid for Young Scientists (B) (No. 23760329) from JSPS, Japan. The work of M. Vehkaperä was supported by the Norwegian Research Council under grant 171133/V30. The work of T. Tanaka was in part supported by the Grant-in-Aid for Scientific Research on Priority Areas (No. 18079010) from MEXT, Japan. The material in this paper was presented in part at 2009 IEEE International Symposium on Information Theory, Seoul, Korea, July 2009, and at 2010 International Symposium on Information Theory and its Applications & 2010 International Symposium on Spread Spectrum Techniques and Applications, Taichung, Taiwan, Oct. 2010.

K. Takeuchi is with the Department of Communication Engineering and Informatics, the University of Electro-Communications, Tokyo 182-8585, Japan (e-mail: ktakeuchi@uec.ac.jp).

R. R. Müller is with the Department of Electronics and Telecommunications, the Norwegian University of Science and Technology (NTNU), NO-7491 Trondheim, Norway (e-mail: ralf@iet.ntnu.no).

M. Vehkaperä is with the School of Electrical Engineering, Royal Institute of Technology (KTH), SE-100 44 Stockholm, Sweden (e-mail: mikkov@kth.se).

T. Tanaka is with the Department of Systems Science, Graduate School of Informatics, Kyoto University, Kyoto, 606-8501, Japan (e-mail: tt@i.kyoto-u.ac.jp).

a significant performance gain in the low-to-moderate SNR regimes, compared to conventional receivers based on one-shot channel estimation.

Index Terms

Multiple-input multiple-output (MIMO) systems, Rayleigh block-fading channels, noncoherent capacity, training-based transmission, linear minimum mean-squared error (LMMSE) channel estimation, successive decoding (SD), biased signaling, large-system analysis, replica method.

I. INTRODUCTION

A. Motivation

Multiple-input multiple-output (MIMO) transmission is a promising scheme for increasing the spectral efficiency of wireless communication systems, and has been applied to several modern standards, such as wireless LAN (IEEE 802.11n) and Mobile WiMAX (IEEE 802.16e). However, the ultimate achievable rate of MIMO systems is not fully understood. Thus, it is an important issue in information theory to elucidate the channel capacity of MIMO systems.

The capacity of MIMO channels with perfect channel state information (CSI) at the receiver was analyzed in the early pioneering works [1], [2]. Telatar [2] proved that independent and identically distributed (i.i.d.) Gaussian signaling is optimal for i.i.d. Rayleigh fading MIMO channels with perfect CSI at the receiver. See e.g. [3] for the case of more sophisticated fading models. The assumption of perfect CSI available at the receiver is a reasonable assumption if the coherence time is sufficiently long compared to the number of transmit antennas. However, this assumption becomes unrealistic for mobile communications with short coherence time or a large number of transmit antennas. Thus, it is worth considering the assumption of CSI available neither to the transmitter nor to the receiver, while the receiver is assumed to know the statistical model of the channel perfectly. In this paper, this assumption is simply referred to as the no CSI assumption.

Marzetta and Hochwald [4] considered i.i.d. Rayleigh block-fading MIMO channels with no CSI, and characterized a class of capacity-achieving signaling schemes. In block-fading channels, the channel is fixed during one fading block and independently changes at the beginning of the next fading block. The assumption of block-fading simplifies analyzing the capacity, although it might be an idealized assumption.¹ See [5], [6] for the capacity of time-varying MIMO channels with no CSI. In this paper, we consider block-fading MIMO channels with no CSI.

The capacity-achieving inputs are not i.i.d. over space or time for block-fading MIMO channels with no CSI [4]. These dependencies over space and time make it difficult to calculate the capacity. In order to circumvent this difficulty, three kinds of strategies have been considered in the literature. A first strategy is to obtain a closed form for a lower bound on the capacity by considering unitary space-time modulation [7], although the insight provided by the closed form is not very clear. It is possible to calculate a lower bound of the capacity numerically for all signal-to-noise ratios (SNRs) [8], [9], while this task is not necessarily easy in terms of computational complexity.

¹ The assumption of block-fading is valid for time-division multiple-access (TDMA) schemes.

A second strategy is to consider the high or low SNR limits. This strategy can provide an analytical formula of the capacity in return for giving up the capacity result in the moderate SNR regime. High SNR approximations of the capacity were derived in [10], [11]. The approximations tolerate an error of $o(1)$ in the high SNR limit. The analytical formula by Zheng and Tse [10] provides a useful geometric insight, i.e., the capacity of MIMO channels with no CSI has an interpretation as sphere packing in the Grassmann manifold, while the capacity for the case of perfect CSI available at the receiver has an interpretation in terms of sphere packing in the Euclidean space.

The power per information bit E_b required for reliable communication is a key performance measure in the low SNR regime. Verdú [12] proved that the SNR per information bit E_b/N_0 , with N_0 denoting noise power, required for MIMO channels with no CSI achieves the minimum $NE_b/N_0 = \ln 2 \approx -1.59$ dB in the low SNR limit, with N denoting the number of receive antennas. This result provides a fundamental limit in terms of energy efficiency. See [13], [14] for more detailed analysis.

The last strategy is to analyze the achievable rate of a training-based system, which obviously provides a lower bound on the capacity. Since accurate channel estimates are assumed to be obtained by training, i.i.d. signaling over space and time is commonly used for training-based systems. This signaling contains practical modulation schemes, such as quadrature phase shift keying (QPSK) or quadrature amplitude modulation (QAM). Results based on this strategy are less explored than those based on the other two strategies. An advantage of the training-based strategy is that it is possible to obtain an *analytical* bound that can be easily evaluated for all SNRs. Hassibi and Hochwald [15] derived an analytical lower bound on the achievable rate of a pilot-assisted system, called the Hassibi-Hochwald (HH) bound in this paper. Another advantage is that it can provide a useful guideline for designing practical training-based MIMO systems. In fact, it was shown in [15] that the optimal number of pilot symbols is equal to the number of transmit antennas in terms of their lower bound. A weakness is that lower bounds derived by the last strategy might be looser than those derived by the first strategy. In this paper, we focus on the last strategy and improve the existing lower bound of the capacity based on training.

Hassibi and Hochwald [15] used a method for lower-bounding the achievable rate of a pilot-assisted system, developed by Médard in [16]. As shown in [17], using this method requires the assumption of one-shot channel estimation, under which the decoder regards the channel estimates provided by the channel estimator as the true ones. In other words, the decoded data symbols are not re-utilized for refining the channel estimates. Thus, a lower bound based on training-based systems should improve by refining the channel estimates with the decoded data symbols.

We follow a successive decoding (SD) strategy considered in [17]–[19], in which the data symbols decoded in the preceding stages are utilized for refining the channel estimates. In the initial channel estimation, the channel estimator utilizes pilot signals transmitted by using a fraction of resources. As a training-based scheme suitable for the SD strategy, we consider a combination of the conventional pilot-assisted scheme and a bias-based scheme [20]. In the bias-based scheme, a probabilistic bias of transmitted symbols is used for the initial channel estimation, while time-division multiplexed pilot symbols are utilized in the pilot-assisted scheme. The bias-based scheme was numerically shown to outperform pilot-assisted schemes for practical iterative receivers [21]–[23]. The goal of this

paper is to derive an analytical bound based on the SD strategy with a combination of the pilot-assisted scheme and the bias-based scheme.

B. Contributions & Methodology

The main contribution of this paper is to derive lower bounds on the achievable rates of SD receivers in the large-system limit, where the number of transmit antennas, the number of receive antennas, and coherence time tend to infinity while their ratios are kept constant. The lower bounds can be evaluated easily, whereas Padmanabhan et al. [19] calculated bounds on the corresponding achievable rate by numerical simulations. Numerical simulations in this paper show that the large-system results can provide a good approximation for not so large systems. The derived lower bounds are used to optimize the overhead for training. It is shown that negligibly small overhead for training is best in terms of the lower bounds. The optimized bound outperforms the HH bound [15] for all SNRs. Furthermore, the comparison between our bound and the high-SNR approximation of the capacity [10], [11] implies that the high-SNR approximation is valid only for quite high SNR.

The derivation of the proposed bounds consists of two steps: First, the optimal channel estimator is replaced by the linear minimum mean-squared error (LMMSE) channel estimator. Since the optimal channel estimator is nonlinear in general, the distribution of the channel estimates becomes non-Gaussian. This non-Gaussianity makes it difficult to calculate the achievable rates of the SD receivers with the optimal channel estimator. In order to circumvent this difficulty, we consider a lower bound based on LMMSE channel estimation.

Next, we take the large-system limit to obtain analytical results. The large-system limit has been extensively considered in the analysis of code-division multiple-access (CDMA) and MIMO systems with perfect CSI at the receiver, by using random matrix theory [24]–[27] and the replica method [28]–[34]. The advantage of taking the large-system limit is that several performance measures, such as mutual information and signal-interference-plus-noise ratio (SINR), are expected to be self-averaging, i.e., they converge in probability to deterministic values in the large-system limit. This self-averaging property allows us to obtain analytical results. The large-system limit in previous works for the perfect CSI case may be regarded as the limit in which the numbers of transmit and receive antennas tend to infinity at the same rate *after* taking the long coherence-time limit, since the receiver can obtain accurate channel estimates in these limits. In order to consider the no CSI case, on the other hand, the coherence time *and* the numbers of transmit and receive antennas tend to infinity at the same rate in this paper. Note that the coherence time must also tend to infinity to obtain meaningful results when the number of antennas tends to infinity, since there is no point in using transmit antennas more than the coherence time [4].

We use the replica method to evaluate the achievable rates in the large-system limit. The replica method was originally developed in statistical physics [35]. See [36]–[38] for the details of the replica method. Recently, it has been recognized that the replica method is useful for analyzing nonlinear receivers [28]–[34]. A weakness of the replica method is that it is based on several non-rigorous assumptions in the present time. See [39], [40] for a recent remarkable progress with respect to the replica method.

C. Notation

For a complex number $z \in \mathbb{C}$, throughout this paper, j , $\Re[z]$, $\Im[z]$, and z^* denote the imaginary unit, the real and imaginary parts of z , and the complex conjugate of z , respectively. For a complex matrix \mathbf{A} , \mathbf{A}^T , \mathbf{A}^H , $\text{Tr}(\mathbf{A})$, and $\det \mathbf{A}$ represent the transpose, the conjugate transpose, the trace, and the determinant of \mathbf{A} , respectively. The vector $\mathbf{1}_n$ denotes the n -dimensional vector whose elements are all one. The $n \times n$ identity matrix is denoted by \mathbf{I}_n . The operator \otimes denotes the Kronecker product of two matrices. The matrix $\text{diag}(a_1, \dots, a_n)$ represents the diagonal matrix with a_i as the i th diagonal element. \mathcal{M}_n^+ denotes the set of all positive definite $n \times n$ Hermitian matrices. $\log x$, $\ln x$, $\delta(\cdot)$, and $\delta_{a,b}$ denote $\log_2 x$, $\log_e x$, the Dirac delta function, and the Kronecker delta, respectively. For random variables X , Y , and Z , $I(X; Y|Z)$ denotes the conditional mutual information between X and Y given Z with the logarithm to base 2. For a complex random vector \mathbf{x} and a random variable Y , $\text{cov}[\mathbf{x}|Y]$ represents the covariance matrix of \mathbf{x} given Y . $\mathcal{CN}(\mathbf{m}, \mathbf{\Sigma})$ denotes a proper complex Gaussian distribution with mean \mathbf{m} and a covariance matrix $\mathbf{\Sigma}$ [41]. For covariance matrices $\mathbf{\Sigma}$ and $\tilde{\mathbf{\Sigma}}$, $D_a(\mathbf{\Sigma}||\tilde{\mathbf{\Sigma}})$ represents the Kullback-Leibler divergence with the logarithm to base a between $\mathcal{CN}(\mathbf{0}, \mathbf{\Sigma})$ and $\mathcal{CN}(\mathbf{0}, \tilde{\mathbf{\Sigma}})$.

As notational convenience for subsets of the natural numbers \mathbb{N} , we use $[a, b) = \{i \in \mathbb{N} : a \leq i < b\}$ for integers a and b ($> a$). The other sets $[a, b]$, (a, b) , and so on are defined in the same manner. The set $\mathcal{J} \setminus \{j\} = \{j' \in \mathcal{J} : j' \neq j\}$ denotes the set obtained by eliminating the element j from a set of indices \mathcal{J} . When \mathcal{J} equals the set of all indices, $\mathcal{J} \setminus \{j\}$ is simply written as $\setminus j$.

For a set of indices $\mathcal{J} = \{j_1, \dots, j_n\}$ and scalars $\{v_j : j \in \mathcal{J}\}$, $\mathbf{v}_{\mathcal{J}}$ denotes the column vector $\mathbf{v} = (v_{j_1}, \dots, v_{j_n})^T$, while $\vec{\mathbf{v}}_{\mathcal{J}}$ does the row vector $\vec{\mathbf{v}}_{\mathcal{J}} = (v_{j_1}, \dots, v_{j_n})$. For example, $\mathbf{v}_{[a,b)} = (v_a, \dots, v_{b-1})^T$ and $\mathbf{v}_{\mathcal{J} \setminus \{j_2\}} = (v_{j_1}, v_{j_3}, \dots, v_{j_n})^T$. Note that $\mathbf{v}_{\mathcal{J} \setminus \{j\}}$ is written as $\mathbf{v}_{\setminus j}$ when \mathcal{J} is the set of all indices, since $\mathcal{J} \setminus \{j\}$ is abbreviated as $\setminus j$. For column vectors $\{\mathbf{a}_j : j \in \mathcal{J}\}$, similarly, $\mathbf{A}_{\mathcal{J}}$ denotes the matrix $\mathbf{A}_{\mathcal{J}} = (\mathbf{a}_{j_1}, \dots, \mathbf{a}_{j_n})$. For example, $\mathbf{A}_{[a,b)} = (\mathbf{a}_a, \dots, \mathbf{a}_{b-1})$ and $\mathbf{A}_{\mathcal{J} \setminus \{j_2\}} = (\mathbf{a}_{j_1}, \mathbf{a}_{j_3}, \dots, \mathbf{a}_{j_n})$. We use symbols with tildes and hats to represent random variables for postulated (or virtual) channels and estimates of random variables, respectively. Underlined symbols are used to represent random variables for decoupled channels.

The remainder of this paper is organized as follows: A Rayleigh block-fading MIMO channel is introduced in Section II. The achievable rates of SD receivers based on LMMSE channel estimation are formulated in Section III. The main results of this paper are presented in Section IV. The obtained analytical bounds are compared to existing results in Section V. We conclude this paper in Section VI. The derivation of the main results is summarized in appendices.

II. CHANNEL MODEL

A. MIMO Channel

A narrowband MIMO system with M transmit antennas and N receive antennas is considered. We assume block-fading with coherence time T_c , i.e., the channel matrix $\mathbf{H} \in \mathbb{C}^{N \times M}$ is kept constant during one fading block consisting of T_c symbol periods, and at the beginning of the next fading block the channel matrix is independently

sampled from a distribution. The received vector $\mathbf{y}_t \in \mathbb{C}^N$ in the t th symbol period within a fading block is given by

$$\mathbf{y}_t = \frac{1}{\sqrt{M}} \mathbf{H} \mathbf{x}_t + \mathbf{n}_t, \quad t = 1, \dots, T_c, \quad (1)$$

where $\mathbf{x}_t = (x_{1,t}, \dots, x_{M,t})^T$ and $\mathbf{n}_t \sim \mathcal{CN}(\mathbf{0}, N_0 \mathbf{I}_N)$ denote the transmitted vector in the t th symbol period and an additive white Gaussian noise (AWGN) vector with a covariance matrix $N_0 \mathbf{I}_N$, respectively. The MIMO channel (1) can be represented in matrix form as

$$\mathbf{Y} = \frac{1}{\sqrt{M}} \mathbf{H} \mathbf{X} + \mathbf{N}, \quad (2)$$

with $\mathbf{Y} = (\mathbf{y}_1, \dots, \mathbf{y}_{T_c})$, $\mathbf{X} = (\mathbf{x}_1, \dots, \mathbf{x}_{T_c})$, and $\mathbf{N} = (\mathbf{n}_1, \dots, \mathbf{n}_{T_c})$.

For the simplicity of analysis, we assume i.i.d. Rayleigh fading MIMO channels, i.e., the channel matrix \mathbf{H} has mutually independent entries, and each entry $h_{n,m} = (\mathbf{H})_{n,m}$ is drawn from the circularly symmetric complex Gaussian (CSCG) distribution $\mathcal{CN}(0, 1)$ with unit variance. Note that the assumption of i.i.d. Rayleigh fading might be an idealized assumption since there can be correlations between the elements of the channel matrix in practice.

We impose a power constraint

$$\frac{1}{MT_c} \sum_{m=1}^M \sum_{t=1}^{T_c} \mathbb{E} [|x_{m,t}|^2] \leq P, \quad (3)$$

for $P > 0$. Marzetta and Hochwald [4] proved that the capacity does not decrease even if the power constraint is strengthened to a power constraint on each transmitted symbol,

$$\mathbb{E} [|x_{m,t}|^2] \leq P. \quad (4)$$

The former power constraint (3) allows us to use power allocation over space and time, whereas the latter power constraint (4) does not. In this paper, we only consider the latter power constraint (4), which simplifies the analysis.

B. Training-Based Transmission

We assume that neither the transmitter nor the receiver has CSI. More precisely, only the statistical properties of the MIMO channel (1) are assumed to be known to the receiver. The previous works [10], [15] showed that pilot-assisted channel estimation can achieve the capacity in the leading order of SNR in the high SNR regime, i.e., the full spatial multiplexing gain, while the obtained lower bounds are loose in the low-to-moderate SNR regime. Channel estimation based on pilot information is also considered in this paper. The main difference between the previous works and this paper appears in the receiver structure. We consider joint channel and data estimation based on SD, whereas in the previous works data symbols decoded successfully were not utilized for refining channel estimates.

One fading block is decomposed into the training phase $\mathcal{T}_{T_{\text{tr}}} = \{1, \dots, T_{\text{tr}}\}$ and the communication phase $\mathcal{C}_{T_{\text{tr}}+1} = \{T_{\text{tr}} + 1, \dots, T_c\}$, which consist of the first T_{tr} symbol periods and of the remaining $(T_c - T_{\text{tr}})$ symbol periods, respectively. The transmitter sends pilot symbol vectors in the training phase, and transmits data symbol vectors in the communication phase. Therefore, the transmitted vector \mathbf{x}_t is assumed to be known to the receiver

for $t \in \mathcal{T}_{\text{tr}}$. For simplicity, we assume that the pilot symbol matrix $\mathbf{X}_{\mathcal{T}_{\text{tr}}} = (\mathbf{x}_1, \dots, \mathbf{x}_{T_{\text{tr}}}) \in \mathbb{C}^{M \times T_{\text{tr}}}$ has zero-mean i.i.d. entries with i.i.d. real and imaginary parts. Furthermore, we assume that each pilot symbol satisfies $\mathbb{E}[|x_{m,t}|^2] = P$ for $t \in \mathcal{T}_{\text{tr}}$, since the accuracy of channel estimation should improve as the power of pilot symbols increases. The transmission of i.i.d. data symbols can achieve the capacity of the MIMO channel (1) with perfect CSI at the receiver. If accurate channel estimates are obtained by joint channel and data estimation, thus, i.i.d. signaling should be a reasonable option for training-based transmissions. We assume that the data symbols $\{x_{m,t} : t \in \mathcal{C}_{T_{\text{tr}}+1}\}$ are i.i.d. random variables with i.i.d. real and imaginary parts for all m and $t \in \mathcal{C}_{T_{\text{tr}}+1}$. Note that zero-mean is not assumed for the data symbols. Under this assumption, the achievable rate is monotonically increasing with the power of each data symbol. We hereinafter let $\mathbb{E}[|x_{m,t}|^2] = P$.

In this paper, we consider a biased signaling scheme, in which the mean $\mathbb{E}[x_{m,t}] = \theta_{m,t}$ of the data symbol for $t \in \mathcal{C}_{T_{\text{tr}}+1}$ is biased while the long-term average $(T_c - T_{\text{tr}})^{-1} \sum_{t=T_{\text{tr}}+1}^{T_c} \theta_{m,t}$ tends to zero as $T_c \rightarrow \infty$. In order to apply the replica method, we assume that $\{\Re[\theta_{m,t}], \Im[\theta_{m,t}] : \text{for all } m, t\}$ are independently drawn from a zero-mean hyperprior probability density function (pdf)² $p(\theta)$ with variance $\sigma_\theta^2/2$. The transmitter informs the receiver in advance about the bias matrix $\Theta = (\mathbf{O}, \boldsymbol{\theta}_{T_{\text{tr}}+1}, \dots, \boldsymbol{\theta}_{T_c}) \in \mathbb{C}^{M \times T_c}$, with $\boldsymbol{\theta}_t = (\theta_{1,t}, \dots, \theta_{M,t})^T$. In other words, Θ is assumed to be known to the receiver. The biased signaling can reduce the overhead for training [20] compared to the conventional pilot-assisted schemes. We present two examples of biased signaling: biased QPSK and biased Gaussian signaling. See [21]–[23] for implementations of biased QPSK.

Example 1 (Biased QPSK). For $\Re[x_{m,t}], \Im[x_{m,t}] \in \{\pm\sqrt{P/2}\}$, the prior pmf of $x_{m,t}$ for biased QPSK is given by

$$p(x_{m,t}|\theta_{m,t}) = \frac{1 + \Re[\theta_{m,t}]/\Re[x_{m,t}]}{2} \frac{1 + \Im[\theta_{m,t}]/\Im[x_{m,t}]}{2}. \quad (5)$$

The non-negativity of probability restricts the support of the hyperprior pdf $p(\theta)$ to $\Re[\theta_{m,t}] \in [-\sqrt{P/2}, \sqrt{P/2}]$ and $\Im[\theta_{m,t}] \in [-\sqrt{P/2}, \sqrt{P/2}]$. It is straightforward to check that $\mathbb{E}[x_{m,t}|\theta_{m,t}] = \theta_{m,t}$ and $\mathbb{E}[|x_{m,t}|^2|\theta_{m,t}] = P$.

Example 2 (Biased Gaussian Signaling). The prior pdf of $x_{m,t} \in \mathbb{C}$ for biased Gaussian signaling is given by

$$p(x_{m,t}|\theta_{m,t}) = \frac{1}{\pi(P - |\theta_{m,t}|^2)} e^{-\frac{|x_{m,t} - \theta_{m,t}|^2}{P - |\theta_{m,t}|^2}}. \quad (6)$$

Note that the support of the hyperprior pdf $p(\theta)$ is restricted to $|\theta_{m,t}| < \sqrt{P}$, due to the positivity of variance.

The main results presented in this paper hold for a general prior of $x_{m,t}$ with finite moments. The performance for the biased Gaussian signaling corresponds to a performance bound for multilevel modulation with trellis shaping [42], [43].

² When $\theta_{m,t}$ is discrete, $p(\theta)$ denotes a probability mass function (pmf).

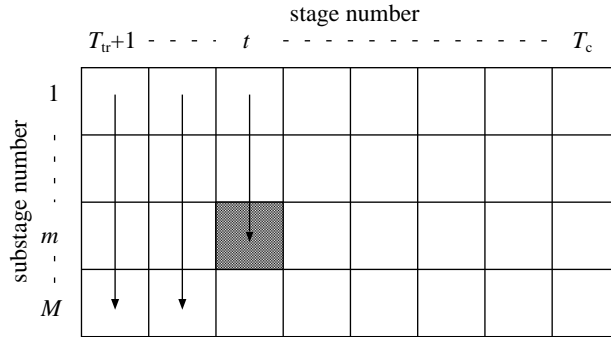


Fig. 1. Successive decoding.

III. RECEIVERS

A. Successive Decoding

We consider an SD receiver [18], [19] (See Fig. 1). The data symbol vectors $\{\mathbf{x}_t\}$ are decoded in the order $t = T_{tr} + 1, \dots, T_c$. In stage t , the matrix $\mathbf{X}_{(T_{tr},t)} = (\mathbf{x}_{T_{tr}+1}, \dots, \mathbf{x}_{t-1}) \in \mathbb{C}^{M \times (t - T_{tr} - 1)}$ contains the data symbol vectors decoded in the preceding stages. Stage t consists of M substages, in which the elements $\{x_{m,t}\}$ are decoded in the order $m = 1, \dots, M$. In substage m within stage t , the vector $\mathbf{x}_{[1,m],t} = (x_{1,t}, \dots, x_{m-1,t})^T \in \mathbb{C}^{m-1}$ consists of the data symbols decoded in the preceding substages. The channel estimator utilizes the data symbols $\mathbf{X}_{(T_{tr},t)}$ decoded in the preceding stages, along with the received matrix $\mathbf{Y}_{\setminus t} \in \mathbb{C}^{N \times (T_c - 1)}$ and the pilot information $\{\mathbf{X}_{\mathcal{T}_{T_{tr}}}, \Theta_{(t,T_c)}\}$, in which the matrices $\mathbf{Y}_{\setminus t}$ and $\Theta_{(t,T_c)} \in \mathbb{C}^{M \times (T_c - t)}$ are obtained by eliminating the t th column vector from the received matrix \mathbf{Y} and the first t column vectors from the bias matrix Θ , respectively. We write the information used for channel estimation in stage t as $\mathcal{I}_t = \{\bar{\mathbf{X}}_{\setminus t}, \mathbf{Y}_{\setminus t}\}$, with $\bar{\mathbf{X}}_{\setminus t} = (\mathbf{X}_{\mathcal{T}_{T_{tr}}}, \mathbf{X}_{(T_{tr},t)}, \Theta_{(t,T_c)}) \in \mathbb{C}^{M \times (T_c - 1)}$. In substage m within stage t , the detector with successive interference cancellation (SIC) uses the data symbols $\mathbf{x}_{[1,m],t}$ decoded in the preceding substages and the bias vector $\boldsymbol{\theta}_{[m,M],t} = (\theta_{m,t}, \dots, \theta_{M,t})^T$ to subtract inter-stream interference from the received vector \mathbf{y}_t , and then perform multiuser detection (MUD).

Let us define the constrained capacity of the MIMO system based on the pilot information $\{\mathbf{X}_{\mathcal{T}_{T_{tr}}}, \Theta\}$ as the conditional mutual information per symbol period between all data symbol vectors $\{\mathbf{x}_t : t \in \mathcal{C}_{T_{tr}+1}\}$ and the received matrix \mathbf{Y} conditioned on the pilot symbol matrix $\mathbf{X}_{\mathcal{T}_{T_{tr}}}$ and the bias matrix Θ [44]

$$C = \frac{1}{T_c} I(\{\mathbf{x}_t : t \in \mathcal{C}_{T_{tr}+1}\}; \mathbf{Y} | \mathbf{X}_{\mathcal{T}_{T_{tr}}}, \Theta). \quad (7)$$

It is straightforward to confirm that the optimal SD receiver can achieve the constrained capacity (7). Applying the

chain rule for mutual information to (7) repeatedly [44], we obtain

$$\begin{aligned}
 C &= \frac{1}{T_c} \sum_{t=T_{\text{tr}}+1}^{T_c} I(\mathbf{x}_t; \mathbf{Y} | \mathbf{X}_{\mathcal{T}_{T_{\text{tr}}}}, \Theta, \mathbf{X}_{(T_{\text{tr}}, t)}) \\
 &= \frac{1}{T_c} \sum_{t=T_{\text{tr}}+1}^{T_c} I(\mathbf{x}_t; \mathbf{y}_t | \mathcal{I}_t, \Theta_{(T_{\text{tr}}, t)}, \boldsymbol{\theta}_t) \\
 &= \frac{1}{T_c} \sum_{t=T_{\text{tr}}+1}^{T_c} \sum_{m=1}^M I(x_{m,t}; \mathbf{y}_t | \mathcal{I}_t, \mathbf{x}_{[1,m),t}, \boldsymbol{\theta}_{[m,M],t}),
 \end{aligned} \tag{8}$$

with $\Theta_{(T_{\text{tr}}, t)} = (\boldsymbol{\theta}_{T_{\text{tr}}+1}, \dots, \boldsymbol{\theta}_{t-1})$. In the derivation of the second equality, we have used the fact that \mathbf{x}_t and $\mathbf{Y}_{\setminus t}$ are independent of each other, due to the i.i.d. assumption of the data symbols. In the last expression, we have omitted conditioning with respect to $\Theta_{(T_{\text{tr}}, t)}$ and $\boldsymbol{\theta}_{[1,m),t} = (\theta_{1,t}, \dots, \theta_{m-1,t})^T$, which are not utilized by the receiver in substage m within stage t since they are the parameters of the known data symbols $\mathbf{X}_{(T_{\text{tr}}, t)}$ and $\mathbf{x}_{[1,m),t}$. For notational simplicity, this omission is applied throughout this paper. Note that $\Theta_{(T_{\text{tr}}, t)}$ and $\boldsymbol{\theta}_{[1,m),t}$ affect the achievable rate (8). Expression (8) implies that the SD scheme results in no loss of information if the detector with SIC can achieve the mutual information $I(x_{m,t}; \mathbf{y}_t | \mathcal{I}_t, \mathbf{x}_{[1,m),t}, \boldsymbol{\theta}_{[m,M],t})$ in substage m within stage t .

It is difficult to evaluate the mutual information $I(x_{m,t}; \mathbf{y}_t | \mathcal{I}_t, \mathbf{x}_{[1,m),t}, \boldsymbol{\theta}_{[m,M],t})$ exactly. Instead, we derive a lower bound based on LMMSE channel estimation. We first introduce the optimal channel estimator and then define the LMMSE channel estimator.

B. Channel Estimators

1) *Optimal Channel Estimator:* We focus on stage t in this section. The optimal channel estimator uses the information \mathcal{I}_t to estimate the channel matrix \mathbf{H} , and sends the joint posterior pdf

$$p(\mathbf{H} | \mathcal{I}_t) = \frac{p(\mathbf{Y}_{\setminus t} | \mathbf{H}, \bar{\mathbf{X}}_{\setminus t}) p(\mathbf{H})}{\int p(\mathbf{Y}_{\setminus t} | \mathbf{H}, \bar{\mathbf{X}}_{\setminus t}) p(\mathbf{H}) d\mathbf{H}}, \tag{9}$$

to the detector with SIC. In (9), the pdf $p(\mathbf{Y}_{\setminus t} | \mathbf{H}, \bar{\mathbf{X}}_{\setminus t})$ is decomposed into the product of pdfs $p(\mathbf{Y}_{\setminus t} | \mathbf{H}, \bar{\mathbf{X}}_{\setminus t}) = \prod_{t'=1}^{t-1} p(\mathbf{y}_{t'} | \mathbf{H}, \mathbf{x}_{t'}) \prod_{t'=t+1}^{T_c} p(\mathbf{y}_{t'} | \mathbf{H}, \boldsymbol{\theta}_{t'})$, given by

$$p(\mathbf{y}_{t'} | \mathbf{H}, \boldsymbol{\theta}_{t'}) = \int p(\mathbf{y}_{t'} | \mathbf{H}, \mathbf{x}_{t'}) p(\mathbf{x}_{t'} | \boldsymbol{\theta}_{t'}) d\mathbf{x}_{t'}, \tag{10}$$

where $p(\mathbf{y}_{t'} | \mathbf{H}, \mathbf{x}_{t'})$ represents the MIMO channel (1). Note that the joint posterior pdf (9) is decomposed into the product $\prod_{n=1}^N p(\vec{\mathbf{h}}_n | \mathcal{I}_t)$ of the marginal posterior pdfs, with $\vec{\mathbf{h}}_n \in \mathbb{C}^{1 \times M}$ denoting the n th row vector of \mathbf{H} , due to the assumption of i.i.d. fading.

The optimal channel estimator is nonlinear in general, which makes it difficult to analyze detectors with SIC, while it is possible to evaluate the performance of the optimal channel estimator. In order to circumvent this difficulty, we reduce the optimal channel estimator to an LMMSE channel estimator by considering a virtual MIMO channel.

2) *LMMSE Channel Estimator:* We use Médard's method [16] to replace the MIMO channels (1) for $t' = t+1, \dots, T_c$ by virtual MIMO channels

$$\tilde{\mathbf{y}}_{t'} = \frac{1}{\sqrt{M}} \mathbf{H} \boldsymbol{\theta}_{t'} + \mathbf{w}_{t'} + \mathbf{n}_{t'}, \tag{11}$$

where $\mathbf{w}_{t'} \in \mathbb{C}^N$ denotes a CSCG random vector with the covariance matrix $(P - \sigma_{t'}^2)\mathbf{I}_N$, with $\sigma_{t'}^2 = M^{-1} \sum_{m=1}^M |\theta_{m,t'}|^2$. The virtual MIMO channel (11) is obtained by extracting the term $M^{-1/2}\mathbf{H}(\mathbf{x}_{t'} - \boldsymbol{\theta}_{t'})$ from the first term of the right-hand side (RHS) in the original MIMO channel (1) and then replacing it by the AWGN term $\mathbf{w}_{t'}$ with the covariance matrix $\text{cov}[M^{-1/2}\mathbf{H}(\mathbf{x}_{t'} - \boldsymbol{\theta}_{t'})|\boldsymbol{\theta}_{t'}]$. This replacement implies that information about the channel matrix included in $\mathbf{H}(\mathbf{x}_{t'} - \boldsymbol{\theta}_{t'})$ is discarded. Thus, channel estimation based on the virtual MIMO channel (11) should be inferior to that based on the original MIMO channel (1). In other words, the mutual information $I(x_{m,t}; \mathbf{y}_t | \mathcal{I}_t, \mathbf{x}_{[1,m],t}, \boldsymbol{\theta}_{[m,M],t})$ should be bounded from below by

$$I(x_{m,t}; \mathbf{y}_t | \mathcal{I}_t, \mathbf{x}_{[1,m],t}, \boldsymbol{\theta}_{[m,M],t}) \geq I(x_{m,t}; \mathbf{y}_t | \tilde{\mathcal{I}}_t, \mathbf{x}_{[1,m],t}, \boldsymbol{\theta}_{[m,M],t}), \quad (12)$$

which denotes the constrained capacity of the MIMO channel (1) in symbol period t with side information $\tilde{\mathcal{I}}_t = \{\tilde{\mathbf{X}}_{\setminus t}, \tilde{\mathbf{Y}}_{\setminus t}\}$, $\mathbf{x}_{[1,m],t}$, and $\boldsymbol{\theta}_{[m,M],t}$, in which $\tilde{\mathbf{Y}}_{\setminus t} = (\mathbf{y}_1, \dots, \mathbf{y}_{t-1}, \tilde{\mathbf{y}}_{t+1}, \dots, \tilde{\mathbf{y}}_{T_c})$ contains the received vectors of the virtual MIMO channel (11) in the last $(T_c - t)$ elements while the first $(t - 1)$ elements of $\tilde{\mathbf{Y}}_{\setminus t}$ are the same as those of the original one $\mathbf{Y}_{\setminus t}$. From (1) and (11), the matrix $\tilde{\mathbf{Y}}_{\setminus t}$ is explicitly given by

$$\tilde{\mathbf{Y}}_{\setminus t} = \frac{1}{\sqrt{M}} \mathbf{H} \tilde{\mathbf{X}}_{\setminus t} + (\mathbf{O}, \mathbf{W}_{(t, T_c]}) + \mathbf{N}_{\setminus t}, \quad (13)$$

with $\mathbf{W}_{(t, T_c]} = (\mathbf{w}_{t+1}, \dots, \mathbf{w}_{T_c}) \in \mathbb{C}^{N \times (T_c - t)}$. In (13), the matrix $\mathbf{N}_{\setminus t} \in \mathbb{C}^{N \times (T_c - 1)}$ is obtained by eliminating the t th column vector from the noise matrix \mathbf{N} .

Let us consider channel estimation based on the information $\tilde{\mathcal{I}}_t$. The optimal channel estimator for this case constructs the joint posterior pdf $p(\mathbf{H} | \tilde{\mathcal{I}}_t)$ and feeds it to the detector with SIC. The joint posterior pdf of \mathbf{H} given $\tilde{\mathcal{I}}_t$ is defined by (9) in which the pdf (10) for $t' = t + 1, \dots, T_c$ is replaced by

$$p(\tilde{\mathbf{y}}_{t'} | \mathbf{H}, \boldsymbol{\theta}_{t'}) = \int p(\tilde{\mathbf{y}}_{t'} | \mathbf{H}, \boldsymbol{\theta}_{t'}, \mathbf{w}_{t'}) p(\mathbf{w}_{t'} | \boldsymbol{\theta}_{t'}) d\mathbf{w}_{t'}, \quad (14)$$

where $p(\tilde{\mathbf{y}}_{t'} | \mathbf{H}, \boldsymbol{\theta}_{t'}, \mathbf{w}_{t'})$ represents the virtual MIMO channel (11). A straightforward calculation indicates that the joint posterior pdf $p(\mathbf{H} | \tilde{\mathcal{I}}_t)$ is a proper complex Gaussian pdf with mean $\hat{\mathbf{H}}_t \in \mathbb{C}^{N \times M}$ and covariance $\text{cov}[(\vec{\mathbf{h}}_1, \dots, \vec{\mathbf{h}}_N)^T | \tilde{\mathcal{I}}_t] = \mathbf{I}_N \otimes \boldsymbol{\Xi}_t$, given by

$$\hat{\mathbf{H}}_t = \frac{1}{\sqrt{M}} \left[\sum_{t'=1}^{t-1} \frac{\mathbf{y}_{t'} \mathbf{x}_{t'}^H}{N_0} + \sum_{t'=t+1}^{T_c} \frac{\tilde{\mathbf{y}}_{t'} \boldsymbol{\theta}_{t'}^H}{P - \sigma_{t'}^2 + N_0} \right] \boldsymbol{\Xi}_t, \quad (15)$$

$$\boldsymbol{\Xi}_t = \left[\mathbf{I}_M + \frac{1}{M} \left(\sum_{t'=1}^{t-1} \frac{\mathbf{x}_{t'} \mathbf{x}_{t'}^H}{N_0} + \sum_{t'=t+1}^{T_c} \frac{\boldsymbol{\theta}_{t'} \boldsymbol{\theta}_{t'}^H}{P - \sigma_{t'}^2 + N_0} \right) \right]^{-1}. \quad (16)$$

The posterior mean $\hat{\mathbf{H}}_t$ coincides with the LMMSE estimator of \mathbf{H} based on the received matrix $\tilde{\mathbf{Y}}_{\setminus t}$ and the known information $\tilde{\mathbf{X}}_{\setminus t}$. Furthermore, $\boldsymbol{\Xi}_t$ is equal to the error covariance matrix of the LMMSE estimator for each row vector of \mathbf{H} . Thus, we refer to the optimal channel estimator for the virtual MIMO channel (11) as the LMMSE channel estimator.

Note that the linear filter given by (15) provides the LMMSE estimates of \mathbf{H} for the original MIMO channel (1). One should not confuse the LMMSE channel estimator for the virtual MIMO channel (11) with that for the original MIMO channel (1). The former, which is considered in this paper, is the optimal channel estimator for the virtual MIMO channel (11), while the latter is a suboptimal channel estimator for the original MIMO channel (1).

C. Detectors

1) *Optimal Detector*: We focus on substage m within stage t and define the optimal detector with SIC, which achieves the lower bound (12). The optimal detector with SIC feeds to the associated decoder the posterior pdf³ of $x_{m,t}$ based on the knowledge about the received vector \mathbf{y}_t , the data symbols $\mathbf{x}_{[1,m],t}$ decoded in the preceding substages, the bias $\boldsymbol{\theta}_{[m,M],t}$ for the unknown data symbols $\mathbf{x}_{[m,M],t} = (x_{m,t}, \dots, x_{M,t})^T$, and the joint posterior pdf $p(\mathbf{H}|\tilde{\mathcal{I}}_t)$ provided by the LMMSE channel estimator, given by

$$p(x_{m,t}|\mathbf{y}_t, \tilde{\mathcal{I}}_t, \mathbf{x}_{[1,m],t}, \boldsymbol{\theta}_{[m,M],t}) = \frac{\int p(\mathbf{y}_t|\mathbf{x}_t, \tilde{\mathcal{I}}_t)p(\mathbf{x}_{[m,M],t}|\boldsymbol{\theta}_{[m,M],t})d\mathbf{x}_{[m,M],t}}{\int p(\mathbf{y}_t|\mathbf{x}_t, \tilde{\mathcal{I}}_t)p(\mathbf{x}_{[m,M],t}|\boldsymbol{\theta}_{[m,M],t})d\mathbf{x}_{[m,M],t}} \quad (17)$$

with $\mathbf{x}_{(m,M),t} = (x_{m+1,t}, \dots, x_{M,t})^T \in \mathbb{C}^{M-m}$. In (17), the pdf $p(\mathbf{y}_t|\mathbf{x}_t, \tilde{\mathcal{I}}_t)$ is given by

$$p(\mathbf{y}_t|\mathbf{x}_t, \tilde{\mathcal{I}}_t) = \int p(\mathbf{y}_t|\mathbf{H}, \mathbf{x}_t)p(\mathbf{H}|\tilde{\mathcal{I}}_t)d\mathbf{H}, \quad (18)$$

where $p(\mathbf{y}_t|\mathbf{H}, \mathbf{x}_t)$ represents the MIMO channel (1). The use of SIC appears in the pdf (18), which is a proper complex Gaussian pdf with mean $M^{-1/2}\hat{\mathbf{H}}_t\mathbf{x}_t$ and covariance $(N_0 + M^{-1}\mathbf{x}_t^H\boldsymbol{\Xi}_t\mathbf{x}_t)\mathbf{I}_N$. Expression (17) implies that the optimal detector with SIC subtracts the known inter-stream interference $M^{-1/2}\hat{\mathbf{H}}_t(\mathbf{x}_{[1,m],t}^T, 0, \boldsymbol{\theta}_{(m,M),t}^T)^T$ from the received vector \mathbf{y}_t , with $\boldsymbol{\theta}_{(m,M),t} = (\theta_{m+1,t}, \dots, \theta_{M,t})^T$, and then mitigates residual inter-stream interference by performing the optimal nonlinear MUD.

Let $\tilde{x}_{m,t} \in \mathbb{C}$ denote a random variable following the marginal posterior pdf (17). Since the lower bound (12) is equal to the mutual information $I(x_{m,t}; \tilde{x}_{m,t}|\tilde{\mathcal{I}}_t, \mathbf{x}_{[1,m],t}, \boldsymbol{\theta}_{[m,M],t})$, the achievable rate (8) of the optimal SD receiver is bounded from below by

$$C \geq \frac{1}{T_c} \sum_{t=T_{\text{tr}}+1}^{T_c} \sum_{m=1}^M I(x_{m,t}; \tilde{x}_{m,t}|\tilde{\mathcal{I}}_t, \mathbf{x}_{[1,m],t}, \boldsymbol{\theta}_{[m,M],t}), \quad (19)$$

which is given via the equivalent channel between the data symbol $x_{m,t}$ and the associated decoder

$$\begin{aligned} & p(\tilde{x}_{m,t}|x_{m,t}, \tilde{\mathcal{I}}_t, \mathbf{x}_{[1,m],t}, \boldsymbol{\theta}_{[m,M],t}) \\ &= \int p(x_{m,t} = \tilde{x}_{m,t}|\mathbf{y}_t, \tilde{\mathcal{I}}_t, \mathbf{x}_{[1,m],t}, \boldsymbol{\theta}_{[m,M],t})p(\mathbf{y}_t|\mathbf{x}_t, \tilde{\mathcal{I}}_t)p(\mathbf{x}_{(m,M),t}|\boldsymbol{\theta}_{(m,M),t})d\mathbf{x}_{(m,M),t}d\mathbf{y}_t. \end{aligned} \quad (20)$$

2) *LMMSE Detector*: Since the optimal detector is infeasible in terms of the complexity, it is important in practice to obtain a lower bound based on the LMMSE detector with SIC. We follow [17] to derive the LMMSE detector that feeds to the associated decoder an approximate posterior pdf of $x_{m,t}$ based on the knowledge about the received vector \mathbf{y}_t , the data symbols $\mathbf{x}_{[1,m],t}$ decoded in the preceding substages, the bias $\boldsymbol{\theta}_{[m,M],t}$ for the unknown data symbols $\mathbf{x}_{[m,M],t} = (x_{m,t}, \dots, x_{M,t})^T$, and the joint posterior pdf $p(\mathbf{H}|\tilde{\mathcal{I}}_t)$ provided by the LMMSE channel estimator.

We first divide the RHS of the MIMO channel (1) into two terms:

$$\mathbf{y}_t = \frac{1}{\sqrt{M}}\hat{\mathbf{H}}_t\mathbf{x}_t + \frac{1}{\sqrt{M}}(\mathbf{H} - \hat{\mathbf{H}}_t)\mathbf{x}_t + \mathbf{n}_t, \quad (21)$$

³The marginal posterior pdf (17) is replaced by the posterior pmf of $x_{m,t}$ if $x_{m,t}$ is a discrete random variable.

with $\hat{\mathbf{H}}_t$ denoting the LMMSE estimate (15) of the channel matrix. Let $\hat{\mathbf{H}}_{[1,m],t} \in \mathbb{C}^{N \times (m-1)}$ and $\hat{\mathbf{H}}_{[m,M],t} \in \mathbb{C}^{N \times (M-m+1)}$ denote the matrices that consist of the first $(m-1)$ column vectors of the LMMSE estimate (15) and of the last $(M-m+1)$ column vectors, respectively. The first term of the RHS in (21) is further decomposed into two terms:

$$\mathbf{y}_t = \frac{1}{\sqrt{M}} \hat{\mathbf{H}}_{[1,m],t} \mathbf{x}_{[1,m],t} + \frac{1}{\sqrt{M}} \hat{\mathbf{H}}_{[m,M],t} \mathbf{x}_{[m,M],t} + \frac{1}{\sqrt{M}} (\mathbf{H} - \hat{\mathbf{H}}_t) \mathbf{x}_t + \mathbf{n}_t, \quad (22)$$

where the first term of the RHS is a known quantity. From this expression, the LMMSE detector is defined via the postulated MIMO channel

$$\tilde{\mathbf{y}}_t^{(L)} - \frac{1}{\sqrt{M}} \hat{\mathbf{H}}_{[1,m],t} \mathbf{x}_{[1,m],t} = \frac{1}{\sqrt{M}} \hat{\mathbf{H}}_{[m,M],t} \tilde{\mathbf{x}}_{[m,M],t}^{(L)} + \tilde{\mathbf{w}}_t^{(L)} + \mathbf{n}_t, \quad (23)$$

where $\tilde{\mathbf{y}}_t^{(L)} \in \mathbb{C}^N$ and $\tilde{\mathbf{x}}_{[m,M],t}^{(L)} = (\tilde{x}_{m,t}^{(L)}, \dots, \tilde{x}_{M,t}^{(L)})^T \in \mathbb{C}^{M-m+1}$ denote the received vector and the data symbol vector postulated by the LMMSE detector, respectively. The postulated data symbol vector $\tilde{\mathbf{x}}_{[m,M],t}^{(L)}$ is assumed to be a proper complex Gaussian random vector with mean $\boldsymbol{\theta}_{[m,M],t}$ and covariance

$$\boldsymbol{\Sigma}_{m,t} = P \mathbf{I}_{M-m+1} - \text{diag}(|\theta_{m,t}|^2, \dots, |\theta_{M,t}|^2), \quad (24)$$

which are the same as the mean and covariance of the original vector $\mathbf{x}_{[m,M],t}$, respectively. Furthermore, $\tilde{\mathbf{w}}_t^{(L)} \in \mathbb{C}^N$ is a CSCG random vector with the covariance matrix $\zeta_{m,t} \mathbf{I}_N$, in which

$$\zeta_{m,t} = \frac{1}{M} \text{Tr} (\mathbb{E}[\mathbf{x}_t \mathbf{x}_t^H | \mathbf{x}_{[1,m],t}] \boldsymbol{\Xi}_t), \quad (25)$$

with

$$\mathbb{E}[\mathbf{x}_t \mathbf{x}_t^H | \mathbf{x}_{[1,m],t}] = \text{diag}(|x_{1,t}|^2, \dots, |x_{m-1,t}|^2, P, \dots, P). \quad (26)$$

Note that $\tilde{\mathbf{w}}_t^{(L)}$ has the same first and second moments as those of the third term on the RHS of (22).

The posterior distribution of $\tilde{\mathbf{x}}_{[m,M],t}^{(L)}$ given $\tilde{\mathbf{y}}_t^{(L)}$, $\tilde{\mathcal{I}}_t$, $\mathbf{x}_{[1,m],t}$, and $\boldsymbol{\theta}_{[m,M],t}$ is a proper complex Gaussian distribution with mean $\hat{\mathbf{x}}_{[m,M],t}^{(L)}$ and covariance $\boldsymbol{\Xi}_{m,t}^{(L)}$, given by

$$\hat{\mathbf{x}}_{[m,M],t}^{(L)} = (\boldsymbol{\Xi}_{m,t}^{(L)})^{-1} \left\{ \frac{1}{\sqrt{M}} (N_0 + \zeta_{m,t})^{-1} \hat{\mathbf{H}}_{[m,M],t}^H \left(\tilde{\mathbf{y}}_t^{(L)} - \frac{1}{\sqrt{M}} \hat{\mathbf{H}}_{[1,m],t} \mathbf{x}_{[1,m],t} \right) + \boldsymbol{\Sigma}_{m,t}^{-1} \boldsymbol{\theta}_{[m,M],t} \right\}, \quad (27)$$

$$\boldsymbol{\Xi}_{m,t}^{(L)} = \left(\boldsymbol{\Sigma}_{m,t}^{-1} + \frac{1}{M} (N_0 + \zeta_{m,t})^{-1} \hat{\mathbf{H}}_{[m,M],t}^H \hat{\mathbf{H}}_{[m,M],t} \right)^{-1}. \quad (28)$$

Note that the posterior mean (27) with $\tilde{\mathbf{y}}_t^{(L)} = \mathbf{y}_t$ is equal to the LMMSE estimate of $\mathbf{x}_{[m,M],t}$. The LMMSE detector with SIC sends the marginal posterior pdf $p(\tilde{x}_{m,t}^{(L)} | \tilde{\mathbf{y}}_t^{(L)} = \mathbf{y}_t, \tilde{\mathcal{I}}_t, \mathbf{x}_{[1,m],t}, \boldsymbol{\theta}_{[m,M],t})$, corresponding to (17), given via the marginalization of the joint posterior pdf $p(\tilde{\mathbf{x}}_{[m,M],t}^{(L)} | \tilde{\mathbf{y}}_t^{(L)}, \tilde{\mathcal{I}}_t, \mathbf{x}_{[1,m],t}, \boldsymbol{\theta}_{[m,M],t})$. Thus, we have a lower bound of the achievable rate based on the LMMSE detector with SIC

$$C \geq \frac{1}{T_c} \sum_{t=T_{\text{tr}}+1}^{T_c} \sum_{m=1}^M I(x_{m,t}; \tilde{x}_{m,t}^{(L)} | \tilde{\mathcal{I}}_t, \mathbf{x}_{[1,m],t}, \boldsymbol{\theta}_{[m,M],t}), \quad (29)$$

which is given via the equivalent channel between the data symbol $x_{m,t}$ and the associated LMMSE detector in the same manner as in (19).

The goal of this paper is to optimize the length of training phase T_{tr} , the prior pdf of the data symbols, and the hyperprior pdf of the bias in terms of the two lower bounds (19) and (29).

IV. MAIN RESULTS

A. Large-System Analysis

First, the lower bound (19) based on the optimal detector is evaluated in the large-system limit. We focus on substage m within stage t in the SD receiver. In order to calculate $I(x_{m,t}; \tilde{x}_{m,t} | \tilde{\mathcal{L}}_t, \mathbf{x}_{[1,m],t}, \boldsymbol{\theta}_{[m,M],t})$, we have to evaluate the distribution of the equivalent channel (20), which is a probability distribution on the space of distributions and depends on the omitted variables $\Theta_{(T_{\text{tr}},t)}$ and $\boldsymbol{\theta}_{[1,m],t}$ implicitly through the posterior pdf $p(\mathbf{H} | \tilde{\mathcal{L}}_t)$ and $\mathbf{x}_{[1,m],t}$. This evaluation is quite difficult in general for finite-sized systems. A key assumption of circumventing this difficulty is the assumption of the large-system limit in which M , N , T_c , T_{tr} , t , and m tend to infinity while their ratios $\alpha = M/N$, $\beta = M/T_c$, $\tau_0 = T_{\text{tr}}/T_c$, $\tau = t/T_c$, and $\mu = m/M$ are kept constant. The self-averaging property for the equivalent channel (20) is expected to hold in the large-system limit: The distribution of the equivalent channel (20) converges to a Dirac measure on the space of distributions in the large-system limit. See [45] for a mathematical treatment of self-averaging. The assumption of self-averaging implies that the detection performance for each data symbol coincides with the corresponding average performance in the large-system limit. Under this assumption, the replica method allows us to analyze the equivalent channel (20) in the large-system limit.

The self-averaging properties are classified into those for extensive quantities and those for non-extensive quantities. The former quantities are proportional to the size of systems, while the latter quantities are not. The self-averaging property for extensive quantities, such as sum capacity and the so-called free-energy in statistical physics, has been rigorously justified for linear systems [25] and general systems [46], [47]. It might be possible to prove the self-averaging property for the lower bound (19) by using the method developed in [46], [47]. However, we need the self-averaging property for *each* equivalent channel (20), which is non-extensive. The self-averaging property for non-extensive quantities is less understood except for several simple cases.

We also need the self-averaging property for each element of the error covariance matrix (16), along with that for the equivalent channel (20). Note that the error covariance matrix (16) is a random matrix depending on $\tilde{\mathbf{X}}_{\setminus t}$ explicitly and on $\Theta_{(T_{\text{tr}},t)}$ implicitly through the data symbol vectors decoded in the preceding stages. See [48] for the self-averaging property of each diagonal element for random covariance matrices.

Assumption 1. *Each element of the error covariance matrix (16) for the LMMSE channel estimation converges in probability to a deterministic value in the large-system limit, i.e.,*

$$(\Xi_t)_{\tilde{m}, \tilde{m}'} \rightarrow \begin{cases} \xi^2(\tau) & \text{for } \tilde{m} = \tilde{m}' \\ \rho(\tau) & \text{for } \tilde{m} < \tilde{m}' \\ \rho^*(\tau) & \text{for } \tilde{m} > \tilde{m}'. \end{cases} \quad (30)$$

The error covariance matrix (16) does not depend on the number of receive antennas N or the current substage m . Thus, the limits (30) do not depend on α or μ , while they may depend on β , τ_0 , and τ . Assumption 1 has been rigorously proved for the unbiased case $\theta_{m,t} = 0$ in [26].

Assumption 2. *The equivalent channel (20) is self-averaging with respect to $\tilde{\mathbf{Y}}_{\setminus t}$ and $\mathbf{x}_{[1,m),t}$: (20) converges in law to a conditional pdf of $\tilde{x}_{m,t}$ given $x_{m,t}$, $\bar{\mathbf{X}}_{\setminus t}$, and $\boldsymbol{\theta}_t$, which does not depend on $\tilde{\mathbf{Y}}_{\setminus t}$ or $\mathbf{x}_{[1,m),t}$, in the large-system limit.*

The self-averaging property for equivalent channels has been rigorously proved in the case of linear receivers by using random matrix theory [24], [26], while its justification is still open for nonlinear receivers. The equivalent channel (20) is also expected to be self-averaging with respect to the other random variables. However, Assumption 2 is sufficient for using the replica method. We postulate Assumptions 1 and 2 since their justification is beyond the scope of this paper.

Following the replica methodology raises the issue of whether replica symmetry (RS) or replica symmetry breaking (RSB) should be assumed. The formal definition of the RS assumption will be presented in Appendices B and C. Roughly speaking, RSB should be assumed for complicated optimization problems in which the object function has multi-valley structure [36], [37]. There are many local optima for such an object function. On the other hand, the RS assumption is applicable to simple problems such that the object function has the unique global optimum or a few local optima. Nishimori's rigorous result [49] suggests that the individually optimal (IO) detection [50] considered in this paper should have a simple structure corresponding to the RS assumption, while the jointly optimal (JO) detection [50] should be a complicated problem corresponding to the RSB assumption. A recent rigorous study [51] also supports the RS assumption for the IO detection. Thus, the RS assumption is postulated in this paper. Note that the self-averaging property for the equivalent channel might not hold if the system had a complicated structure corresponding to the RSB assumption [37], [52].

The lower bound (19) is given as a double integral of the constrained capacity for AWGN channels. We first derive the AWGN channels in a heuristic manner. The heuristic derivation described below provides an intuitive interpretation of the AWGN channels, although the formal derivation is based on the replica method. In the current stage $t = \tau T_c$, with $\tau_0 \leq \tau \leq 1$, we consider fading channels with time diversity for channel estimation,

$$\underline{y}_{n,t'} = \frac{1}{\sqrt{M}} h_{n,m} x_{m,t'} + \underline{w}_{n,t'}, \quad \text{for all } t' < t, \quad (31)$$

$$\underline{y}_{n,t'} = \frac{1}{\sqrt{M}} h_{n,m} \theta_{m,t'} + \underline{w}_{n,t'}, \quad \text{for all } t' > t, \quad (32)$$

with $\underline{w}_{n,t'} \sim \mathcal{CN}(0, \sigma_{\text{tr}}^2)$ for $t' < t$ and with $\underline{w}_{n,t'} \sim \mathcal{CN}(0, \sigma_c^2)$ for $t' > t$. The fading channels are obtained by extracting the first terms in (31) and (32) from the original and virtual MIMO channels (1) and (11), and then by approximating the remaining terms by CSCG random vectors with covariance $\sigma_{\text{tr}}^2 \mathbf{I}_N$ and $\sigma_c^2 \mathbf{I}_N$, respectively. We apply maximal-ratio combining (MRC) to (31) and (32),

$$\underline{z}_{\text{tr}} = \frac{1}{\sqrt{P(\tau T_c - 1)}} \sum_{t'=1}^{\tau T_c - 1} x_{m,t'}^* \underline{y}_{n,t'}, \quad (33)$$

$$\underline{z}_c = \frac{1}{\sqrt{\sigma_\theta^2 (1 - \tau) T_c}} \sum_{t'=\tau T_c + 1}^{T_c} \theta_{m,t'}^* \underline{y}_{n,t'}. \quad (34)$$

Taking the large-system limit, due to the weak law of large numbers, we obtain

$$\begin{pmatrix} \underline{z}_{\text{tr}} \\ \underline{z}_{\text{c}} \end{pmatrix} = \frac{1}{\sqrt{\beta}} \begin{pmatrix} \sqrt{\tau P} \\ \sqrt{(1-\tau)\sigma_{\theta}^2} \end{pmatrix} h_{n,m} + \begin{pmatrix} w_{\text{tr}} \\ w_{\text{c}} \end{pmatrix}, \quad (35)$$

where w_{tr} and w_{c} are mutually independent CSCG random variables with variances σ_{tr}^2 and σ_{c}^2 , respectively. The minimum mean-squared error (MMSE) estimate of $h_{n,m}$ for the channel (35) is given by [53]

$$\hat{h}_{n,m} = \frac{1}{\sqrt{\beta}\xi^2(\tau)} \left(\frac{\sqrt{\tau P}}{\sigma_{\text{tr}}^2} z_{\text{tr}} + \frac{\sqrt{(1-\tau)\sigma_{\theta}^2}}{\sigma_{\text{c}}^2} z_{\text{c}} \right). \quad (36)$$

where the mean-squared error (MSE) $\xi^2(\tau)$ for the MMSE estimate (36) is explicitly given by

$$\xi^2(\tau) = \left(1 + \frac{\tau P}{\sigma_{\text{tr}}^2 \beta} + \frac{(1-\tau)\sigma_{\theta}^2}{\sigma_{\text{c}}^2 \beta} \right)^{-1}. \quad (37)$$

It is well known that the MMSE estimate $\hat{h}_{n,m}$ and the estimation error $\Delta \underline{h}_{n,m} = h_{n,m} - \hat{h}_{n,m}$ are uncorrelated CSCG random variables with variances $(1 - \xi^2(\tau))$ and $\xi^2(\tau)$, respectively.

We next consider fading channels with spatial diversity for data estimation in the current substage $m = \mu M$ for $0 \leq \mu \leq 1$,

$$\underline{y}_{n,t} = \frac{1}{\sqrt{M}} \left\{ \hat{h}_{n,m} x_{m,t} + \Delta \underline{h}_{n,m} x_{m,t} \right\} + \underline{w}_{n,t}, \quad n = 1, \dots, N, \quad (38)$$

where $\underline{w}_{n,t} \in \mathbb{C}$ denotes a CSCG random variable with variance $\sigma^2(\tau, \mu)$. Applying the MRC to $\{\underline{y}_{n,t}\}$, we obtain

$$\underline{z} = \frac{1}{\sqrt{N(1 - \xi^2(\tau))}} \sum_{n=1}^N \hat{h}_{n,m}^* \underline{y}_{n,t}. \quad (39)$$

Taking the large-system limit gives the AWGN channel

$$\underline{z} = \sqrt{\frac{1 - \xi^2(\tau)}{\alpha}} x_{m,t} + \underline{w}, \quad (40)$$

with $\underline{w} \sim \mathcal{CN}(0, \sigma^2(\tau, \mu))$. The MMSE estimate $\hat{x}_{m,t}$ of $x_{m,t}$ for the AWGN channel (40) is given as the mean $\hat{x}_{m,t} = \int x_{m,t} p(x_{m,t} | \underline{z}, \theta_{m,t}) dx_{m,t}$ with respect to the posterior pdf

$$p(x_{m,t} | \underline{z}, \theta_{m,t}) = \frac{p(\underline{z} | x_{m,t}) p(x_{m,t} | \theta_{m,t})}{\int p(\underline{z} | x_{m,t}) p(x_{m,t} | \theta_{m,t}) x_{m,t}}, \quad (41)$$

where $p(\underline{z} | x_{m,t})$ represents the AWGN channel (40). The MSE for the MMSE estimate $\hat{x}_{m,t}$ given $\theta_{m,t}$ is defined as

$$\text{MSE}(\sigma^2, \theta_{m,t}) = \mathbb{E} [|x_{m,t} - \hat{x}_{m,t}|^2 | \theta_{m,t}]. \quad (42)$$

We have not so far specified the variances σ_{tr}^2 , σ_{c}^2 , and $\sigma^2(\tau, \mu)$. The constrained capacity of the AWGN channel (40) corresponds to the mutual information in the lower bound (19) when the three variances are determined as solutions to fixed-point equations.

Proposition 1 (Optimal Detector). *Suppose that Assumption 1, Assumption 2, and the RS assumption hold. Then, the constrained capacity (7) per transmit antenna is bounded from below by*

$$\frac{C}{M} \geq \int_{\tau \in [\tau_0, 1]} \int_{\mu \in [0, 1]} I(x_{m,t}; \underline{z} | \theta_{m,t}) d\tau d\mu, \quad (43)$$

in the large-system limit, in which the mutual information $I(x_{m,t}; \underline{z}|\theta_{m,t})$ is equal to the constrained capacity of the AWGN channel (40). In evaluating $I(x_{m,t}; \underline{z}|\theta_{m,t})$, $\{\sigma_{\text{tr}}^2, \sigma_c^2\}$ is given as the solution to the coupled fixed-point equations

$$\sigma_{\text{tr}}^2 = N_0 + P\xi^2(\tau), \quad (44)$$

$$\sigma_c^2 = N_0 + (P - \sigma_\theta^2) + \sigma_\theta^2 \xi^2(\tau), \quad (45)$$

where $\xi^2(\tau)$ is given by (37). Furthermore, $\sigma^2(\tau, \mu)$ is given as a solution σ^2 to the fixed-point equation

$$\sigma^2 = N_0 + P\xi^2(\tau) + (1 - \mu)(1 - \xi^2(\tau))\mathbb{E} [\text{MSE}(\sigma^2, \theta_{m,t})], \quad (46)$$

where $\text{MSE}(\sigma^2, \theta_{m,t})$ is given by (42). If the fixed-point equation (46) has multiple solutions, one should choose the solution minimizing the following quantity

$$(1 - \mu)I(x_{m,t}; \underline{z}|\theta_{m,t}) + \frac{1}{\alpha} \left[D_2(N_0 \|\sigma^2) + \frac{\xi^2(\tau)}{\sigma^2} \log_2 e \right]. \quad (47)$$

Derivation of Proposition 1: See Appendix A. ■

Note that the last terms in the coupled fixed-point equations (44) and (45) depend on σ_{tr}^2 and σ_c^2 through (37). Equation (46) for given $\xi^2(\tau)$ provides a fixed-point equation with respect to σ^2 . The second and last terms in the RHS of (46) correspond to contributions from channel estimation errors and inter-stream interference, respectively. The integrand in (43) depends on the variables τ and μ through the SNR $P(1 - \xi^2(\tau))/(\alpha\sigma^2(\tau, \mu))$.

The existence of multiple solutions in (46) relates to the so-called phase transition in statistical physics. See [28], [31] for an interpretation in the context of communications. Numerical evaluation of (46) for QPSK modulation implies that multiple solutions do not appear when $\alpha \leq 1$. In the high SNR regime there is no point to use transmit antennas more than receive antennas or half the coherence time. In fact, Zheng and Tse [10] proved that the full spatial multiplexing gain of the MIMO channel with no CSI is given by $\bar{M}(1 - \bar{M}/T_c)$, with $\bar{M} = \min\{M, N, \lfloor T_c/2 \rfloor\}$, which is achieved by using $\min\{N, \lfloor T_c/2 \rfloor\}$ transmit antennas out of M transmit antennas if $M > N$ or $M > \lfloor T_c/2 \rfloor$. Thus, we consider $\alpha \leq 1$ and $\beta \leq 1/2$ in the high SNR regime.

Next, the lower bound (29) based on the LMMSE detector is evaluated in the large-system limit. The following proposition is obtained in the same manner as in the derivation of Proposition 1.

Assumption 3. *The equivalent channel for the LMMSE detector is self-averaging with respect to $\tilde{\mathbf{Y}}_{\setminus t}$ and $\mathbf{x}_{[1,m],t}$ in the large-system limit.*

Proposition 2 (LMMSE Detector). *Suppose that Assumption 1, Assumption 3, and the RS assumption hold. Then, the constrained capacity (7) per transmit antenna is bounded from below by (43) in the large-system limit. In evaluating (43), $\{\sigma_{\text{tr}}^2, \sigma_c^2\}$ is given as the solution to the coupled fixed-point equations (44) and (45). On the other hand, $\sigma^2(\tau, \mu)$ is given as the unique solution σ^2 to the fixed-point equation*

$$\sigma^2 = N_0 + P\xi^2(\tau) + (1 - \mu)(1 - \xi^2(\tau))\mathbb{E} \left[\frac{(P - |\theta_{m,t}|^2)\alpha\sigma^2}{(1 - \xi^2(\tau))(P - |\theta_{m,t}|^2) + \alpha\sigma^2} \right]. \quad (48)$$

Derivation of Proposition 2: Proposition 2 is obtained by repeating the derivation of Proposition 1. Thus, we only prove the uniqueness of the solution to the fixed-point equation (48). The RHS of (48) is a concave function of σ^2 , which intersects with a straight line passing the origin with slope 1 at two points. Since the concave function passes the point $(0, N_0 + \xi^2(\tau))$, which is above the origin, one intersection must be in $\sigma^2 < 0$. Thus, the fixed-point equation (48) has the unique solution in the region $\sigma^2 > 0$. ■

The expectation in the RHS of (48) corresponds to the MSE for the LMMSE estimator of the data symbol $x_{m,t}$ transmitted through the AWGN channel (40), while (42) in the fixed-point equation (46) is the MSE for the MMSE estimator.

B. Optimization

The next goal is to optimize the lower bound (43) based on the optimal detector with respect to τ_0 , the hyperprior pdf of $\theta_{m,t}$, and the prior pdf of $x_{m,t}$. We first notice that the lower bound (43) is monotonically nonincreasing with respect to τ_0 since the integrand is non-negative and does not depend on τ_0 . Thus, the lower bound (43) is maximized as $\tau_0 \rightarrow 0$. Note that the limit $\tau_0 \rightarrow 0$ does not necessarily indicate no pilot symbols, since we have taken the limit $\tau_0 \rightarrow 0$ after the large-system limit. In other words, the effect of pilot symbols is negligible in Proposition 1 if T_{tr} is sublinear in T_c , i.e., $T_{\text{tr}} = o(T_c)$.

Next, we maximize the lower bound (43) with respect to the hyperprior pdf of $\theta_{m,t}$. For a fixed hyperprior pdf, the SNR $P(1 - \xi^2(\tau))/(\alpha\sigma^2(\tau, \mu))$ improves as the variance σ_θ^2 grows, since the increase of σ_θ^2 results in reductions of the channel estimator error $\xi^2(\tau)$ and the inter-stream interference given by the last term in the RHS of (46). However, increasing σ_θ^2 reduces the mutual information $I(x_{m,t}; \underline{z}|\theta_{m,t})$ for a fixed SNR, due to the reduction of payload. Interestingly, numerical results presented in Section V show that the lower bound (43) is maximized as $\sigma_\theta^2 \rightarrow 0$ for a fixed hyperprior pdf of $\theta_{m,t}$. This indicates that the lower bound (43) is maximized when $\theta_{m,t} = 0$ with probability one.

The arguments described above indicate that negligible pilot information, or more precisely, the limits $\tau_0, \sigma_\theta^2 \rightarrow 0$ are best in the large-system limit, while $\tau_0 = \beta$ is best in terms of the HH bound [15]. Thus, we can conclude that the SD scheme can reduce the overhead for training significantly. It is worth noting that using a capacity-achieving error-correcting code is assumed in our analysis. We conjecture that if some practical coding is used finite τ_0 or σ_θ^2 are required for getting accurate channel estimates in the initial stage. See [54] for the case of practical coding.

Finally, we optimize the lower bound (43) with respect to the prior pdf of $x_{m,t}$. This optimization problem is nonlinear since the prior pdf of $x_{m,t}$ depends on σ^2 through the last term in the RHS of the fixed-point equation (46). Instead of solving the nonlinear optimization problem exactly, we consider the biased Gaussian signaling $x_{m,t} \sim \mathcal{CN}(\theta_{m,t}, P - |\theta_{m,t}|^2)$ as a suboptimal solution. This choice of the prior pdf should be reasonable since Gaussian signaling is optimal if accurate channel estimates can be obtained. In this case, Proposition 1 reduces to the following corollary.

Corollary 1. *Suppose that Assumption 1, Assumption 2, and the RS assumption hold. If $x_{m,t} \sim \mathcal{CN}(\theta_{m,t}, P -$*

$|\theta_{m,t}|^2$), then the constrained capacity (7) per transmit antenna is bounded from below by c_g given by

$$\frac{C}{M} \geq c_g = \int_{\tau \in [\tau_0, 1]} \int_{\mu \in [0, 1]} \mathbb{E} \left[\log \left(1 + \frac{(1 - \xi^2(\tau))(P - |\theta_{m,t}|^2)}{\alpha \sigma^2(\tau, \mu)} \right) \right] d\tau d\mu, \quad (49)$$

in the large-system limit. In evaluating the integrand in (49), $\xi^2(\tau)$ is given by (37), defined via (44) and (45). Furthermore, $\sigma^2(\tau, \mu)$ is given as the unique solution σ^2 to the fixed-point equation (48).

Proof of Corollary 1: It is straightforward to confirm that the lower bound (43) and the fixed-point equation (46) reduce to (49) and (48) under the biased Gaussian signaling, respectively. ■

We believe that the biased Gaussian signaling maximizes the quantity (47), following the argument in [55]. If $\xi^2(\tau) = 0$ and $\sigma^2 = N_0$ were satisfied for all τ and μ , the biased Gaussian signaling would maximize the lower bound (43). However, $\xi^2(\tau)$ is bounded from below by a positive value for $\tau < \beta$. This implies the suboptimality of the i.i.d. Gaussian signaling.

Proposition 2 and Corollary 1 imply that the large-system performance of the LMMSE detector coincides with that of the optimal detector when the i.i.d. Gaussian signaling is used. Note that this observation is not necessarily trivial, since we have made the Gaussian approximation of the third term on the RHS of (22) in the derivation of the LMMSE detector. Our results imply that, for the i.i.d. Gaussian signaling, the performance loss due to the Gaussian approximation vanishes in the large-system limit.

C. High SNR Regime

In the high SNR limit $N_0 \rightarrow 0$, the lower bound (49) is shown to achieve the full spatial multiplexing gain when $T_{\text{tr}} \leq M$.

Proposition 3. *Suppose that Assumption 1, Assumption 2, and the RS assumption hold. For $\alpha \leq 1$ and $\tau_0 \leq \beta \leq 1/2$, the lower bound (49) with the biased Gaussian signaling $x_{m,t} \sim \mathcal{CN}(\theta_{m,t}, P - |\theta_{m,t}|^2)$ achieves the full spatial multiplexing gain in the high SNR limit $N_0 \rightarrow 0$, i.e.,*

$$\liminf_{N_0 \rightarrow 0} \frac{c_g}{\log(P/N_0)} = 1 - \beta. \quad (50)$$

Proof of Proposition 3: We first prove that the solution σ_{tr}^2 to the coupled fixed-point equations (44) and (45) converges to zero in the high SNR limit for $\tau > \beta$. The proof is by contradiction. Suppose that σ_{tr}^2 is strictly positive in the high SNR limit. Dividing both sides of (44) by σ_{tr}^2 and taking the high SNR limit, we have

$$1 = \frac{\beta P \sigma_c^2}{\beta \sigma_{\text{tr}}^2 \sigma_c^2 + \tau P \sigma_c^2 + (1 - \tau) \sigma_\theta^2 \sigma_{\text{tr}}^2}. \quad (51)$$

Rearranging (51), we obtain

$$\sigma_{\text{tr}}^2 = -\frac{(\tau - \beta) P \sigma_c^2}{\beta \sigma_c^2 + (1 - \tau) \sigma_\theta^2}. \quad (52)$$

However, the RHS of (52) is negative, due to $\tau > \beta$, which is a contradiction. Thus, the solution σ_{tr}^2 must converge to zero in the high SNR limit for $\tau > \beta$. This result implies that the MSE (37) also converges to zero in the high SNR limit for $\tau > \beta$.

It is straightforward to show in a similar manner that the solution σ^2 to the fixed-point equation (48) is $O(N_0)$ in the high SNR limit for $\alpha \leq 1$ when the MSE (37) converges to zero. Thus, we have

$$\liminf_{N_0 \rightarrow 0} \frac{c_g}{\log(P/N_0)} = 1 - \beta, \quad (53)$$

which is equal to the full spatial multiplexing gain for $\alpha \leq 1$ and $\beta \leq 1/2$. ■

The proof of Proposition 3 indicates that in the first M stages the performance of the SD receiver is limited by channel estimation errors, rather than inter-stream interference in MUD. This phenomenon is robust in the sense that it occurs regardless of the prior of data symbols.

D. Low SNR Regime

The power per information bit E_b required for reliable communication is a key performance measure in the low SNR regime. Verdú [12] proved that the capacity C_{opt} of the MIMO channel (1) with no CSI is given by $C_{\text{opt}} = NP/(N_0 \ln 2) + o(N_0)$ in the low SNR limit $N_0 \rightarrow \infty$, or $NE_b/N_0 \geq \lim_{N_0 \rightarrow \infty} NP/(N_0 C_{\text{opt}}) = \ln 2 \approx -1.59$ dB. Since using multiple transmit antennas wastes valuable power in the low SNR regime, the number of transmit antennas used should be reduced as N_0 increases. One option is to increase M^{-1} and N_0 at the same rate. Thus, we consider the limit, in which $\alpha, \beta \rightarrow 0$ and $N_0 \rightarrow \infty$ while β/α and $s = P/(\beta N_0)$ are kept constant. The following proposition provides an upper bound on the normalized SNR $NE_b/N_0 = NP/(N_0 C)$ required for the optimal SD receiver, with C denoting the achievable rate (8) of the optimal SD receiver.

Proposition 4. *Suppose that the optimal SD receiver achieves a rate R/M . Then, the normalized SNR NE_b/N_0 is bounded from above by*

$$N \frac{E_b}{N_0} \leq \frac{\beta s}{\alpha R} + o(N_0), \quad (54)$$

in the limit where $\alpha, \beta \rightarrow 0$ and $N_0 \rightarrow \infty$ while β/α and $s = P/(\beta N_0)$ are kept constant. In (54), s is implicitly given by

$$R = \left[1 + \left(s + \frac{\beta}{\alpha} s^2 \right)^{-1} \right] \log \left(1 + s + \frac{\beta}{\alpha} s^2 \right) - \left(1 + \frac{1}{s} \right) \log(1 + s). \quad (55)$$

Proof of Proposition 4: Using the lower bound (49) for Gaussian signaling, we obtain an upper bound $NE_b/N_0 \leq NP/(MN_0 c_g) = \beta s/(\alpha c_g)$. Thus, it is sufficient to prove that the maximum of c_g with respect to τ_0 and σ_θ^2 is given by the RHS of (55).

We evaluate the solutions to the fixed-point equations (44), (45), and (48). It is straightforward to find that σ_{tr}^2/N_0 , σ_c^2/N_0 , and σ^2/N_0 tend to 1 as $N_0 \rightarrow \infty$, since (37) and (42) are bounded. This observation implies

$$c_g \leq \int_{\tau_0}^1 \log \left[1 + \frac{\beta s}{\alpha} \left(1 - \frac{\sigma_\theta^2}{P} \right) \frac{\tau + (1 - \tau)\sigma_\theta^2/P}{s^{-1} + \tau + (1 - \tau)\sigma_\theta^2/P} \right] d\tau + o(N_0), \quad (56)$$

in the limit described in Proposition 4. In the derivation of (56), we have used Jensen's inequality. The equality holds only when $|\theta_{m,t}|^2$ takes σ_θ^2 with probability one. It is easy to confirm that the integrand in (56) is monotonically decreasing with respect to σ_θ^2 . Thus, the maximum of c_g is achieved at $\tau_0 = 0$ and $\sigma_\theta^2 = 0$, and given by

$$\max_{\tau_0, \sigma_\theta^2 \geq 0} c_g = \int_0^1 \log \left[1 + \frac{\beta}{\alpha} \frac{s^2 \tau}{1 + s\tau} \right] d\tau + o(N_0). \quad (57)$$

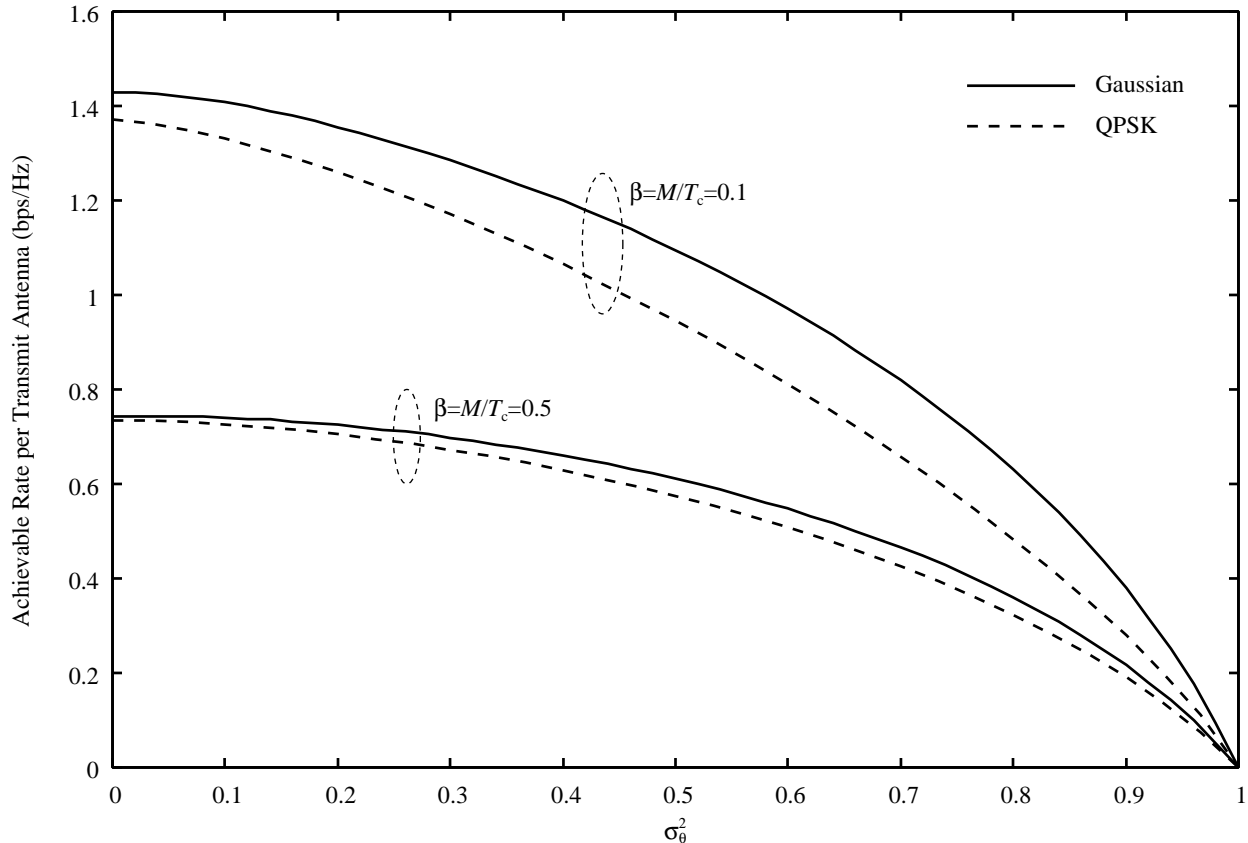


Fig. 2. Achievable rate versus the variance of the bias σ_θ^2 for the SNR $P/N_0 = 6$ dB, $\alpha = M/N = 1$, and $\tau_0 = T_{tr}/T_c = 0$.

Calculating the integration in (57), we find that the first term in the RHS of (57) is equal to the RHS of (55). ■

In the proof of Proposition 4, we have proved that the lower bound (49) is maximized at $\tau_0 = 0$ and $\sigma_\theta^2 = 0$ in the low SNR regime. This result implies that negligible pilot information is best in terms of the lower bound (49) in the low SNR regime.

It is interesting to note that the achievable rate (55) is approximated by $R = \beta s^2 / (2\alpha \ln 2) + O(s^3)$ as $s \rightarrow 0$, which implies that $NE_b/N_0 \leq \sqrt{2\beta \ln 2 / \alpha R} + o(N_0, R)$ in the low rate regime, i.e., the upper bound (54) diverges in $R \rightarrow 0$. In other words, the minimum of the upper bound (54) is achieved at a strictly positive rate, as shown in Section V. We remark that a similar result was reported in [56].

The reason why the minimum is achieved at a positive rate is because we have spread power over all time slots. It is well known that on-off keying is optimal in the low SNR regime, in other words, that spreading power over all time slots results in a waste of valuable power. If on-off keying was used, the normalized SNR required would reduce monotonically as the achievable rate decreases, as shown in [56]. However, on-off keying requires high peak-to-average power ratio (PAPR), which is unfavorable in practice. Thus, the minimum of the upper bound (54) may be interpreted as a practical performance bound in terms of energy efficiency.

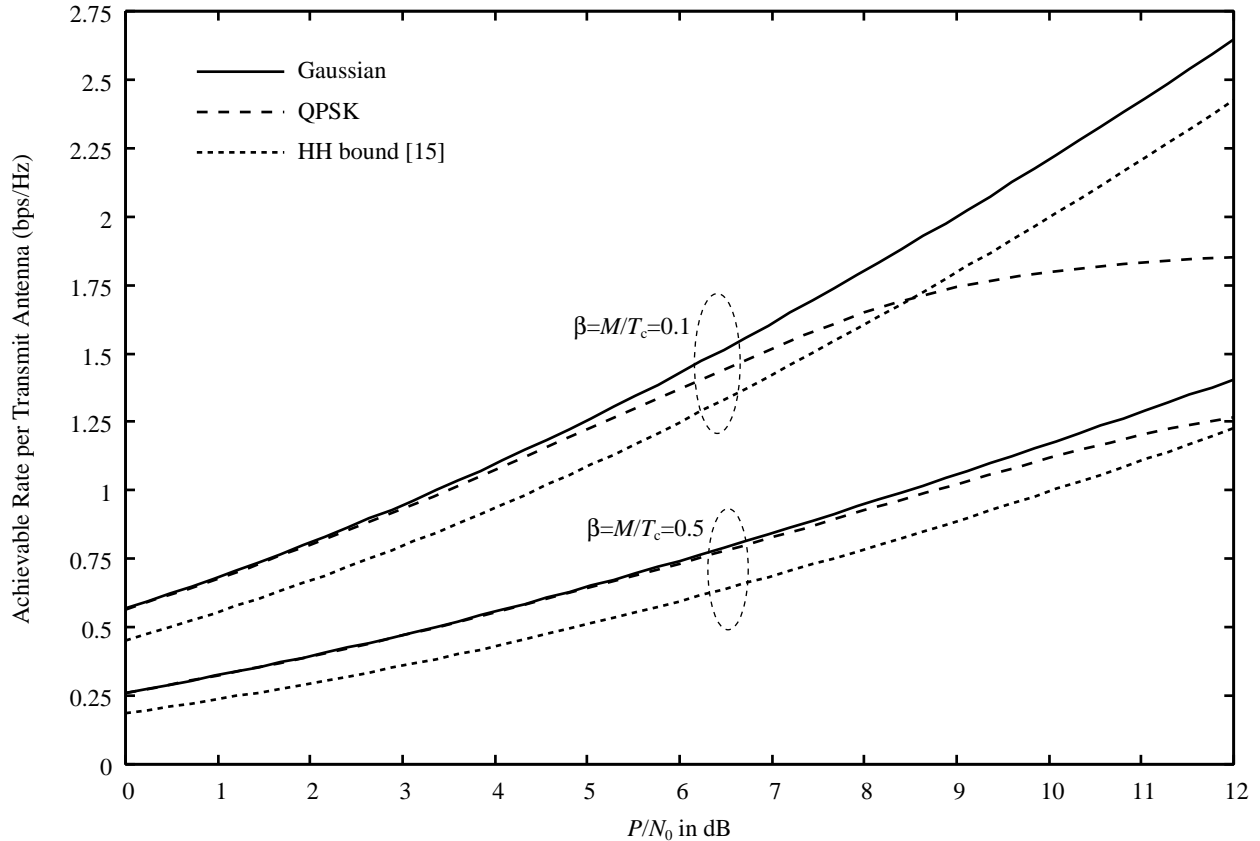


Fig. 3. Achievable rate versus SNR in the moderate SNR regime for the variance of the bias $\sigma_\theta^2 = 0$, $\alpha = M/N = 1$, and $\tau_0 = T_{tr}/T_c = 0$.

V. NUMERICAL RESULTS

A. Large Systems

The lower bound (49) for the biased Gaussian signaling is compared to two existing bounds in this section. One is the HH bound [15], which corresponds to the achievable rate of receivers based on one-shot channel estimation, in which the decoded data symbols are not re-utilized for refining the channel estimates. The other one is the high-SNR approximation of the capacity [10], which includes a deviation of $o(1)$ from the capacity at high SNR. In all numerical results, we chose $\tau_0 = 0$ since the lower bound (49) is maximized at $\tau_0 = 0$. In order to investigate the optimal choice of σ_θ^2 , we display the lower bound (49) for the biased Gaussian signaling with respect to σ_θ^2 in Fig. 2. The lower bound (43) for the biased QPSK signaling is also shown in the same figure. We have used $p(\theta) = [\delta(\theta - \sigma_\theta) + \delta(\theta + \sigma_\theta)]/2$ as the distribution of $\theta_{m,t}$, i.e., $\theta_{m,t}$ takes $\pm\sigma_\theta$ with equal probability. We find that the lower bound for the biased Gaussian signaling is larger than that for the biased QPSK signaling for all σ_θ^2 . Furthermore, both lower bounds are monotonically decreasing as σ_θ^2 grows. The latter observation implies that the lower bounds are maximized at $\sigma_\theta^2 = 0$, in other words, negligible pilot information is best in terms of the lower bounds. Hereinafter, we consider the unbiased case $\sigma_\theta^2 = 0$.

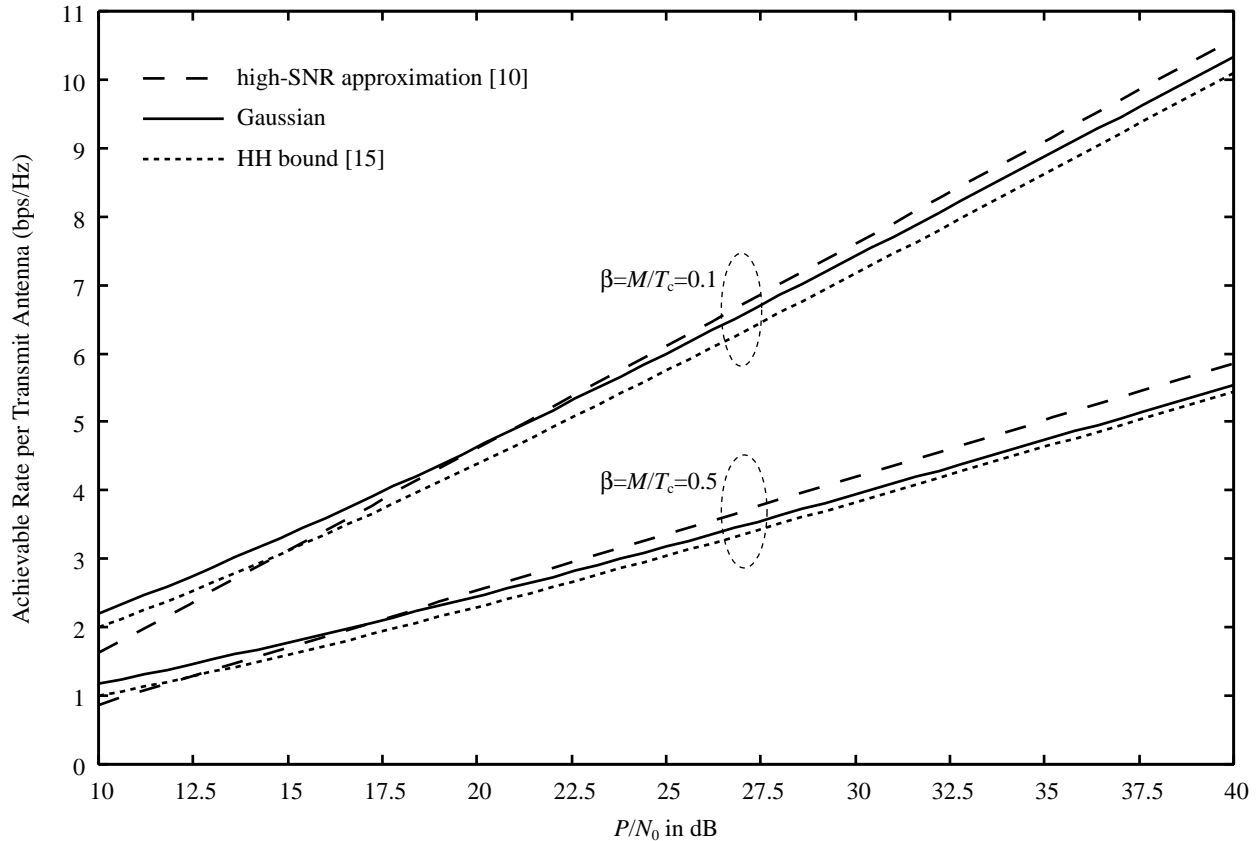


Fig. 4. Achievable rate versus SNR in the high SNR regime for the variance of the bias $\sigma_b^2 = 0$, $\alpha = M/N = 1$, and $\tau_0 = T_{tr}/T_c = 0$.

Figure 3 provides a comparison between the lower bound (49) for unbiased Gaussian signaling and the HH bound in the moderate SNR regime. The lower bound (43) for QPSK modulation is also displayed. The HH bound is a lower bound on the capacity for finite-sized systems [15, Theorem 3]. We have used a large-system formula of the HH bound, which is easily derived in the same manner as in [25]. There is a significant gap of 1 dB to 1.8 dB between the lower bound for unbiased Gaussian signaling and the HH bound for all SNRs. Moreover, the HH bound is inferior even to the lower bound for QPSK modulation in the case of short coherence time ($\beta = 0.5$). These observations imply that SD receivers can provide a substantial performance gain in the moderate SNR regime, compared to receivers based on one-shot channel estimation, since they can reduce overhead for training significantly.

Next, we compare the lower bound for unbiased Gaussian signaling with the high-SNR approximation of the capacity [10, Corollary 11] in the high-SNR regime in Fig. 4. The HH bound is also displayed in the same figure. Note that in the high-SNR approximation the large-system limit is taken after the high SNR limit. Thus, the comparison makes sense under the assumption that the large-system limit and the high SNR limit commute for the high-SNR approximation. We find that the high-SNR approximation is smaller than the lower bound for unbiased

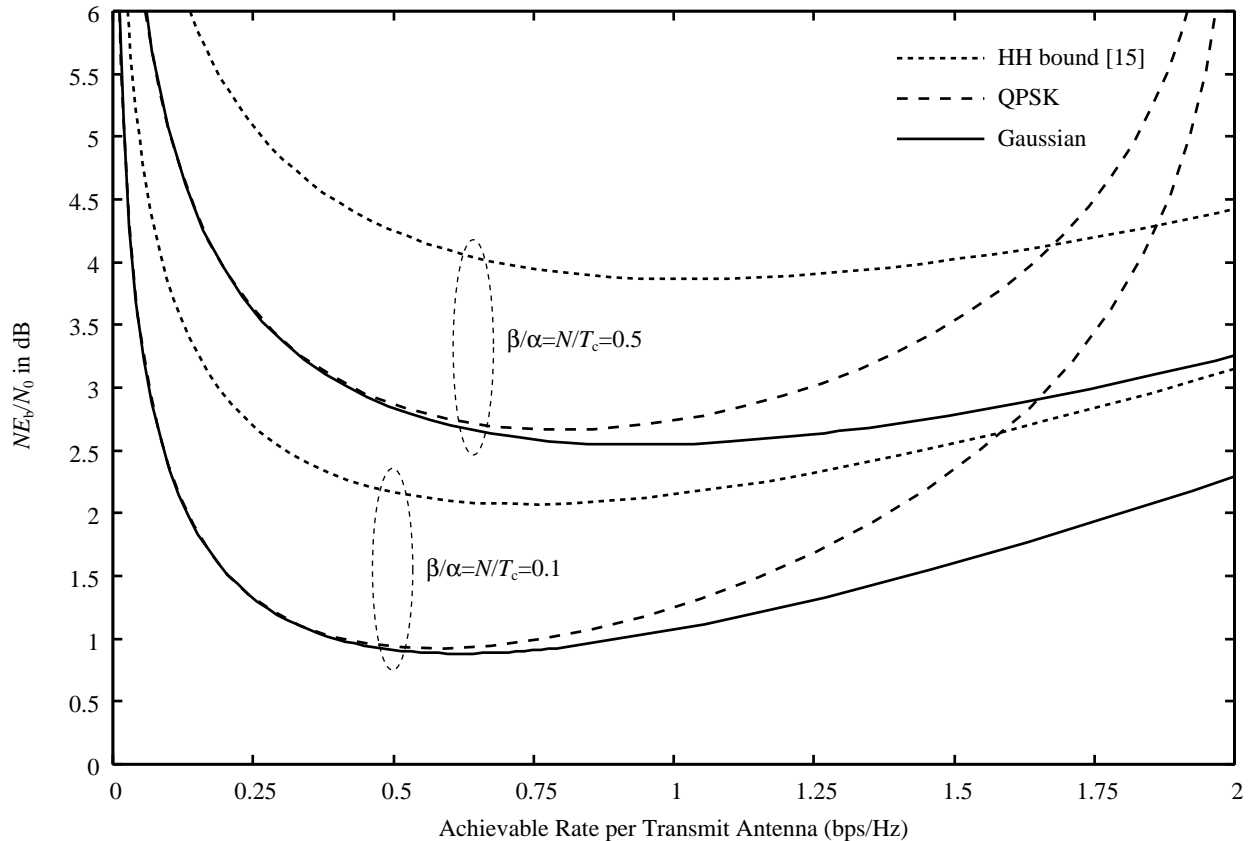


Fig. 5. Normalized SNR versus achievable rate in the low SNR regime for the variance of the bias $\sigma_\theta^2 = 0$ and $\tau_0 = T_{tr}/T_c = 0$.

Gaussian signaling in the SNR region of below 17.5 dB for $\beta = 0.5$ or below 20 dB for $\beta = 0.1$. This implies that the high-SNR approximation derived by Zheng and Tse [10] is valid only for quite high SNR. The lower bound for unbiased Gaussian signaling is close to the HH bound, rather than the high-SNR approximation, in the quite high SNR regime, which indicates the suboptimality of Gaussian signaling in the quite high SNR regime.

Finally, we consider the low SNR regime and take the limit described in Proposition 4, in which the power per information bit E_b required for reliable communication is a key performance measure. Figure 5 displays the upper bound (54) of NE_b/N_0 required for the SD receiver with unbiased Gaussian signaling as a function of the achievable rate per transmit antenna. The normalized SNRs NE_b/N_0 are also plotted for the SD receiver with QPSK modulation and for the HH bound. We find that NE_b/N_0 has a minimum at a positive achievable rate. This observation is due to the suboptimality of i.i.d. Gaussian signaling. If perfect CSI was available at the receiver, the normalized SNR NE_b/N_0 would be monotonically decreasing with the reduction of the achievable rate [12], since i.i.d. Gaussian signaling is optimal in that case. For the case of no CSI, however, the normalized SNR NE_b/N_0 diverges as the achievable rate tends to zero, since i.i.d. signaling wastes valuable power in the low SNR regime, as discussed in Section IV-D. Another observation is that there is a large gap of 1 dB to 1.5 dB between the

minimal normalized SNRs for the SD receivers and the HH bound, while all bounds are far from the ultimate limit $NE_b/N_0 \approx -1.59$ dB. This result implies that the SD scheme can significantly improve the HH bound in the low SNR regime.

B. Finite-Sized Systems

We have so far considered the large-system performance. In order to confirm the usefulness of the large-system analysis in practice, numerical simulations are presented for finite-sized systems with no CSI. Since the optimal detector has high complexity, only the performance of the LMMSE detector is investigated. Unbiased QPSK and unbiased Gaussian signaling are considered. Note that, for the unbiased case, the performance of the LMMSE channel estimator depends on stage t , rather than the coherence time T_c . Figure 6 shows the normalized MSE for the LMMSE estimate (27) of the data symbols in substage m within stage t for the SD receiver. For comparison, we plot the large-system results based on Proposition 2 with $\alpha = M/N$, $\beta/\tau = M/(t-1)$, and $\mu = (m-1)/M$. The normalized MSE is given by the expectation in the RHS of (48) divided by P in the large-system limit. A correction of minus one for the stage index t is because the performance in stage t is approximated by that in stage $t+1$ in the large-system limit. See (33)–(35). A correction for the substage index is also due to the same reason. We find that the large-system results are in good agreement with those for not so large systems.

VI. CONCLUSIONS

We have investigated the achievable rates of SD receivers for the Rayleigh block-fading MIMO channel with no CSI. Analytical formulas for the achievable rates have been derived in the large-system limit, by using the replica method. It has been shown that negligible pilot information is best in terms of the information-theoretical achievable rates. From a theoretical point of view, the formulas provide the best lower bound on the capacity among existing *analytical* lower bounds that can be easily evaluated for all SNRs, while it is far from the true capacity in the low or quite high SNR regimes. From a practical point of view, the analytical lower bounds derived in this paper can be regarded as a fundamental performance limit for practical training-based systems with QPSK or multilevel modulation. We conclude that the SD receiver can reduce overhead for training significantly. Thus, it provides a substantial performance gain, compared to receivers based on one-shot channel estimation, especially in the low-to-moderate SNR regime.

One important future work is to investigate spatially correlated MIMO channels with no CSI. On the one hand, spatial correlations cause a reduction of diversity. On the other hand, they make it possible to estimate the channel matrix more accurately than without correlations, since one can utilize the knowledge about the correlations for channel estimation. Thus, it should be worth investigating impacts of these two effects onto the performance for training-based systems. It does not seem to be straightforward to extend the results presented in this paper to the case of spatially correlated MIMO channels.

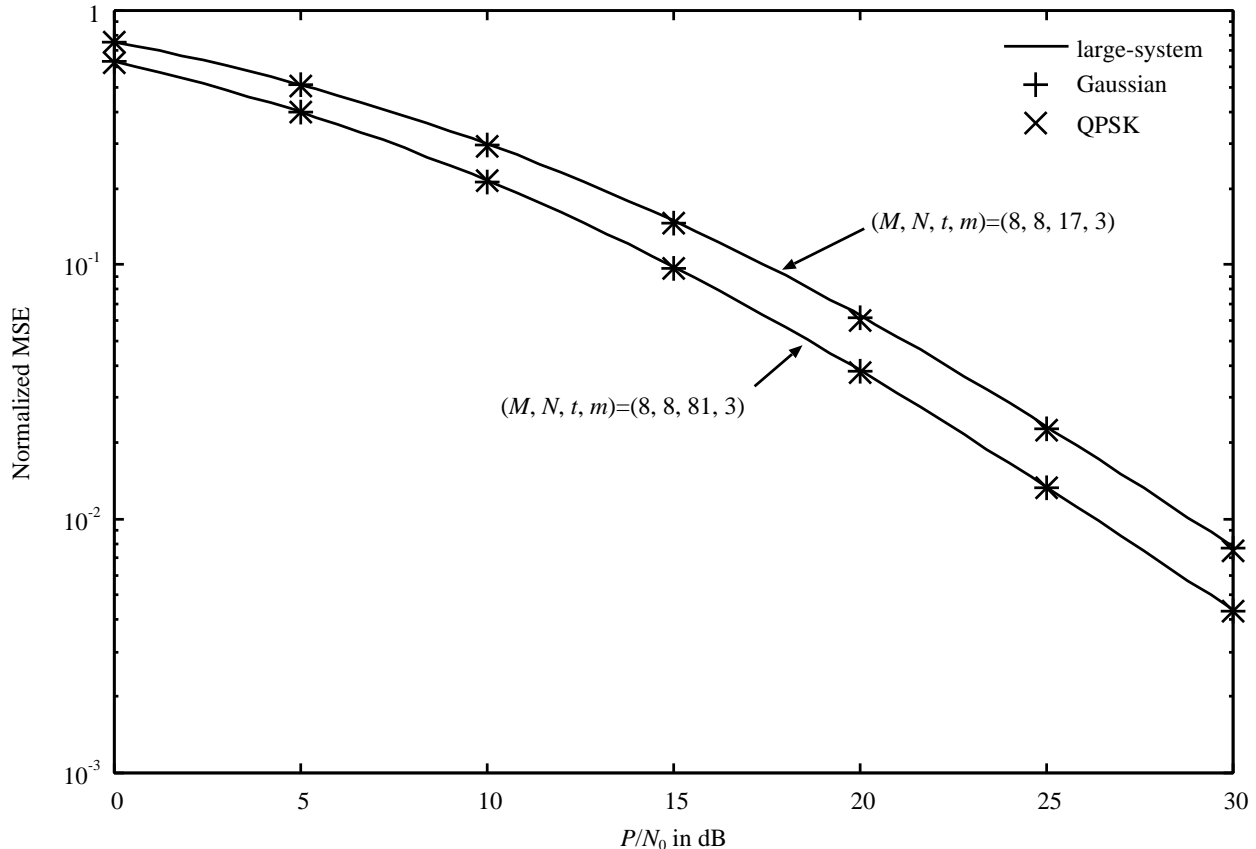


Fig. 6. Normalized MSE for the LMMSE detector versus SNR in substage m within stage t for the SD receiver. $m = 3$, $t = 17, 81$, $M = 8$ transmit antennas, $N = 8$ receive antennas, and the variance of the bias $\sigma_\theta^2 = 0$.

APPENDIX A

DERIVATION OF PROPOSITION 1

A. Sketch

Let us consider substage $m = \mu M$ within stage $t = \tau T_c$ in the SD receiver for $0 \leq \tau \leq 1$ and $0 \leq \mu \leq 1$. For some $\tilde{m} \in \mathbb{N}$, we decompose the lower bound (19) into two terms,

$$\frac{C}{M} \geq \frac{1}{T_c M} \sum_{t=T_{\text{tr}}+1}^{T_c} \left[\sum_{m=1}^{\tilde{m}} I(x_{m,t}; \tilde{x}_{m,t} | \tilde{\mathcal{L}}_t, \mathbf{x}_{[1,m],t}, \boldsymbol{\theta}_{[m,M],t}) + \sum_{m=\tilde{m}+1}^M I(x_{m,t}; \tilde{x}_{m,t} | \tilde{\mathcal{L}}_t, \mathbf{x}_{[1,m],t}, \boldsymbol{\theta}_{[m,M],t}) \right], \quad (58)$$

and then take the limit in which M , N , T_c , T_{tr} , t , m , and \tilde{m} tend to infinity while their ratios $\alpha = M/N$, $\beta = M/T_c$, $\tau_0 = T_{\text{tr}}/T_c$, $\tau = t/T_c$, $\mu = m/M$, and $\mu_0 = \tilde{m}/M$ are kept constant. The second term consists of the mutual information for the decoding problem after an extensive number of users have been decoded, while the first term contains the mutual information for the problem after a finite number of users have been decoded. We will show below that $I(x_{m,t}; \tilde{x}_{m,t} | \tilde{\mathcal{L}}_t, \mathbf{x}_{[1,m],t}, \boldsymbol{\theta}_{[m,M],t})$ for $\mu \geq \mu_0$ converges to the integrand in (43) in the

large-system limit. The definition of the Riemann integral implies that the sum $(T_c M^{-1}) \sum_{t=T_{\text{tr}}+1}^{T_c} \sum_{m=\tilde{m}+1}^M$ in the second term of (58) tends to $\int_{\tau_0}^1 d\tau \int_{\mu_0}^1 d\mu$. Taking the limit $\mu_0 \rightarrow 0$, we arrive at Proposition 1, since the first term of (58) tends to zero as $\mu_0 \rightarrow 0$.

The evaluation of $I(x_{m,t}; \tilde{x}_{m,t} | \tilde{\mathcal{L}}_t, \mathbf{x}_{[1,m],t}, \boldsymbol{\theta}_{[m,M],t})$ consists of two parts: analysis of the error covariance matrix (16) and analysis of the equivalent channel (20). We apply the replica method to both analyses.

B. Analysis of Channel Estimator

We evaluate the error covariance matrix (16) for the LMMSE channel estimation in the large-system limit. Since the joint posterior pdf $p(\mathbf{H} | \tilde{\mathcal{L}}_t)$ is decomposed into $\prod_{n=1}^N p(\vec{\mathbf{h}}_n | \tilde{\mathcal{L}}_t)$, without loss of generality, we focus on the estimation problem for the first row of \mathbf{H} , denoted by $\vec{\mathbf{h}}_1$. The first row vector $\vec{\mathbf{y}}_{\setminus t,1} \in \mathbb{C}^{1 \times (T_c - 1)}$ of (13) is given by

$$\vec{\mathbf{y}}_{\setminus t,1} = \frac{1}{\sqrt{M}} \vec{\mathbf{h}}_1 \bar{\mathbf{X}}_{\setminus t} + (\vec{\mathbf{0}}, \vec{\mathbf{w}}_{(t,T_c),1}) + \vec{\mathbf{n}}_{\setminus t,1}, \quad (59)$$

where $\vec{\mathbf{w}}_{(t,T_c),1} \in \mathbb{C}^{1 \times (T_c - t)}$ and $\vec{\mathbf{n}}_{\setminus t,1} \in \mathbb{C}^{1 \times (T_c - 1)}$ denote the first row vectors of the matrices $\mathbf{W}_{(t,T_c]}$ and $\mathbf{N}_{\setminus t}$, respectively.

The channel (59) can be regarded as a MIMO channel with the channel matrix $\bar{\mathbf{X}}_{\setminus t}$ known to the receiver. The main difference between $\bar{\mathbf{X}}_{\setminus t}$ and zero-mean channel matrices considered in previous works [24]–[26], [28], [30], [31] is that $\bar{\mathbf{X}}_{\setminus t}$ has the nonzero mean $\hat{\mathbf{X}}_{\setminus t} = (\mathbf{O}, \boldsymbol{\Theta}_{(T_{\text{tr}},t)}, \boldsymbol{\Theta}_{(t,T_c]}) \in \mathbb{C}^{M \times (T_c - 1)}$ conditioned on $\boldsymbol{\Theta}$. Let us decompose the channel matrix $\bar{\mathbf{X}}_{\setminus t}$ into the mean $\hat{\mathbf{X}}_{\setminus t}$ and the difference $\bar{\mathbf{X}}_{\setminus t} - \hat{\mathbf{X}}_{\setminus t}$. The problem would reduce to the zero-mean case if the two matrices were independent of each other, since the sum of two independent matrices with i.i.d. zero-mean entries is also a matrix with i.i.d. zero-mean entries. However, the two matrices are not independent while they are uncorrelated zero-mean matrices. Thus, we have to treat the influence of higher-order correlations carefully.

The following proposition implies that the large-system results for each element of the error covariance matrix (16) coincide with those for the case as if the two matrices $\hat{\mathbf{X}}_{\setminus t}$ and $\bar{\mathbf{X}}_{\setminus t} - \hat{\mathbf{X}}_{\setminus t}$ were mutually independent. In other words, higher-order correlations between the two matrices do not affect the results for each element of the error covariance matrix (16) in the large-system limit. Note that we do not claim the norm convergence $\|\boldsymbol{\Xi}_t - \xi^2(\tau) \mathbf{I}_M\| \rightarrow 0$.

Proposition 5. *Suppose that Assumption 1 and the RS assumption hold. Then, each diagonal element of the error covariance matrix (16) converges in probability to (37), defined by (44) and (45), in the large-system limit. Furthermore, each off-diagonal element of the error covariance matrix (16) converges in probability to zero in the large-system limit.*

Proof: See Appendix B. ■

Proposition 5 was rigorously proved without Assumption 1 for the unbiased case $\theta_{m,t} = 0$ in [26]. Since we cannot claim the norm convergence $\|\boldsymbol{\Xi}_t - \xi^2(\tau) \mathbf{I}_M\| \rightarrow 0$, a careful treatment of $\boldsymbol{\Xi}_t$ is required in the analysis of the equivalent channel (20).

We remark that the convergence of each off-diagonal element to zero results from the fact that the MMSE estimate $\hat{\mathbf{h}}_1$ of $\vec{\mathbf{h}}_1$ and its error $\vec{\mathbf{h}}_1 - \hat{\mathbf{h}}_1$ are uncorrelated with each other. In fact, we can show a stronger result for the off-diagonal elements without the replica method.

Lemma 1. *Suppose that Assumption 1 holds. For a constant $A \geq 0$, each off-diagonal element $(\Xi_t)_{\tilde{m}, \tilde{m}'}$ ($\tilde{m} \neq \tilde{m}'$) of (16) satisfies*

$$\limsup_{M \rightarrow \infty} M^{3/4} |(\Xi_t)_{\tilde{m}, \tilde{m}'}| = A \quad \text{in probability,} \quad (60)$$

where the limit denotes the large-system limit.

Proof: We use the fact that the covariance matrices Ξ_t and $\mathbf{I} - \Xi_t$ for $\vec{\mathbf{h}}_1 - \hat{\mathbf{h}}_1$ and $\hat{\mathbf{h}}_1$ are positive definite. Let $\{\lambda_{\tilde{m}} > 0 : \tilde{m} = 1, \dots, M\}$ denote the eigenvalues of Ξ_t . The positive definiteness of $\mathbf{I} - \Xi_t$ implies $1 - \lambda_{\tilde{m}} > 0$ for all \tilde{m} , or, $0 < \lambda_{\tilde{m}} < 1$ for all \tilde{m} . This observation implies that $\mathbf{I}_M - \Xi_t^k$ is also positive definite for any $k \in \mathbb{N}$, or

$$\limsup_{M \rightarrow \infty} \frac{1}{M} \text{Tr}(\Xi_t^k) < 1 \quad (61)$$

in the large-system limit. Note that Assumption 1 implies that the left-hand side (LHS) of (61) tends to the expected one $M^{-1} \text{Tr}(\mathbb{E}[\Xi_t^k])$.

In order to prove Lemma 1, we evaluate $\text{Tr}(\mathbb{E}[\Xi_t^4])$. Let ρ_t denote the elements of $\mathbb{E}[\Xi_t]$ in the strictly upper triangular part. A direct calculation implies that the the leading term of $\text{Tr}(\mathbb{E}[\Xi_t^4])$ is given by $|\rho_t|^2 M^4 (2|\rho_t|^2 - \Re[\rho_t^2])/3$ as $M \rightarrow \infty$. Applying this result and $\Re[\rho_t^2] \leq |\rho_t|^2$ to (61), we have

$$\limsup_{M \rightarrow \infty} M^3 |\rho_t|^4 < 3, \quad (62)$$

which implies that Lemma 1 holds. ■

Lemma 1 implies $(\Xi_t)_{\tilde{m}, \tilde{m}'} = O(M^{-3/4})$ in the large-system limit. We believe that it is possible to prove $(\Xi_t)_{\tilde{m}, \tilde{m}'} = O(M^{-1})$ by calculating $\text{Tr}(\mathbb{E}[\Xi_t^k])$ and taking $k \rightarrow \infty$ after the large-system limit. However, Lemma 1 is sufficient for deriving Proposition 1.

C. Analysis of Detector

We focus on substage m within stage t and analyze the equivalent channel (20) in the large-system limit. It is shown that the equivalent channel reduces to a MIMO channel with perfect CSI at the receiver in the large-system limit. Let $\Xi_t^{(c)} \in \mathbb{C}^{(M-m+1) \times (M-m+1)}$ denote the posterior covariance matrix of $(h_{1,m}, \dots, h_{1,M})^T \in \mathbb{C}^{M-m+1}$ given $\tilde{\mathcal{L}}_t$, i.e., the bottom-right block of the error covariance matrix (16),

$$\Xi_t = \begin{pmatrix} * & * \\ * & \Xi_t^{(c)} \end{pmatrix}. \quad (63)$$

The equivalent MIMO channel with perfect CSI at the receiver is defined as

$$\underline{\mathbf{z}} = \alpha^{-1/2} \sqrt{\mathbf{I} - \Xi_t^{(c)}} \mathbf{x}_{[m,M],t} + \underline{\mathbf{w}}, \quad (64)$$

with $\underline{\mathbf{w}} \sim \mathcal{CN}(\mathbf{0}, \sigma^2 \mathbf{I}_{M-m+1})$. In (64), the matrix $\sqrt{\mathbf{I} - \Xi_t^{(c)}}$ denotes a squared root of $\mathbf{I} - \Xi_t^{(c)}$, i.e., $\mathbf{I} - \Xi_t^{(c)} = \sqrt{\mathbf{I} - \Xi_t^{(c)}}^H \sqrt{\mathbf{I} - \Xi_t^{(c)}}$.

The equivalent channel between $x_{m,t}$ and the associated decoder for the MIMO channel (64) with perfect CSI at the receiver is given by

$$\begin{aligned} & p(\tilde{x}_{m,t} | x_{m,t}, \Xi_t^{(c)}, \boldsymbol{\theta}_{[m,M],t}) \\ &= \int p(x_{m,t} = \tilde{x}_{m,t} | \underline{\mathbf{z}}, \Xi_t^{(c)}, \boldsymbol{\theta}_{[m,M],t}) p(\underline{\mathbf{z}} | \Xi_t^{(c)}, \mathbf{x}_{[m,M],t}) p(\mathbf{x}_{[m,M],t} | \boldsymbol{\theta}_{[m,M],t}) d\underline{\mathbf{z}}, \end{aligned} \quad (65)$$

where $p(x_{m,t} | \underline{\mathbf{z}}, \Xi_t^{(c)}, \boldsymbol{\theta}_{[m,M],t})$ represents the pdf of $x_{m,t}$ conditioned on $\underline{\mathbf{z}}$, $\Xi_t^{(c)}$, and $\boldsymbol{\theta}_{[m,M],t}$.

Proposition 6. *Suppose that Assumption 2 and the RS assumption hold. Then, the equivalent channel (20) converges in law to the equivalent channel (65) for the MIMO channel (64) with perfect CSI at the receiver in the large-system limit. In evaluating (65), the variance σ^2 of $\underline{\mathbf{w}}$ is given as the solution to the fixed-point equation,*

$$\sigma^2 = N_0 + \lim_{M \rightarrow \infty} \frac{P}{M} \text{Tr}(\Xi_t) + V(\sigma^2), \quad (66)$$

with

$$V(\sigma^2) = \lim_{M \rightarrow \infty} \frac{1}{M} \mathbb{E} \left[(\mathbf{x}_{[m,M],t} - \langle \mathbf{x}_{[m,M],t} \rangle)^H (\mathbf{I} - \Xi_t^{(c)}) (\mathbf{x}_{[m,M],t} - \langle \mathbf{x}_{[m,M],t} \rangle) \middle| \Xi_t^{(c)}, \boldsymbol{\theta}_{[m,M],t} \right], \quad (67)$$

where $\langle \mathbf{x}_{[m,M],t} \rangle$ denotes the mean of $\mathbf{x}_{[m,M],t}$ with respect to the posterior pdf $p(\mathbf{x}_{[m,M],t} | \underline{\mathbf{z}}, \Xi_t^{(c)}, \boldsymbol{\theta}_{[m,M],t})$. If there are multiple solutions, one should choose the solution σ^2 minimizing the following quantity

$$\lim_{M \rightarrow \infty} \frac{1}{M} I(\mathbf{x}_{[m,M],t}; \underline{\mathbf{z}}) + \frac{1}{\alpha} \left[D_2(N_0 | \sigma^2) + \lim_{M \rightarrow \infty} \frac{\log_2 e}{\sigma^2 M} \text{Tr}(\Xi_t) \right], \quad (68)$$

where $I(\mathbf{x}_{[m,M],t}; \underline{\mathbf{z}})$ denotes the mutual information between $\mathbf{x}_{[m,M],t}$ and $\underline{\mathbf{z}}$ given realizations of Ξ_t and $\boldsymbol{\theta}_{[m,M],t}$.

Proof: See Appendix C. ■

We have implicitly assumed that the equivalent channel (65) and the last two terms in (66) converge as $M \rightarrow \infty$. This assumption is justified below by using Proposition 5 and Lemma 1.

Proposition 6 implies that the mutual information $I(x_{m,t}; \tilde{x}_{m,t} | \tilde{\mathcal{I}}_t, \mathbf{x}_{[1,m],t}, \boldsymbol{\theta}_{[m,M],t})$ tends to the constrained capacity $I(x_{m,t}; \tilde{x}_{m,t} | \Xi_t^{(c)}, \boldsymbol{\theta}_{[m,M],t})$ of the MIMO channel (64) with perfect CSI at the receiver in the large-system limit. In order to complete the derivation of Proposition 1, we show that $I(x_{m,t}; \tilde{x}_{m,t} | \Xi_t^{(c)}, \boldsymbol{\theta}_{[m,M],t})$ tends to the integrand in (43). A proof of this statement is given in Appendix D. One may expect that if the convergence of each off-diagonal element of the error covariance matrix (16) to zero is fast enough, the off-diagonal elements of the channel matrix $\sqrt{\mathbf{I} - \Xi_t^{(c)}}$ for the MIMO channel (64) with perfect CSI at the receiver are negligible. Thus, the MIMO channel (64) with perfect CSI at the receiver is decoupled into the bank of the AWGN channels (40). The proof presented in Appendix D implies that the convergence speed shown in Lemma 1, i.e., $(\Xi_t^{(c)})_{\tilde{m}, \tilde{m}'} = O(M^{-3/4})$ for $\tilde{m} \neq \tilde{m}'$, is fast enough. In order to explain this argument intuitively, we apply the matched filter (MF) $\mathbf{r} = \alpha^{-1/2} \sqrt{\mathbf{I} - \Xi_t^{(c)}}^H \underline{\mathbf{z}}$ for the received vector $\underline{\mathbf{z}}$ of the MIMO channel (64) with perfect CSI at the receiver,

$$\mathbf{r} = \frac{\xi_{t,m}}{\alpha} x_{m,t} + \sum_{m'=m+1}^M \frac{\xi_{t,m'}}{\alpha} x_{m',t} + \boldsymbol{\eta}, \quad (69)$$

with $\boldsymbol{\eta} \sim \mathcal{CN}(\mathbf{0}, \sigma^2(\mathbf{I} - \boldsymbol{\Xi}_t^{(c)})/\alpha)$. In (69), the vector $\boldsymbol{\xi}_{t,m'}$ denotes the $(m' - m + 1)$ th column vector of $\mathbf{I} - \boldsymbol{\Xi}_t^{(c)}$ for $m' = m, \dots, M$. Note that the MF output vector (69) contains sufficient information for the estimation of $\mathbf{x}_{[m,M],t}$. The magnitude of the inter-stream interference, given by the second term of the RHS in (69), would be proportional to the magnitude of each interfering signal multiplied by $M - m$ if a *constructive* superposition of all interfering signals occurred. However, it does not occur due to the independence of data symbols with high probability. On average, the magnitude of the inter-stream interference is proportional to the magnitude of each interfering signal multiplied by $\sqrt{M - m}$. Since the magnitude of each interfering signal is $O(M^{-3/4})$, the magnitude of inter-stream interference is $O(M^{-1/4})$. Thus, the inter-stream interference is negligible in the large-system limit.

We have so far presented the derivation of Proposition 1. Finally, we discuss the performance degradation caused by using the LMMSE channel estimator. Let us consider the estimation problem for the first row vector $\vec{\mathbf{h}}_1$ of \mathbf{H} based on the first row vector of the received matrix $\mathbf{Y}_{\setminus t}$, instead of $\tilde{\mathbf{Y}}_{\setminus t}$. It is worth noticing the similarity between this problem and the detection problem of $x_{m,t}$ in stage t . This similarity allows us to analyze the performance of the optimal channel estimator (9) in the large-system limit.

Proposition 7. *Suppose that the error covariance matrix for the optimal channel estimator (9) is self-averaging in the large-system limit. Under the RS assumption, then, each diagonal element of the error covariance matrix converges in probability to the same value as that for the LMMSE channel estimator, defined in Proposition 5, in the large-system limit.*

The derivation of Proposition 7 is omitted since it is straightforwardly derived by combining the methods for deriving Propositions 5 and 6. Proposition 7 allows us to expect that the gap between the achievable rate of the optimal SD receiver and its lower bound (43) may be quite small in the large-system limit, although we cannot immediately conclude that the lower bound (43) is tight in the large-system limit.

APPENDIX B

DERIVATION OF PROPOSITION 5

A. Formulation

It is sufficient from Assumption 1 to show that the averaged quantities $\bar{\xi}_t^2 = M^{-1} \sum_{\tilde{m}=1}^M \mathbb{E}[(\boldsymbol{\Xi}_t)_{\tilde{m},\tilde{m}}]$ and $\bar{\rho}_t = (M - 1)^{-1} \sum_{\tilde{m}=2}^M \mathbb{E}[(\boldsymbol{\Xi}_t)_{1,\tilde{m}}]$ converge to $\xi^2(\tau)$ and zero, respectively, in the large-system limit, in which M , T_c , T_{tr} , and t tend to infinity while $\beta = M/T_c$, $\tau_0 = T_{\text{tr}}/T_c$, and $\tau = t/T_c$ are kept constant.

For notational convenience, hereinafter, we drop the subscript 1 in (59) from all variables. For example, $\vec{\mathbf{y}}_{\setminus t,1}$ and $\vec{\mathbf{h}}_1$ are written as $\vec{\mathbf{y}}_{\setminus t}$ and $\vec{\mathbf{h}}$, respectively. Let $\vec{\mathbf{h}}^{(a)} = (h_1^{(a)}, \dots, h_M^{(a)}) \in \mathbb{C}^{1 \times M}$ denote replicas of $\vec{\mathbf{h}}$ for $a \in \mathbb{N}$: $\{\vec{\mathbf{h}}^{(a)} : a \in \mathbb{N}\}$ are i.i.d. random vectors drawn from $p(\vec{\mathbf{h}})$. Furthermore, we write $\vec{\mathbf{h}}$ as $\vec{\mathbf{h}}^{(0)} = (h_1^{(0)}, \dots, h_M^{(0)})$. The replica analysis is based on the following lemma.

Lemma 2. *Let us define a function $Z_n(\omega; f)$ as*

$$Z_n(\omega; f) = \mathbb{E} \left[\int e^{M\omega f} \left\{ \int p(\vec{\mathbf{y}}_{\setminus t} | \vec{\mathbf{h}}, \bar{\mathbf{X}}_{\setminus t}) p(\vec{\mathbf{h}}) d\vec{\mathbf{h}} \right\}^{n-2} \prod_{a=0}^2 \left\{ p(\vec{\mathbf{y}}_{\setminus t} | \vec{\mathbf{h}} = \vec{\mathbf{h}}^{(a)}, \bar{\mathbf{X}}_{\setminus t}) p(\vec{\mathbf{h}}^{(a)}) d\vec{\mathbf{h}}^{(a)} \right\} d\vec{\mathbf{y}}_{\setminus t} \right], \quad (70)$$

with a complex function f of $\{\vec{\mathbf{h}}^{(a)} : a = 0, 1, 2\}$. In (70), $p(\vec{\mathbf{y}}_{\setminus t} | \vec{\mathbf{h}}, \vec{\mathbf{X}}_{\setminus t})$ represents the virtual MIMO channel (59). For $n \geq 0$ and $\omega \in R$,

$$\bar{\xi}_t^2 = \lim_{n \rightarrow +0} \lim_{\omega \rightarrow 0} \frac{1}{M} \frac{\partial}{\partial \omega} \ln Z_n(\omega; f_1), \quad (71)$$

$$\bar{\rho}_t = \lim_{n \rightarrow +0} \lim_{\omega \rightarrow 0} \frac{1}{M} \frac{\partial}{\partial \omega} \ln Z_n(\omega; f_2), \quad (72)$$

where the functions f_1 and f_2 are given by $f_1 = M^{-1} \sum_{\tilde{m}=1}^M f_{\tilde{m}, \tilde{m}}$ and $f_2 = (M-1)^{-1} \sum_{\tilde{m}=2}^M f_{1, \tilde{m}}$, respectively, with

$$f_{\tilde{m}, \tilde{m}'} = (h_{\tilde{m}}^{(0)} - h_{\tilde{m}}^{(1)})(h_{\tilde{m}'}^{(0)} - h_{\tilde{m}'}^{(2)})^*. \quad (73)$$

Proof: We only present the proof of (71) since the proof of (72) is the same as that of (71). Let $\hat{\mathbf{h}}_t \in \mathbb{C}^{1 \times M}$ denote the first row vector of the LMMSE estimate (15), i.e., the mean of $\vec{\mathbf{h}}$ with respect to $p(\vec{\mathbf{h}} | \tilde{\mathcal{L}}_t)$. Then, we have

$$\bar{\xi}_t^2 = \frac{1}{M} \mathbb{E} \left[\int (\vec{\mathbf{h}} - \vec{\mathbf{h}}^{(2)})^H (\vec{\mathbf{h}} - \vec{\mathbf{h}}^{(1)}) \prod_{a=1}^2 \left\{ p(\vec{\mathbf{h}} = \vec{\mathbf{h}}^{(a)} | \tilde{\mathcal{L}}_t) d\vec{\mathbf{h}}^{(a)} \right\} \right], \quad (74)$$

where we have used the fact that the error covariance matrix (16) is the posterior covariance of $\vec{\mathbf{h}}$ given $\tilde{\mathcal{L}}_t$. The introduction of a non-negative real number n gives

$$\bar{\xi}_t^2 = \lim_{n \rightarrow +0} \mathbb{E} \left[\int f_1 \left\{ \int p(\vec{\mathbf{y}}_{\setminus t} | \vec{\mathbf{h}}, \vec{\mathbf{X}}_{\setminus t}) p(\vec{\mathbf{h}}) d\vec{\mathbf{h}} \right\}^{n-2} \prod_{a=0}^2 \left\{ p(\vec{\mathbf{y}}_{\setminus t} | \vec{\mathbf{h}} = \vec{\mathbf{h}}^{(a)}, \vec{\mathbf{X}}_{\setminus t}) p(\vec{\mathbf{h}}^{(a)}) d\vec{\mathbf{h}}^{(a)} \right\} d\vec{\mathbf{y}}_{\setminus t} \right]. \quad (75)$$

It is straightforward to confirm that (71) is equivalent to (75), since $Z_n(\omega; f_1) = 1$ as $n, \omega \rightarrow 0$. ■

It is difficult to evaluate (70) for a real number n . The main trick of the replica method is that n is regarded as a non-negative integer in evaluating (70). For $n = 2, 3, \dots$, we have a simple expression of (70),

$$Z_n(\omega; f) = \mathbb{E} \left[e^{M\omega f} \int \prod_{a=0}^n p(\vec{\mathbf{y}}_{\setminus t} | \vec{\mathbf{h}} = \vec{\mathbf{h}}^{(a)}, \vec{\mathbf{X}}_{\setminus t}) d\vec{\mathbf{y}}_{\setminus t} \right]. \quad (76)$$

In order to use Lemma 2, we have to take the operations with respect to ω before the large-system limit. However, we need to take the operations after the large-system limit, since it is possible to get an analytical formula of (76) only in the large-system limit, as shown in the next section. We circumvent this dilemma by assuming the commutativity of the large-system limit and the operations.

Assumption 4. For a non-negative integer n ,

$$\lim_{M \rightarrow \infty} \lim_{\omega \rightarrow 0} \frac{1}{M} \frac{\partial}{\partial \omega} \ln Z_n(\omega; f) = \lim_{\omega \rightarrow 0} \frac{\partial}{\partial \omega} \lim_{M \rightarrow \infty} \frac{1}{M} \ln Z_n(\omega; f), \quad (77)$$

where $\lim_{M \rightarrow \infty}$ denotes the large-system limit.

An analytical formula of (76) obtained in the large-system limit is not generally defined for $n \geq 0$. In order to predict the correct asymptotic formula of (70) in a neighborhood of $n = 0$, we will assume a symmetric statistics with respect to replica indices, called the RS assumption. Assuming that the order of the large-system limit and the operations with respect to n and ω in (71) and (72) is commutative, we obtain analytical expressions of (71) and (72) in the large-system limit. It is a challenging open problem to prove whether these assumptions are valid or whether the obtained result is correct.

B. Average over Non-Replicated Variables

In this section, we evaluate the expectations in (76) with respect to the non-replicated variables $\Theta_{(T_{\text{tr}}, t)}$ and $\bar{\mathbf{X}}_{\setminus t} = (\mathbf{X}_{\mathcal{T}_{T_{\text{tr}}}}, \mathbf{X}_{(T_{\text{tr}}, t)}, \Theta_{(t, T_c)})$. The matrix $\bar{\mathbf{X}}_{\setminus t}$ consists of three kinds of random vectors: $\{\mathbf{x}_{t'}\}$ for $t' = 1, \dots, T_{\text{tr}}$ are the pilot symbol vectors, $\{\mathbf{x}_{t'}\}$ for $t' = T_{\text{tr}} + 1, \dots, t - 1$ are the data symbol vectors decoded in the preceding stages, and $\{\theta_{t'}\}$ for $t' = t + 1, \dots, T_c$ are the bias vectors for the data symbol vectors unknown in the current stage. Since the elements of $\bar{\mathbf{y}}_{\setminus t}$, given by (59), are mutually independent conditioned on $\mathcal{H} = \{\mathbf{h}^{(a)} : a = 0, 1, \dots\}$ and $\bar{\mathbf{X}}_{\setminus t}$, (76) yields

$$Z_n(\omega; f) = \mathbb{E} \left\{ e^{M\omega f} \left[e_n(v_p^{(a)}, N_0, \mathcal{H}) \right]^{T_{\text{tr}}} \left[e_n(v_d^{(a)}, N_0, \mathcal{H}) \right]^{t - T_{\text{tr}} - 1} \prod_{t'=t+1}^{T_c} \left[e_n(v_c^{(a)}, N_0 + P - \sigma_{t'}^2, \mathcal{H}) \right] \right\}, \quad (78)$$

with

$$e_n(v^{(a)}, \sigma^2, \mathcal{H}) = \mathbb{E} \left[\int \prod_{a=0}^n g(y; v^{(a)}, \sigma^2) dy \middle| \mathcal{H} \right], \quad (79)$$

where $g(y; v^{(a)}, \sigma^2)$ denotes the pdf of a proper complex Gaussian random variable $y \in \mathbb{C}$ with mean $v^{(a)}$ and variance σ^2 . In (78), $\sigma_{t'}^2$ is given by $\sigma_{t'}^2 = M^{-1} \sum_{\tilde{m}=1}^M |\theta_{\tilde{m}, t'}|^2$. Furthermore, $v_p^{(a)} \in \mathbb{C}$, $v_d^{(a)} \in \mathbb{C}$, and $v_c^{(a)} \in \mathbb{C}$ are given by

$$v_p^{(a)} = \frac{1}{\sqrt{M}} \sum_{\tilde{m}=1}^M h_{\tilde{m}}^{(a)} x_{\tilde{m}, 1}, \quad (80)$$

$$v_d^{(a)} = \frac{1}{\sqrt{M}} \sum_{\tilde{m}=1}^M h_{\tilde{m}}^{(a)} x_{\tilde{m}, t-1}, \quad (81)$$

$$v_c^{(a)} = \frac{1}{\sqrt{M}} \sum_{\tilde{m}=1}^M h_{\tilde{m}}^{(a)} \theta_{\tilde{m}, T_c}, \quad (82)$$

respectively.

We first evaluate $e_n(v_p^{(a)}, N_0, \mathcal{H})$ in the large-system limit, following [28], [31]. Calculating the Gaussian integration with respect to y , we obtain

$$e_n(v_p^{(a)}, N_0, \mathcal{H}) = \frac{\mathbb{E} \left[e^{-N_0^{-1} \mathbf{v}_p^H \mathbf{A} \mathbf{v}_p} \middle| \mathcal{H} \right]}{(\pi N_0)^n (1+n)}, \quad (83)$$

with $\mathbf{v}_p = (v_p^{(0)}, \dots, v_p^{(n)})^T$ and

$$\mathbf{A} = \frac{1}{(1+n)} \begin{pmatrix} n & -\mathbf{1}_n^T \\ -\mathbf{1}_n & (1+n)\mathbf{I}_n - \mathbf{1}_n \mathbf{1}_n^T \end{pmatrix}. \quad (84)$$

In $M \rightarrow \infty$, due to the central limit theorem, \mathbf{v}_p conditioned on \mathcal{H} converges in distribution to a CSCG random vector with the covariance matrix $P\mathbf{Q}$, given by

$$\mathbf{Q} = \frac{1}{M} \sum_{\tilde{m}=1}^M \mathbf{h}_{\tilde{m}} \mathbf{h}_{\tilde{m}}^H, \quad (85)$$

with $\mathbf{h}_{\tilde{m}} = (h_{\tilde{m}}^{(0)}, \dots, h_{\tilde{m}}^{(n)})^T$. Thus,

$$e_n(v_p^{(a)}, N_0, \mathcal{H}) = \exp \left\{ G \left(\frac{P}{N_0} \mathbf{Q} \right) \right\} + O(M^{-1}), \quad (86)$$

in the large-system limit, in which the function $G(\mathbf{Q})$ is given by

$$G(\mathbf{Q}) = -\ln \det(\mathbf{I}_{n+1} + \mathbf{A}\mathbf{Q}) - n \ln(\pi N_0) - \ln(1+n). \quad (87)$$

We next calculate $e_n(v_c^{(a)}, N_0 + P - \sigma_{v'}^2, \mathcal{H})$. Expanding it with respect to the difference $\sigma_{v'}^2 - \sigma_\theta^2$, we have

$$e_n(v_c^{(a)}, N_0 + P - \sigma_{v'}^2, \mathcal{H}) = e_n(v_c^{(a)}, N_0 + P - \sigma_\theta^2, \mathcal{H}) + O(M^{-1/2}), \quad (88)$$

in the large-system limit, since the standard deviation of $\sigma_{v'}^2 - \sigma_\theta^2$ is $O(1/\sqrt{M})$. In the same manner as in the derivation of (86), we have

$$e_n(v_c^{(a)}, N_0 + P - \sigma_{v'}^2, \mathcal{H}) = \exp \left\{ G \left(\frac{\sigma_\theta^2}{N_0 + P - \sigma_\theta^2} \mathbf{Q} \right) \right\} + O(M^{-1/2}). \quad (89)$$

The quantity $e_n(v_d^{(a)}, N_0, \mathcal{H})$ is different from the other two quantities since $\mathbf{v}_d = (v_d^{(0)}, \dots, v_d^{(n)})^T$ has the nonzero mean $\mathbf{v}_\theta = (v_\theta^{(0)}, \dots, v_\theta^{(n)})^T$, with

$$v_\theta^{(a)} = \frac{1}{\sqrt{M}} \sum_{\tilde{m}=1}^M h_{\tilde{m}}^{(a)} \theta_{\tilde{m}, t-1}. \quad (90)$$

The difference $\mathbf{v}_d - \mathbf{v}_\theta$ conditioned on \mathcal{H} and $\boldsymbol{\theta}_{t-1}$ converges in distribution to a CSCG random vector with the covariance matrix $\mathbf{Q}_d = P\mathbf{Q} - \frac{1}{M} \sum_{\tilde{m}=1}^M |\theta_{\tilde{m}, t-1}|^2 \mathbf{h}_{\tilde{m}} \mathbf{h}_{\tilde{m}}^H$ in the large-system limit. We first take the expectation with respect to \mathbf{x}_{t-1} to obtain

$$e_n(v_d^{(a)}, N_0, \mathcal{H}) = \mathbb{E} \left[e^{G(N_0^{-1} \mathbf{Q}_d)} e^{-\mathbf{v}_\theta^H \mathbf{B}(\mathbf{Q}_d, N_0^{-1} \mathbf{A}) \mathbf{v}_\theta} \middle| \mathcal{H} \right] + O(M^{-1}), \quad (91)$$

with

$$\mathbf{B}(\mathbf{Q}, \mathbf{A}) = \mathbf{Q}^{-1} - \mathbf{Q}^{-1}(\mathbf{A} + \mathbf{Q}^{-1})^{-1} \mathbf{Q}^{-1}. \quad (92)$$

In order to eliminate the dependence of $\boldsymbol{\theta}_{m-1}$ on \mathbf{Q}_d , we use $\|\mathbf{Q}_d - (P - \sigma_\theta^2)\mathbf{Q}\| = O(1/\sqrt{M})$ in the large-system limit. Expanding the exponent in (91) around $\mathbf{Q}_d = (P - \sigma_\theta^2)\mathbf{Q}$, we obtain

$$e_n(v_d^{(a)}, N_0, \mathcal{H}) = \exp \left\{ G \left(\frac{P - \sigma_\theta^2}{N_0} \mathbf{Q} \right) \right\} \mathbb{E} \left[\exp \left\{ -N_0^{-1} \mathbf{v}_\theta^H \mathbf{B} \left(\frac{P - \sigma_\theta^2}{N_0} \mathbf{Q}, \mathbf{A} \right) \mathbf{v}_\theta \right\} \middle| \mathcal{H} \right] + O(M^{-1/2}), \quad (93)$$

where we have used the identity $\mathbf{B}(\mathbf{Q}, N_0^{-1} \mathbf{A}) = N_0^{-1} \mathbf{B}(N_0^{-1} \mathbf{Q}, \mathbf{A})$. Applying the central limit theorem with respect to \mathbf{v}_θ to (93), after some calculation, we arrive at

$$e_n(v_d^{(a)}, N_0, \mathcal{H}) = \exp \left\{ G \left(\frac{P}{N_0} \mathbf{Q} \right) \right\} + O(M^{-1/2}). \quad (94)$$

It is interesting to compare (86) for the pilot symbols and (94) for the data symbols decoded in the preceding stages. These expressions imply that random biases do not contribute to the performance of channel estimation in the leading order.

We substitute (86), (89), and (94) into (78) to obtain

$$\frac{1}{M} \ln Z_n(\omega; f) = \frac{1}{M} \ln \mathbb{E} \left\{ e^{M[\omega f + \tilde{G}(\mathbf{Q})]} \right\} + O(1/\sqrt{M}), \quad (95)$$

in the large-system limit, with

$$\tilde{G}(\mathbf{Q}) = \frac{\tau}{\beta} G \left(\frac{P}{N_0} \mathbf{Q} \right) + \frac{1-\tau}{\beta} G \left(\frac{\sigma_\theta^2}{N_0 + P - \sigma_\theta^2} \mathbf{Q} \right). \quad (96)$$

Differentiating (95) with respect to ω and using Assumption 4, we have

$$\lim_{M \rightarrow \infty} \lim_{\omega \rightarrow 0} \frac{1}{M} \frac{\partial}{\partial \omega} \ln Z_n(\omega; f) = \lim_{M \rightarrow \infty} \frac{\mathbb{E} \left[f_{m_1, m_2} e^{M\tilde{G}(\mathbf{Q})} \right]}{\mathbb{E} \left[e^{M\tilde{G}(\mathbf{Q})} \right]}, \quad (97)$$

with $f_{m_1, m_2} = f_{1,1}$ for $f = f_1$ and $f_{m_1, m_2} = f_{1,2}$ for $f = f_2$. Expression (97) implies that the problem of evaluating (71) and (72) reduces to that of evaluating (97) for $f = f_{m_1, m_2}$.

C. Average over Replicated Variables

In this section, we take the expectation in (97) with respect to the replicated variables \mathcal{H} , following [57]. For notational convenience, we define a set $\mathcal{M} = \{m_1, m_2\}$ of integers. We first evaluate the conditional pdf $\mu(\mathbf{Q})$ of \mathbf{Q} given $\mathcal{H}_{\mathcal{M}} = \{\mathbf{h}_{\tilde{m}} : \tilde{m} \in \mathcal{M}\}$.

$$\mu(\mathbf{Q}) = \mathbb{E} \left[\delta \left(\mathbf{Q} - \frac{1}{M} \sum_{\tilde{m}=1}^M \mathbf{h}_{\tilde{m}} \mathbf{h}_{\tilde{m}}^H \right) \middle| \mathcal{H}_{\mathcal{M}} \right]. \quad (98)$$

It might be possible to obtain the analytical expression of the pdf (98) since \mathbf{Q} is a Wishart matrix. However, we derive an asymptotic expression in the large-system limit by using the inversion formula for the moment generating function $F(\tilde{\mathbf{Q}})$ of \mathbf{Q} given by

$$F(\tilde{\mathbf{Q}}) = \mathbb{E} \left[e^{M \text{Tr}(\mathbf{Q}\tilde{\mathbf{Q}})} \middle| \mathcal{H}_{\mathcal{M}} \right], \quad (99)$$

where a positive definite $(n+1) \times (n+1)$ Hermitian matrix $\tilde{\mathbf{Q}}$ is given by

$$\tilde{\mathbf{Q}} = \begin{pmatrix} \tilde{q}_{0,0} & \frac{1}{2}\tilde{q}_{0,1} & \cdots & \frac{1}{2}\tilde{q}_{0,n} \\ \frac{1}{2}\tilde{q}_{0,1}^* & \ddots & \ddots & \vdots \\ \vdots & \ddots & \ddots & \frac{1}{2}\tilde{q}_{n-1,n} \\ \frac{1}{2}\tilde{q}_{0,n}^* & \cdots & \frac{1}{2}\tilde{q}_{n-1,n}^* & \tilde{q}_{n,n} \end{pmatrix}. \quad (100)$$

The inversion formula for moment generating functions implies

$$\mu(\mathbf{Q}) = \left(\frac{M}{2\pi j} \right)^{(n+1)^2} \int e^{-M \text{Tr}(\mathbf{Q}\tilde{\mathbf{Q}})} F(\tilde{\mathbf{Q}}) d\tilde{\mathbf{Q}}, \quad (101)$$

with $d\tilde{\mathbf{Q}} = \prod_{a=0}^n d\tilde{q}_{a,a} \prod_{a < a'} \{d\Re[\tilde{q}_{a,a'}] d\Im[\tilde{q}_{a,a'}]\}$. In (101), the integrations with respect to $d\tilde{q}_{a,a}$, $d\Re[\tilde{q}_{a,a'}]$, and $d\Im[\tilde{q}_{a,a'}]$ are taken along the imaginary axes from $-j\infty$ to $j\infty$, respectively. Since $\{\mathbf{h}_{\tilde{m}}\}$ are i.i.d. for all \tilde{m} , the moment generating function (99) reduces to $\{F_1(\tilde{\mathbf{Q}})\}^{M-|\mathcal{M}|} \prod_{\tilde{m} \in \mathcal{M}} \exp(\mathbf{h}_{\tilde{m}}^H \tilde{\mathbf{Q}} \mathbf{h}_{\tilde{m}})$, given by

$$F_1(\tilde{\mathbf{Q}}) = \mathbb{E} \left[e^{\mathbf{h}_1^H \tilde{\mathbf{Q}} \mathbf{h}_1} \right]. \quad (102)$$

Substituting this expression into (101) gives

$$\mu(\mathbf{Q}) = \left(\frac{M}{2\pi j} \right)^{(n+1)^2} \prod_{\tilde{m} \in \mathcal{M}} e^{\mathbf{h}_{\tilde{m}}^H \tilde{\mathbf{Q}} \mathbf{h}_{\tilde{m}}} \int e^{-M I(\mathbf{Q}, \tilde{\mathbf{Q}})} d\tilde{\mathbf{Q}}, \quad (103)$$

with

$$I(\mathbf{Q}, \tilde{\mathbf{Q}}) = \text{Tr}(\mathbf{Q}\tilde{\mathbf{Q}}) - \left(1 - \frac{|\mathcal{M}|}{M} \right) \ln F_1(\tilde{\mathbf{Q}}). \quad (104)$$

In order to obtain an analytical expression of (103), we use the saddle-point method. Let us define $\tilde{\mathbf{q}} \in \mathbb{R}^{(n+1)^2}$ as $\tilde{\mathbf{q}} = (\tilde{\mathbf{q}}_0^T, \dots, \tilde{\mathbf{q}}_n^T)^T$, given by $\tilde{\mathbf{q}}_a = (\tilde{q}_{a,a}, \Re[\tilde{q}_{a,a+1}], \Im[\tilde{q}_{a,a+1}], \dots, \Re[\tilde{q}_{a,n}], \Im[\tilde{q}_{a,n}])^T \in \mathbb{R}^{2(n-a)+1}$. Expanding (104) with respect to $\tilde{\mathbf{Q}}$ around the saddle-point

$$\tilde{\mathbf{Q}}_s = \operatorname{argsup}_{\tilde{\mathbf{Q}} \in \mathcal{M}_{n+1}^+} \lim_{M \rightarrow \infty} I(\mathbf{Q}, \tilde{\mathbf{Q}}), \quad (105)$$

with \mathcal{M}_{n+1}^+ denoting the space of positive definite $(n+1) \times (n+1)$ Hermitian matrices, we have

$$\mu(\mathbf{Q}) = \left(\frac{\sqrt{M}}{2\pi} \right)^{(n+1)^2} \prod_{\tilde{m} \in \mathcal{M}} e^{\mathbf{h}_{\tilde{m}}^H \tilde{\mathbf{Q}}_s \mathbf{h}_{\tilde{m}}} e^{-MI(\mathbf{Q}, \tilde{\mathbf{Q}}_s)} \int_{\mathbb{R}^{(n+1)^2}} \exp \left\{ \frac{1}{2} \tilde{\mathbf{q}}^T \nabla_{\tilde{\mathbf{q}}}^2 I(\mathbf{Q}, \tilde{\mathbf{Q}}_s) \tilde{\mathbf{q}} \right\} \left[1 + O(1/\sqrt{M}) \right] d\tilde{\mathbf{q}}, \quad (106)$$

where $\nabla_{\tilde{\mathbf{q}}}^2 I(\mathbf{Q}, \tilde{\mathbf{Q}}_s)$ denotes the Hesse matrix of $I(\mathbf{Q}, \tilde{\mathbf{Q}})$ with respect to $\tilde{\mathbf{q}}$. In the derivation of (106), we have transformed the variable $\tilde{\mathbf{Q}}$ into $\tilde{\mathbf{Q}}' = \sqrt{M}(\tilde{\mathbf{Q}} - \tilde{\mathbf{Q}}_s)/j$ and then rewritten $\tilde{\mathbf{Q}}'$ as $\tilde{\mathbf{Q}}$. The Hesse matrix $\nabla_{\tilde{\mathbf{q}}}^2 I(\mathbf{Q}, \tilde{\mathbf{Q}}_s)$ is negative definite since the cumulant generating function $\ln F_1(\tilde{\mathbf{Q}})$ is convex. Thus, we can perform the Gaussian integration in (106) to obtain

$$\mu(\mathbf{Q}) = \left(\sqrt{\frac{M}{2\pi}} \right)^{(n+1)^2} |\det\{\nabla_{\tilde{\mathbf{q}}}^2 I(\mathbf{Q}, \tilde{\mathbf{Q}}_s)\}|^{-1} \prod_{\tilde{m} \in \mathcal{M}} e^{\mathbf{h}_{\tilde{m}}^H \tilde{\mathbf{Q}}_s \mathbf{h}_{\tilde{m}}} e^{-MI(\mathbf{Q}, \tilde{\mathbf{Q}}_s)} \left[1 + O(1/\sqrt{M}) \right]. \quad (107)$$

We next calculate the numerator in (97) by using the pdf (107). Substituting (107) into the quantity $\mathbb{E}[f_{m_1, m_2} e^{M\tilde{G}(\mathbf{Q})}]$ and then using the saddle-point method, we have

$$\mathbb{E} \left[f_{m_1, m_2} e^{M\tilde{G}(\mathbf{Q})} \right] = C_n(\mathbf{Q}, \mathbf{Q}_s) e^{-M\Phi(\mathbf{Q}_s)} \mathbb{E} \left[f_{m_1, m_2} \prod_{\tilde{m} \in \mathcal{M}} e^{\mathbf{h}_{\tilde{m}}^H \tilde{\mathbf{Q}}_s \mathbf{h}_{\tilde{m}}} \right] \left[1 + O(1/\sqrt{M}) \right], \quad (108)$$

with $\Phi(\mathbf{Q}) = I(\mathbf{Q}, \tilde{\mathbf{Q}}_s) - \tilde{G}(\mathbf{Q})$ and $C_n(\mathbf{Q}, \mathbf{Q}_s) = |\det\{\nabla_{\tilde{\mathbf{q}}}^2 I(\mathbf{Q}, \tilde{\mathbf{Q}}_s)\}|^{-1} \det\{\nabla^2 \Phi(\mathbf{Q}_s)\}^{-1}$. In (108), \mathbf{Q}_s denotes the saddle-point

$$\mathbf{Q}_s = \operatorname{arginf}_{\mathbf{Q} \in \mathcal{M}_{n+1}^+} \lim_{M \rightarrow \infty} \Phi(\mathbf{Q}). \quad (109)$$

Furthermore, $\nabla^2 \Phi(\mathbf{Q}_s)$ represents the Hesse matrix of $\Phi(\mathbf{Q})$ at the saddle-point $\mathbf{Q} = \mathbf{Q}_s$, and is assumed to be positive definite.

Similarly, we can obtain an analytical expression of the denominator in (97). Substituting the obtained expression and (108) into (97), we arrive at

$$\lim_{M \rightarrow \infty} \lim_{\omega \rightarrow 0} \frac{1}{M} \frac{\partial}{\partial \omega} \ln Z_n(\omega; f) = \mathbb{E} \left[f_{m_1, m_2} \prod_{\tilde{m} \in \mathcal{M}} \frac{e^{\mathbf{h}_{\tilde{m}}^H \tilde{\mathbf{Q}}_s \mathbf{h}_{\tilde{m}}}}{\mathbb{E}[e^{\mathbf{h}_{\tilde{m}}^H \tilde{\mathbf{Q}}_s \mathbf{h}_{\tilde{m}}}]}, \quad (110)$$

with $f_{m_1, m_2} = f_{1,1}$ for $f = f_1$ and $f_{m_1, m_2} = f_{1,2}$ for $f = f_2$.

The calculations of the stationarity conditions for (105) and (109) implies that $(\mathbf{Q}_s, \tilde{\mathbf{Q}}_s)$ is given as the solution to the coupled fixed-point equations

$$\mathbf{Q} = \frac{\mathbb{E} \left[\mathbf{h}_1 \mathbf{h}_1^H e^{\mathbf{h}_1^H \tilde{\mathbf{Q}} \mathbf{h}_1} \right]}{\mathbb{E} \left[e^{\mathbf{h}_1^H \tilde{\mathbf{Q}} \mathbf{h}_1} \right]}, \quad (111)$$

$$\tilde{\mathbf{Q}} = -\frac{\tau P}{\beta N_0} \left(\mathbf{I}_{n+1} + \frac{P}{N_0} \mathbf{A} \mathbf{Q} \right)^{-1} \mathbf{A} - \frac{(1-\tau)\sigma_\theta^2}{\beta(N_0 + P - \sigma_\theta^2)} \left(\mathbf{I}_{n+1} + \frac{\sigma_\theta^2}{N_0 + P - \sigma_\theta^2} \mathbf{A} \mathbf{Q} \right)^{-1} \mathbf{A}. \quad (112)$$

D. Replica Symmetry

The expression (110) is defined only for $n \in \mathbb{N}$, since $(n+1)$ is the dimension of \mathbf{Q} and $\tilde{\mathbf{Q}}$. In order to obtain a formula of (110) defined for $n \in \mathbb{R}$, we assume RS for the solution to the coupled fixed-point equations (111) and (112).

Assumption 5. *The solution $(\mathbf{Q}_s, \tilde{\mathbf{Q}}_s)$ is invariant under all permutations of replica indices:*

$$\mathbf{Q}_s = \begin{pmatrix} a & b\mathbf{1}_n^\top \\ b^*\mathbf{1}_n & (d-c)\mathbf{I}_n + c\mathbf{1}_n\mathbf{1}_n^\top \end{pmatrix}, \quad (113)$$

$$\tilde{\mathbf{Q}}_s = \begin{pmatrix} \tilde{a} & \tilde{b}\mathbf{1}_n^\top \\ \tilde{b}^*\mathbf{1}_n & (\tilde{d}-\tilde{c})\mathbf{I}_n + \tilde{c}\mathbf{1}_n\mathbf{1}_n^\top \end{pmatrix}. \quad (114)$$

We first evaluate the fixed-point equation (112). Let us define $(\sigma_{\text{tr}}^{(0)})^2$, σ_{tr}^2 , $(\sigma_c^{(0)})^2$, and σ_c^2 as

$$\begin{aligned} (\sigma_{\text{tr}}^{(0)})^2 &= N_0 + P(a - b - b^* + c), \\ \sigma_{\text{tr}}^2 &= N_0 + P(d - c), \\ (\sigma_c^{(0)})^2 &= N_0 + P - \sigma_\theta^2 + \sigma_\theta^2(a - b - b^* + c), \\ \sigma_c^2 &= N_0 + P - \sigma_\theta^2 + \sigma_\theta^2(d - c), \end{aligned} \quad (115)$$

respectively. After some calculation for (112), we obtain

$$\begin{aligned} \tilde{a} &= -\frac{\tau P}{\beta} \frac{n}{\sigma_{\text{tr}}^2 + n(\sigma_{\text{tr}}^{(0)})^2} - \frac{(1-\tau)\sigma_\theta^2}{\beta} \frac{n}{\sigma_c^2 + n(\sigma_c^{(0)})^2}, \\ \tilde{b} &= \frac{\tau P}{\beta} \frac{1}{\sigma_{\text{tr}}^2 + n(\sigma_{\text{tr}}^{(0)})^2} + \frac{(1-\tau)\sigma_\theta^2}{\beta} \frac{1}{\sigma_c^2 + n(\sigma_c^{(0)})^2}, \\ \tilde{c} &= \frac{\tau P}{\beta} \frac{(\sigma_{\text{tr}}^{(0)})^2}{(\sigma_{\text{tr}}^2 + n(\sigma_{\text{tr}}^{(0)})^2)\sigma_{\text{tr}}^2} + \frac{(1-\tau)\sigma_\theta^2}{\beta} \frac{(\sigma_c^{(0)})^2}{(\sigma_c^2 + n(\sigma_c^{(0)})^2)\sigma_c^2}, \\ \tilde{d} &= \tilde{c} - \frac{\tau P}{\beta\sigma_{\text{tr}}^2} - \frac{(1-\tau)\sigma_\theta^2}{\beta\sigma_c^2}. \end{aligned} \quad (116)$$

We next evaluate the fixed-point equation (111) by calculating $e^{\mathbf{h}_m^H \tilde{\mathbf{Q}} \mathbf{h}_m}$ with (116).

$$e^{\mathbf{h}_m^H \tilde{\mathbf{Q}} \mathbf{h}_m} = \exp \left\{ \frac{\tau P}{\beta} \left[\tilde{\sigma}_{\text{tr}}^2 \left| \sum_{a=0}^n \frac{h_m^{(a)}}{(\sigma_{\text{tr}}^{(a)})^2} \right|^2 - \sum_{a=0}^n \frac{|h_m^{(a)}|^2}{(\sigma_{\text{tr}}^{(a)})^2} \right] + \frac{(1-\tau)\sigma_\theta^2}{\beta} \left[\tilde{\sigma}_c^2 \left| \sum_{a=0}^n \frac{h_m^{(a)}}{(\sigma_c^{(a)})^2} \right|^2 - \sum_{a=0}^n \frac{|h_m^{(a)}|^2}{(\sigma_c^{(a)})^2} \right] \right\}, \quad (117)$$

with $\tilde{\sigma}_{\text{tr}}^2 = (n\sigma_{\text{tr}}^{-2} + (\sigma_{\text{tr}}^{(0)})^{-2})^{-1}$ and $\tilde{\sigma}_c^2 = (n\sigma_c^{-2} + (\sigma_c^{(0)})^{-2})^{-1}$. In (117), $(\sigma_{\text{tr}}^{(a)})^2$, and $(\sigma_c^{(a)})^2$ are given by $(\sigma_{\text{tr}}^{(a)})^2 = \sigma_{\text{tr}}^2$, and $(\sigma_c^{(a)})^2 = \sigma_c^2$ for $a = 1, \dots, n$. In order to linearize the two quadratic forms in (117), we use the identity

$$e^{\tilde{\sigma}^2 |a|^2} = \int_{\mathbb{C}} \frac{1}{\pi \tilde{\sigma}^2} e^{-\frac{|y|^2}{\tilde{\sigma}^2} + a^* \underline{y} + a \underline{y}^*} d\underline{y}, \quad (118)$$

for $\underline{y} = \underline{y}_{\text{tr}} \in \mathbb{C}$ or $\underline{y} = \underline{y}_{\text{c}} \in \mathbb{C}$. Substituting (118) with $(a, \tilde{\sigma}^2) = (\sqrt{\tau P/\beta} \sum_{a=0}^n h_{\tilde{m}}^{(a)} / (\sigma_{\text{tr}}^{(a)})^2, \tilde{\sigma}_{\text{tr}}^2)$ or $(a, \tilde{\sigma}^2) = (\sqrt{(1-\tau)\sigma_{\theta}^2/\beta} \sum_{a=0}^n h_{\tilde{m}}^{(a)} / (\sigma_{\text{c}}^{(a)})^2, \tilde{\sigma}_{\text{c}}^2)$ into (117), we have

$$e^{\mathbf{h}_{\tilde{m}}^H \tilde{\mathbf{Q}} \mathbf{h}_{\tilde{m}}} = D_n \int \prod_{a=0}^n q(\underline{\mathbf{y}} | h_{\tilde{m}}^{(a)}) d\underline{\mathbf{y}}, \quad (119)$$

with $D_n = (\pi^2 \sigma_{\text{tr}}^2 \sigma_{\text{c}}^2)^n (1+n(\sigma_{\text{tr}}^{(0)})^2/\sigma_{\text{tr}}^2)(1+n(\sigma_{\text{c}}^{(0)})^2/\sigma_{\text{c}}^2)$. In (119), the function $q(\underline{\mathbf{y}} | h_{\tilde{m}}^{(a)})$ for $\underline{\mathbf{y}} = (\underline{y}_{\text{tr}}, \underline{y}_{\text{c}})^T \in \mathbb{C}^2$ is defined as

$$q(\underline{\mathbf{y}} | h_{\tilde{m}}^{(a)}) = q\left(\underline{y}_{\text{tr}} \left| \sqrt{\frac{\tau P}{\beta}} h_{\tilde{m}}^{(a)}; \sigma_{\text{tr}}^{(a)}\right.\right) q\left(\underline{y}_{\text{c}} \left| \sqrt{\frac{(1-\tau)\sigma_{\theta}^2}{\beta}} h_{\tilde{m}}^{(a)}; \sigma_{\text{c}}^{(a)}\right.\right), \quad (120)$$

with

$$q(\underline{y} | h; \sigma) = \frac{1}{\pi \sigma^2} e^{-\frac{|\underline{y}-h|^2}{\sigma^2}}. \quad (121)$$

Applying the expression (119) to (111), we arrive at

$$a - b - b^* + c = \frac{\mathbb{E} \left[\int |h_1^{(0)} - \langle h_1^{(1)} \rangle|^2 q(\underline{\mathbf{y}} | h_1^{(0)}) \left\{ \mathbb{E}_{h_1^{(1)}} \left[q(\underline{\mathbf{y}} | h_1^{(1)}) \right] \right\}^n d\underline{\mathbf{y}} \right]}{\mathbb{E} \left[\int q(\underline{\mathbf{y}} | h_1^{(0)}) \left\{ \mathbb{E}_{h_1^{(1)}} \left[q(\underline{\mathbf{y}} | h_1^{(1)}) \right] \right\}^n d\underline{\mathbf{y}} \right]}, \quad (122)$$

$$d - c = \frac{\mathbb{E} \left[\int \left\langle |h_1^{(1)} - \langle h_1^{(1)} \rangle|^2 \right\rangle q(\underline{\mathbf{y}} | h_1^{(0)}) \left\{ \mathbb{E}_{h_1^{(1)}} \left[q(\underline{\mathbf{y}} | h_1^{(1)}) \right] \right\}^n d\underline{\mathbf{y}} \right]}{\mathbb{E} \left[\int q(\underline{\mathbf{y}} | h_1^{(0)}) \left\{ \mathbb{E}_{h_1^{(1)}} \left[q(\underline{\mathbf{y}} | h_1^{(1)}) \right] \right\}^n d\underline{\mathbf{y}} \right]}, \quad (123)$$

with

$$\langle h_1^{(1)} \rangle = \frac{\mathbb{E}_{h_1^{(1)}} \left[h_1^{(1)} q(\underline{\mathbf{y}} | h_1^{(1)}) \right]}{\mathbb{E}_{h_1^{(1)}} \left[q(\underline{\mathbf{y}} | h_1^{(1)}) \right]}. \quad (124)$$

E. Replica Continuity

Equations (115), (122), and (123) provide the coupled fixed-point equations of $(a - b - b^* + c, d - c)$ under the RS assumption, and are well defined for $n \in \mathbb{R}$. We regard n as a real number and take the limit $n \rightarrow +0$ to obtain

$$(\sigma_{\text{tr}}^{(0)})^2 = N_0 + P \mathbb{E} \left[|h_1^{(0)} - \langle h_1^{(1)} \rangle|^2 \right], \quad (125)$$

$$\sigma_{\text{tr}}^2 = N_0 + P \mathbb{E} \left[|h_1^{(1)} - \langle h_1^{(1)} \rangle|^2 \right], \quad (126)$$

$$(\sigma_{\text{c}}^{(0)})^2 = N_0 + P - \sigma_{\theta}^2 + \sigma_{\theta}^2 \mathbb{E} \left[|h_1^{(0)} - \langle h_1^{(1)} \rangle|^2 \right], \quad (127)$$

$$\sigma_{\text{c}}^2 = N_0 + P - \sigma_{\theta}^2 + \sigma_{\theta}^2 \mathbb{E} \left[|h_1^{(1)} - \langle h_1^{(1)} \rangle|^2 \right], \quad (128)$$

where the expectations for $\underline{\mathbf{y}}$ are taken with respect to the measure $p(\underline{\mathbf{y}} | h_1^{(0)}) d\underline{\mathbf{y}}$. Note that $\mathbb{E}[|h_1^{(1)} - \langle h_1^{(1)} \rangle|^2]$ and $\mathbb{E}[|h_1^{(1)} - \langle h_1^{(1)} \rangle|^2]$ depend on $(\sigma_{\text{tr}}^{(0)})^2$, σ_{tr}^2 , $(\sigma_{\text{c}}^{(0)})^2$, and σ_{c}^2 . Furthermore, the quantity (110) is given by

$$\lim_{M \rightarrow \infty} \lim_{\omega \rightarrow 0} \frac{1}{M} \frac{\partial}{\partial \omega} \ln Z_n(\omega; f) = \begin{cases} \mathbb{E}[|h_1^{(0)} - \langle h_1^{(1)} \rangle|^2] & \text{for } f = f_1 \\ 0 & \text{for } f = f_2. \end{cases} \quad (129)$$

Under the assumption of the commutativity between the large-system limit and the limit $n \rightarrow +0$, the substitution of (129) into (71) or (72) gives

$$\lim_{M \rightarrow \infty} \bar{\xi}_t^2 = \mathbb{E} \left[\left| h_1^{(0)} - \langle h_1^{(1)} \rangle \right|^2 \right], \quad (130)$$

$$\lim_{M \rightarrow \infty} \bar{\rho}_t = 0, \quad (131)$$

in the large-system limit. Note that we have implicitly assumed that the RHSs of (130) and (131), obtained by the replica method, coincide with the correct ones.

In order to complete the derivation of Proposition 5, we show that (130) reduces to (37), defined by the fixed-point equations (44) and (45). Since $h_1^{(a)} \sim \mathcal{CN}(0, 1)$, the quantities $\mathbb{E}[|h_1^{(0)} - \langle h_1^{(1)} \rangle|^2]$ and $\mathbb{E}[|h_1^{(1)} - \langle h_1^{(1)} \rangle|^2]$ reduce to

$$\mathbb{E} \left[\left| h_1^{(0)} - \langle h_1^{(1)} \rangle \right|^2 \right] = \xi^4 \left(1 + \frac{(\sigma_{\text{tr}}^{(0)})^2 \tau P}{\sigma_{\text{tr}}^4 \beta} + \frac{(\sigma_c^{(0)})^2 (1 - \tau) \sigma_\theta^2}{\sigma_c^4 \beta} \right), \quad (132)$$

$$\mathbb{E} \left[\left| h_1^{(1)} - \langle h_1^{(1)} \rangle \right|^2 \right] = \xi^2, \quad (133)$$

with

$$\xi^2 = \left(1 + \frac{\tau P}{\sigma_{\text{tr}}^2 \beta} + \frac{(1 - \tau) \sigma_\theta^2}{\sigma_c^2 \beta} \right)^{-1}. \quad (134)$$

Equations (126), (128), and (133) provide a closed form for $(\sigma_{\text{tr}}^2, \sigma_c^2)$. Furthermore, (125), (127), and (132) for a given solution $(\sigma_{\text{tr}}^2, \sigma_c^2)$ form two independent linear equations with respect to $(\sigma_{\text{tr}}^{(0)})^2$ and $(\sigma_c^{(0)})^2$, and have the unique solution $((\sigma_{\text{tr}}^{(0)})^2, (\sigma_c^{(0)})^2) = (\sigma_{\text{tr}}^2, \sigma_c^2)$. These observations indicate that the averaged MSE (130) is given as (37), defined by the fixed-point equations (44) and (45).

APPENDIX C

DERIVATION OF PROPOSITION 6

A. Formulation

Let $\mathbb{E}_{\tilde{\mathbf{Y}}_{\setminus t}, \mathbf{x}_{[1, m], t}}[\cdot \cdot \cdot]$ denote the expectation with respect to $\tilde{\mathbf{Y}}_{\setminus t}$ and $\mathbf{x}_{[1, m], t}$ given $\tilde{x}_{m, t}$, $x_{m, t}$, $\tilde{\mathbf{X}}_{\setminus t}$ and $\boldsymbol{\theta}_t$. It is sufficient from Assumption 2 to show that $\mathbb{E}_{\tilde{\mathbf{Y}}_{\setminus t}, \mathbf{x}_{[1, m], t}}[p(\tilde{x}_{m, t} | x_{m, t}, \tilde{\mathcal{I}}_t, \mathbf{x}_{[1, m], t}, \boldsymbol{\theta}_{[m, M], t})]$, given by (20), converges in law to the equivalent channel (65) in the large-system limit. Substituting the posterior pdf (17) into (20) and then introducing a non-negative number n , we have

$$\mathbb{E}_{\tilde{\mathbf{Y}}_{\setminus t}, \mathbf{x}_{[1, m], t}} \left[p(\tilde{x}_{m, t} | x_{m, t}, \tilde{\mathcal{I}}_t, \mathbf{x}_{[1, m], t}, \boldsymbol{\theta}_{[m, M], t}) \right] = \lim_{n \rightarrow +0} Z_n^{(d)}, \quad (135)$$

with

$$\begin{aligned} Z_n^{(d)} &= \mathbb{E}_{\tilde{\mathbf{Y}}_{\setminus t}, \mathbf{x}_{[1, m], t}} \left[\int \left\{ \int p(\mathbf{y}_t | \tilde{\mathbf{x}}_t, \tilde{\mathcal{I}}_t) p(\tilde{\mathbf{x}}_{[m, M], t} | \boldsymbol{\theta}_{[m, M], t}) d\tilde{\mathbf{x}}_{[m, M], t} \right\}^{n-1} p(\mathbf{y}_t | \tilde{\mathbf{x}}_t, \tilde{\mathcal{I}}_t) \right. \\ &\quad \left. \times p(\tilde{\mathbf{x}}_{[m, M], t} | \boldsymbol{\theta}_{[m, M], t}) d\tilde{\mathbf{x}}_{(m, M], t} p(\mathbf{y}_t | \mathbf{x}_t, \tilde{\mathcal{I}}_t) p(\mathbf{x}_{(m, M], t} | \boldsymbol{\theta}_{(m, M], t}) d\mathbf{x}_{(m, M], t} d\mathbf{y}_t \right], \end{aligned} \quad (136)$$

where we have introduced $\tilde{\mathbf{x}}_t = ((\mathbf{x}_{[1, m], t})^\top, (\tilde{\mathbf{x}}_{[m, M], t})^\top)^\top$, in which $\tilde{\mathbf{x}}_{[m, M], t} = (\tilde{x}_{m, t}, \dots, \tilde{x}_{M, t})^\top$ has the same statistical properties as $\mathbf{x}_{[m, M], t}$. Furthermore, $\tilde{\mathbf{x}}_{(m, M], t}$ is given by $\tilde{\mathbf{x}}_{(m, M], t} = (\tilde{x}_{m+1, t}, \dots, \tilde{x}_{M, t})^\top$. Note that

(136) is a quantity of $O(1)$, while (70) is exponential in M . Thus, we have to evaluate (136) up to $O(1)$ in the large-system limit.

Let us regard n in (136) as a positive integer. For $n = 2, 3, \dots$, (136) reduces to a special expression,

$$Z_n^{(d)} = \mathbb{E}_{\tilde{\mathbf{Y}}_{\setminus t}, \mathbf{x}_{[1,m],t}} \left[\int \prod_{a=0}^n p(\mathbf{y}_t | \mathbf{x}_t^{(a)}, \tilde{\mathcal{L}}_t) \prod_{a=2}^n \left\{ p(\mathbf{x}_{[m,M],t}^{(a)} | \boldsymbol{\theta}_{[m,M],t}) d\mathbf{x}_{[m,M],t}^{(a)} \right\} \right. \\ \left. \times p(\mathbf{x}_{[m,M],t}^{(0)} | \boldsymbol{\theta}_{(m,M),t}) d\mathbf{x}_{(m,M),t}^{(0)} p(\mathbf{x}_{[m,M],t}^{(1)} | \boldsymbol{\theta}_{[m,M],t}) d\mathbf{x}_{(m,M),t}^{(1)} d\mathbf{y}_t \right]. \quad (137)$$

In (137), $\mathbf{x}_t^{(a)} = ((\mathbf{x}_{[1,m],t})^T, (\mathbf{x}_{[m,M],t}^{(a)})^T)^T \in \mathbb{C}^M$ denotes replicas of $\tilde{\mathbf{x}}_t$ for $a = 2, \dots, n$, in which $\{\mathbf{x}_{[m,M],t}^{(a)} = (x_{m,t}^{(a)}, \dots, x_{M,t}^{(a)})^T\}$ conditioned on $\boldsymbol{\theta}_{[m,M],t}$ are independent random vectors drawn from $p(\mathbf{x}_{[m,M],t} | \boldsymbol{\theta}_{[m,M],t})$. For notational convenience, we have written $\mathbf{x}_{[m,M],t}$ and $\tilde{\mathbf{x}}_{[m,M],t}$ as $\mathbf{x}_{[m,M],t}^{(a)} = (x_{m,t}^{(a)}, \dots, x_{M,t}^{(a)})^T$ for $a = 0$ and $a = 1$, respectively. The vector $\mathbf{x}_{(m,M),t}^{(a)}$ is defined as $\mathbf{x}_{(m,M),t}^{(a)} = (x_{m+1,t}^{(a)}, \dots, x_{M,t}^{(a)})^T$. Furthermore, we have written \mathbf{x}_t and $\tilde{\mathbf{x}}_t$ as $\mathbf{x}_t^{(a)} = ((\mathbf{x}_{[1,m],t})^T, (\mathbf{x}_{[m,M],t}^{(a)})^T)^T$ for $a = 0$ and $a = 1$, respectively.

B. Average over Non-Replicated Variables

The goal of this section is to evaluate the expectation in (137) with respect to the non-replicated variables $\tilde{\mathbf{Y}}_{\setminus t}$. We first calculate the integration in (137) with respect to \mathbf{y}_t . The substitution of (18) into (137) gives

$$Z_n^{(d)} = \mathbb{E}_{\tilde{\mathbf{Y}}_{\setminus t}, \mathbf{x}_{[1,m],t}} \left[\int \prod_{a=0}^n \left\{ p(\mathbf{y}_t | \mathbf{H}^{(a)}, \mathbf{x}_t^{(a)}) p(\mathbf{H}^{(a)} | \tilde{\mathcal{L}}_t) d\mathbf{H}^{(a)} \right\} \prod_{a=2}^n \left\{ p(\mathbf{x}_{[m,M],t}^{(a)} | \boldsymbol{\theta}_{[m,M],t}) d\mathbf{x}_{[m,M],t}^{(a)} \right\} \right. \\ \left. \times p(\mathbf{x}_{(m,M),t}^{(0)} | \boldsymbol{\theta}_{(m,M),t}) d\mathbf{x}_{(m,M),t}^{(0)} p(\mathbf{x}_{(m,M),t}^{(1)} | \boldsymbol{\theta}_{[m,M],t}) d\mathbf{x}_{(m,M),t}^{(1)} d\mathbf{y}_t \right], \quad (138)$$

where $\mathbf{H}^{(a)} = ((\tilde{\mathbf{h}}_1^{(a)})^T, \dots, (\tilde{\mathbf{h}}_N^{(a)})^T)^T \in \mathbb{C}^{N \times M}$ denotes replicas of \mathbf{H} for $a = 0, \dots, n$: $\{\mathbf{H}^{(a)}\}$ conditioned on $\tilde{\mathcal{L}}_t$ are mutually independent random matrices drawn from $p(\mathbf{H} | \tilde{\mathcal{L}}_t)$. This expression is useful since the covariance matrix of \mathbf{y}_t for $p(\mathbf{y}_t | \mathbf{H}^{(a)}, \mathbf{x}_t^{(a)})$ does not depend on $\mathbf{x}_t^{(a)}$, while the covariance matrix of \mathbf{y}_t for $p(\mathbf{y}_t | \mathbf{x}_t^{(a)}, \tilde{\mathcal{L}}_t)$ depends on $\mathbf{x}_t^{(a)}$. Using the fact that the row vectors $\{\tilde{\mathbf{h}}_{n'}^{(a)}\}$ of $\mathbf{H}^{(a)}$ are mutually independent, we obtain

$$Z_n^{(d)} = p(x_{m,t}^{(1)} | \boldsymbol{\theta}_{m,t}^{(1)}) \mathbb{E} \left\{ \prod_{n'=1}^N \mathbb{E}_{\{\tilde{\mathbf{h}}_{n'}^{(a)}\}} \left[\int \prod_{a=0}^n \left\{ \frac{1}{\pi N_0} e^{-\frac{1}{N_0} |y - v_{n',m,t}^{(a)}|^2} \right\} dy \right] \middle| x_{m,t}^{(1)}, x_{m,t}^{(0)}, \bar{\mathbf{X}}_{\setminus t}, \boldsymbol{\theta}_t \right\}, \quad (139)$$

with

$$v_{n',m,t}^{(a)} = \frac{1}{\sqrt{M}} \left[\sum_{m'=1}^{m-1} \Delta h_{n',m',t}^{(a)} x_{m',t} + \sum_{m'=m}^M h_{n',m',t}^{(a)} x_{m',t}^{(a)} \right], \quad (140)$$

where $h_{n',m'}^{(a)}$ and $\Delta h_{n',m',t}^{(a)}$ denote the (n', m') th element of $\mathbf{H}^{(a)}$ and the LMMSE estimation error $\Delta h_{n',m',t}^{(a)} = h_{n',m'}^{(a)} - \hat{h}_{n',m',t}$, respectively, with $\hat{h}_{n',m',t}$ denoting the (n', m') th element of the LMMSE estimate (15). In (139), the expectation $\mathbb{E}_{\{\tilde{\mathbf{h}}_{n'}^{(a)}\}}[\dots]$ is taken with respect to the measure $p(\tilde{\mathbf{h}}_{n'}^{(a)} | \tilde{\mathcal{L}}_t) d\tilde{\mathbf{h}}_{n'}^{(a)}$. In the derivation of (139), we have eliminated the bias $b = M^{-1/2} \sum_{m'=1}^{m-1} \hat{h}_{n',m',t} x_{m',t}$ known to the receiver by transforming $(\mathbf{y}_t)_{n'}$ into $y = (\mathbf{y}_t)_{n'} - b$. Performing the Gaussian integration with respect to y , we have

$$Z_n^{(d)} = p(x_{m,t}^{(1)} | \boldsymbol{\theta}_{m,t}^{(1)}) \mathbb{E} \left[\prod_{n'=1}^N \frac{\mathbb{E}_{\{\tilde{\mathbf{h}}_{n'}^{(a)}\}} \left[e^{-N_0^{-1} \mathbf{v}_{n',m,t}^H \mathbf{A} \mathbf{v}_{n',m,t}} \right]}{(\pi N_0)^n (1+n)} \middle| x_{m,t}^{(1)}, x_{m,t}^{(0)}, \bar{\mathbf{X}}_{\setminus t}, \boldsymbol{\theta}_t \right], \quad (141)$$

with $\mathbf{v}_{n',m,t} = (v_{n',m,t}^{(0)}, \dots, v_{n',m,t}^{(n)})^T$. In (141), the matrix \mathbf{A} is given by (84).

We next calculate the expectation in (141) with respect to $\{\tilde{\mathbf{h}}_{n'}^{(a)}\}$. Since $\{h_{n',m'}^{(a)}\}$ conditioned on $\tilde{\mathcal{I}}_t$ are proper complex Gaussian random vectors⁴, the random vector $\mathbf{v}_{n',m,t}$ conditioned on $\mathcal{X}_t = \{\mathbf{x}_t^{(a)} : \text{for all } a\}$ and $\tilde{\mathcal{I}}_t$ is also a proper complex Gaussian random variable with mean

$$\mathbf{u}_{n',m,t} = \frac{1}{\sqrt{M}} \sum_{m'=m}^M \hat{h}_{n',m',t} \mathbf{x}_{m',t}, \quad (142)$$

and with the covariance matrix $\mathbf{D} = M^{-1} \text{diag}\{(\mathbf{x}_t^{(0)})^H \tilde{\boldsymbol{\Xi}}_t \mathbf{x}_t^{(0)}, \dots, (\mathbf{x}_t^{(n)})^T \tilde{\boldsymbol{\Xi}}_t \mathbf{x}_t^{(n)}\}$, in which $\mathbf{x}_{m',t} \in \mathbb{C}^{n+1}$ is given by $\mathbf{x}_{m',t} = (x_{m',t}^{(0)}, \dots, x_{m',t}^{(n)})^T$. In the same manner as in the derivation of (91), we take the expectation with respect to $\mathbf{v}_{n',m,t}$ conditioned on \mathcal{X}_t and $\tilde{\mathcal{I}}_t$ to obtain

$$Z_n^{(d)} = p(x_{m,t}^{(1)} | \theta_{m,t}^{(1)}) \mathbb{E} \left[\prod_{n'=1}^N e^{G(N_0^{-1} \mathbf{D}) - \mathbf{u}_{n',m,t}^H \mathbf{B}(\mathbf{D}, N_0^{-1} \mathbf{A}) \mathbf{u}_{n',m,t}} \middle| x_{m,t}^{(1)}, x_{m,t}^{(0)}, \bar{\mathbf{X}}_{\setminus t}, \boldsymbol{\theta}_t \right], \quad (143)$$

where $G(\mathbf{Q})$ and $\mathbf{B}(\mathbf{D}, N_0^{-1} \mathbf{A})$ are given by (87) and (92), respectively.

Finally, we evaluate the expectation in (143) with respect to $\tilde{\mathbf{Y}}_{\setminus t}$. Expression (15) implies that the LMMSE estimates $\{\{\hat{h}_{n',m,t}, \dots, \hat{h}_{n',M,t}\} : \text{for all } n'\}$ conditioned on $\bar{\mathbf{X}}_{\setminus t}$ are mutually independent CSCG random vectors with the covariance matrix $\mathbf{I} - \tilde{\boldsymbol{\Xi}}_t^{(c)}$. Thus, the vectors $\{\mathbf{u}_{n',m,t}\}$ conditioned on $\bar{\mathbf{X}}_{\setminus t}$ and \mathcal{X}_t are also mutually independent CSCG random vectors with covariance $\mathbb{E}[(\mathbf{u}_{n',m,t})_a (\mathbf{u}_{n',m,t})_{a'}^* | \bar{\mathbf{X}}_{\setminus t}, \mathcal{X}_t] = M^{-1} (\mathbf{x}_{[m,M],t}^{(a')})^H (\mathbf{I} - \tilde{\boldsymbol{\Xi}}_t^{(c)}) \mathbf{x}_{[m,M],t}^{(a)}$ for all n' . Taking the expectation with respect to $\tilde{\mathbf{Y}}_{\setminus t}$, after some calculation, we have

$$Z_n^{(d)} = p(x_{m,t}^{(1)} | \theta_{m,t}^{(1)}) \mathbb{E} \left[e^{NG(N_0^{-1} \mathbf{Q}_d)} \middle| x_{m,t}^{(1)}, x_{m,t}^{(0)}, \tilde{\boldsymbol{\Xi}}_t, \boldsymbol{\theta}_t \right], \quad (144)$$

where the $(n+1) \times (n+1)$ Hermitian matrix \mathbf{Q}_d is given by

$$(\mathbf{Q}_d)_{a,a'} = M^{-1} \delta_{a,a'} (\mathbf{x}_t^{(a)})^H \tilde{\boldsymbol{\Xi}}_t \mathbf{x}_t^{(a)} + M^{-1} (\mathbf{x}_{[m,M],t}^{(a')})^H (\mathbf{I} - \tilde{\boldsymbol{\Xi}}_t^{(c)}) \mathbf{x}_{[m,M],t}^{(a)}. \quad (145)$$

C. Average over Replicated Variables

In order to evaluate the conditional expectation in (144) with respect to the replicated variables \mathbf{Q}_d , we evaluate the pdf of \mathbf{Q}_d conditioned on $x_{m,t}^{(1)}$, $x_{m,t}^{(0)}$, $\tilde{\boldsymbol{\Xi}}_t$, and $\boldsymbol{\theta}_t$. Let us define the function $\tilde{I}_d(\mathbf{Q}_d, \tilde{\mathbf{Q}}_d)$ as

$$\tilde{I}_d(\mathbf{Q}_d, \tilde{\mathbf{Q}}_d) = \text{Tr}(\mathbf{Q}_d \tilde{\mathbf{Q}}_d) - \lim_{M \rightarrow \infty} \frac{1}{M} \ln \tilde{F}_d(\tilde{\mathbf{Q}}_d), \quad (146)$$

with

$$\tilde{F}_d(\tilde{\mathbf{Q}}_d) = \mathbb{E} \left[e^{M \text{Tr}(\mathbf{Q}_d \tilde{\mathbf{Q}}_d)} \middle| \tilde{\boldsymbol{\Xi}}_t, \boldsymbol{\theta}_t \right], \quad (147)$$

where a positive definite $(n+1) \times (n+1)$ Hermitian matrix $\tilde{\mathbf{Q}}_d$ is defined in the same manner as in (100). In (146), we have implicitly assumed that the limit in the RHS of (146) exists. Furthermore, we define the saddle-point $\tilde{\mathbf{Q}}_d^{(s)}$ as

$$\tilde{\mathbf{Q}}_d^{(s)} = \underset{\tilde{\mathbf{Q}}_d \in \mathcal{M}_{n+1}^+}{\text{argsup}} \tilde{I}_d(\mathbf{Q}_d, \tilde{\mathbf{Q}}_d). \quad (148)$$

⁴ We could not immediately conclude the Gaussianity of $\mathbf{v}_{n',m,t}$ if the optimal channel estimator (9) were used.

We represent the pdf $\mu(\mathbf{Q}_d)$ of \mathbf{Q}_d conditioned on $x_{m,t}^{(1)}$, $x_{m,t}^{(0)}$, Ξ_t , and θ_t by using the inversion formula for the moment generating function of \mathbf{Q}_d , given by

$$F_d(\tilde{\mathbf{Q}}_d) = \mathbb{E} \left[e^{M\text{Tr}(\mathbf{Q}_d \tilde{\mathbf{Q}}_d)} \middle| x_{m,t}^{(1)}, x_{m,t}^{(0)}, \Xi_t, \theta_t \right]. \quad (149)$$

Using the saddle-point method in the same manner as in the derivation of (107) gives

$$\mu(\mathbf{Q}_d) = \left(\frac{M}{2\pi} \right)^{(n+1)^2} |\det\{\nabla_{\tilde{\mathbf{Q}}_d}^2 I_d(\mathbf{Q}_d, \tilde{\mathbf{Q}}_d^{(s)})\}|^{-1} e^{-MI_d(\mathbf{Q}_d, \tilde{\mathbf{Q}}_d^{(s)}) + O(M^{-1})} [1 + O(M^{-1/2})], \quad (150)$$

in the large-system limit. In (150), the function $I_d(\mathbf{Q}_d, \tilde{\mathbf{Q}}_d)$ is given by

$$I_d(\mathbf{Q}_d, \tilde{\mathbf{Q}}_d) = \text{Tr}(\mathbf{Q}_d \tilde{\mathbf{Q}}_d) - \frac{1}{M} \ln F_d(\tilde{\mathbf{Q}}_d). \quad (151)$$

Furthermore, $\nabla_{\tilde{\mathbf{Q}}_d}^2 I_d(\mathbf{Q}_d, \tilde{\mathbf{Q}}_d)$ denotes the Hesse matrix of (151) with respect to $\tilde{\mathbf{Q}}_d$.

The factor $O(M^{-1})$ in the exponent in (150) is due to a small deviation of the saddle-point (148). The removal or addition of one transmit antenna results in a small change of $M\text{Tr}(\mathbf{Q}_d \tilde{\mathbf{Q}}_d)$, more precisely, in a change of $O(1)$. This observation implies that $I_d(\mathbf{Q}_d, \tilde{\mathbf{Q}}_d) = \tilde{I}_d(\mathbf{Q}_d, \tilde{\mathbf{Q}}_d) + O(M^{-1})$ in the large-system limit. Differentiating both sides with respect to $\tilde{\mathbf{Q}}_d$ at the saddle-point (148), we find that the gradient $\nabla_{\tilde{\mathbf{Q}}_d} I_d(\mathbf{Q}_d, \tilde{\mathbf{Q}}_d^{(s)})$ of (151) with respect to $\tilde{\mathbf{Q}}_d$ at the saddle-point is $O(M^{-1})$, which explains the factor $O(M^{-1})$ in the exponent in (150) since a deviation of the saddle-point results in a deviation of the exponent which is proportional to $M\|\nabla_{\tilde{\mathbf{Q}}_d} I_d(\mathbf{Q}_d, \tilde{\mathbf{Q}}_d^{(s)})\|^2$.

We repeat the same argument to evaluate (144). Applying (150) to (144) and using the saddle-point method, we arrive at

$$Z_n^{(d)} = p(x_{m,t}^{(1)} | \theta_{m,t}^{(1)}) C_n^{(d)}(\mathbf{Q}_d^{(s)}, \tilde{\mathbf{Q}}_d^{(s)}) e^{-M\Phi_d(\mathbf{Q}_d^{(s)})} [1 + O(M^{-1/2})]. \quad (152)$$

In (152), the function $\Phi_d(\mathbf{Q}_d)$ is defined as

$$\Phi_d(\mathbf{Q}_d) = I_d(\mathbf{Q}_d, \tilde{\mathbf{Q}}_d^{(s)}) - \alpha^{-1} G(N_0^{-1} \mathbf{Q}_d). \quad (153)$$

The saddle-point $\mathbf{Q}_d^{(s)}$ is given by

$$\mathbf{Q}_d^{(s)} = \underset{\mathbf{Q}_d \in \mathcal{M}_{n+1}^+}{\text{arginf}} \tilde{\Phi}_d(\mathbf{Q}_d), \quad (154)$$

with

$$\tilde{\Phi}_d(\mathbf{Q}_d) = \tilde{I}_d(\mathbf{Q}_d, \tilde{\mathbf{Q}}_d^{(s)}) - \alpha^{-1} G(N_0^{-1} \mathbf{Q}_d). \quad (155)$$

Furthermore, $C_n^{(d)}(\mathbf{Q}_d, \tilde{\mathbf{Q}}_d)$ is defined as

$$C_n^{(d)}(\mathbf{Q}_d, \tilde{\mathbf{Q}}_d) = |\det\{\nabla_{\tilde{\mathbf{Q}}_d}^2 I_d(\mathbf{Q}_d, \tilde{\mathbf{Q}}_d)\}|^{-1} \det\{\alpha^{-1} \nabla_{\mathbf{Q}_d}^2 G(N_0^{-1} \mathbf{Q}_d)\}^{-1}, \quad (156)$$

where $\nabla_{\mathbf{Q}_d}^2 G(N_0^{-1} \mathbf{Q}_d)$ denotes the Hesse matrix of $G(N_0^{-1} \mathbf{Q}_d)$ with respect to \mathbf{Q}_d . Note that we have assumed the positive definiteness of the Hesse matrix $\nabla_{\mathbf{Q}_d}^2 G(N_0^{-1} \mathbf{Q}_d)$ at the saddle-point $\mathbf{Q}_d = \mathbf{Q}_d^{(s)}$.

The calculation of the stationarity conditions for (148) and (154) implies that $(\mathbf{Q}_d^{(s)}, \tilde{\mathbf{Q}}_d^{(s)})$ is given as the solution to the coupled fixed-point equations

$$\mathbf{Q}_d = \lim_{M \rightarrow \infty} \frac{\mathbb{E} \left[\mathbf{Q}_d e^{M\text{Tr}(\mathbf{Q}_d \tilde{\mathbf{Q}}_d)} \middle| \Xi_t, \theta_t \right]}{\mathbb{E} \left[e^{M\text{Tr}(\mathbf{Q}_d \tilde{\mathbf{Q}}_d)} \middle| \Xi_t, \theta_t \right]}, \quad (157)$$

$$\tilde{\mathbf{Q}}_d = -\frac{\alpha^{-1}}{N_0} \left(\mathbf{I}_{n+1} + \frac{\mathbf{A}}{N_0} \mathbf{Q}_d \right)^{-1} \mathbf{A}. \quad (158)$$

D. Evaluation of Fixed-Point Equations

In order to evaluate the coupled fixed-point equations (157) and (158), we assume RS. The assumption of RS is consistent with Assumption 2, i.e., the assumption of the self-averaging property for the equivalent channel (20) [52].

Assumption 6. *The solution $(\mathbf{Q}_d^{(s)}, \tilde{\mathbf{Q}}_d^{(s)})$ is invariant under all permutations of replica indices:*

$$\mathbf{Q}_d^{(s)} = \begin{pmatrix} a_d & b_d \mathbf{1}_n^T \\ b_d^* \mathbf{1}_n & (d_d - c_d) \mathbf{I}_n + c_d \mathbf{1}_n \mathbf{1}_n^T \end{pmatrix}, \quad (159)$$

$$\tilde{\mathbf{Q}}_d^{(s)} = \begin{pmatrix} \tilde{a}_d & \tilde{b}_d \mathbf{1}_n^T \\ \tilde{b}_d^* \mathbf{1}_n & (\tilde{d}_d - \tilde{c}_d) \mathbf{I}_n + \tilde{c}_d \mathbf{1}_n \mathbf{1}_n^T \end{pmatrix}. \quad (160)$$

We first evaluate the fixed-point equation (158). Let us define σ_0^2 and σ^2 as

$$\sigma_0^2 = N_0 + (a_d - b_d - b_d^* + c_d), \quad (161)$$

$$\sigma^2 = N_0 + (d_d - c_d), \quad (162)$$

respectively. After some calculation, we obtain

$$\tilde{a}_d = -\frac{\alpha^{-1}n}{\sigma^2 + n\sigma_0^2}, \quad \tilde{b}_d = \frac{\alpha^{-1}}{\sigma^2 + n\sigma_0^2}, \quad \tilde{c}_d = \frac{\alpha^{-1}\sigma_0^2}{(\sigma^2 + n\sigma_0^2)\sigma^2}, \quad \tilde{d}_d = \tilde{c}_d - \frac{\alpha^{-1}}{\sigma^2}. \quad (163)$$

We next calculate the quantity $\exp\{M\text{Tr}(\mathbf{Q}_d^{(s)} \tilde{\mathbf{Q}}_d^{(s)})\}$. Let $\sqrt{\mathbf{I} - \Xi_t^{(c)}}$ denote a square root of $\mathbf{I} - \Xi_t^{(c)}$, i.e., $\mathbf{I} - \Xi_t^{(c)} = \sqrt{\mathbf{I} - \Xi_t^{(c)}}^H \sqrt{\mathbf{I} - \Xi_t^{(c)}}$. Substituting (163) into that quantity gives

$$e^{M\text{Tr}(\mathbf{Q}_d^{(s)} \tilde{\mathbf{Q}}_d^{(s)})} = \exp \left\{ \tilde{\sigma}_0^2 \left\| \sum_{a=0}^n \frac{\sqrt{\mathbf{I} - \Xi_t^{(c)}} \mathbf{x}_{[m,M],t}^{(a)}}{\sqrt{\alpha}\sigma_a^2} \right\|^2 - \sum_{a=0}^n \frac{\|\sqrt{\mathbf{I} - \Xi_t^{(c)}} \mathbf{x}_{[m,M],t}^{(a)}\|^2}{\alpha\sigma_a^2} + \tilde{a}_d (\mathbf{x}_t^{(0)})^H \Xi_t \mathbf{x}_t^{(0)} + \tilde{d}_d \sum_{a=1}^n (\mathbf{x}_t^{(a)})^H \Xi_t \mathbf{x}_t^{(a)} \right\}, \quad (164)$$

with $\tilde{\sigma}_0^2 = (n\sigma^{-2} + \sigma_0^{-2})^{-1}$ and $\sigma_a^2 = \sigma^2$ for $a = 1, \dots, n$. In order to linearize the quadratic form in (164), we use the identity

$$e^{\tilde{\sigma}_0^2 \|\mathbf{a}\|^2} = \int_{\mathbb{C}^{M-m+1}} \frac{1}{(\pi\tilde{\sigma}_0^2)^{M-m+1}} e^{-\frac{\|\underline{\mathbf{z}}\|^2}{\tilde{\sigma}_0^2} + \mathbf{a}^H \underline{\mathbf{z}} + \underline{\mathbf{z}}^H \mathbf{a}} d\underline{\mathbf{z}}, \quad (165)$$

with $\mathbf{a} = \sum_{a=0}^n \sqrt{\mathbf{I} - \Xi_t^{(c)}} \mathbf{x}_{[m,M],t}^{(a)} / (\sqrt{\alpha}\sigma_a^2)$ to obtain

$$e^{M\text{Tr}(\mathbf{Q}_d^{(s)} \tilde{\mathbf{Q}}_d^{(s)})} = D_n^{(d)} \int \prod_{a=0}^n \left\{ \tilde{q}_a(\underline{\mathbf{z}} | \mathbf{x}_t^{(a)}, \Xi_t) \right\} d\underline{\mathbf{z}}, \quad (166)$$

with $D_n^{(d)} = (\pi\sigma^2)^{n(M-m+1)} (1 + n\sigma_0^2/\sigma^2)^{M-m+1}$. In (166), the functions $\tilde{q}_0(\underline{\mathbf{z}} | \mathbf{x}_t^{(0)}, \Xi_t)$ and $\tilde{q}_a(\underline{\mathbf{z}} | \mathbf{x}_t^{(a)}, \Xi_t)$ for $a = 1, \dots, n$ are given by

$$\tilde{q}_0(\underline{\mathbf{z}} | \mathbf{x}_t^{(0)}, \Xi_t) = q_0(\underline{\mathbf{z}} | \mathbf{x}_{[m,M],t}^{(0)}, \Xi_t^{(c)}) e^{\tilde{a}_d (\mathbf{x}_t^{(0)})^H \Xi_t \mathbf{x}_t^{(0)}}, \quad (167)$$

$$\tilde{q}_a(\underline{\mathbf{z}}|\mathbf{x}_t^{(a)}, \Xi_t) = q_a(\underline{\mathbf{z}}|\mathbf{x}_{[m,M],t}^{(a)}, \Xi_t^{(c)})e^{\tilde{d}_d(\mathbf{x}_t^{(a)})^H \Xi_t \mathbf{x}_t^{(a)}}, \quad (168)$$

respectively, where $q_a(\underline{\mathbf{z}}|\mathbf{x}_{[m,M],t}^{(a)}, \Xi_t^{(c)})$ represents the pdf of a proper complex Gaussian random vector $\underline{\mathbf{z}} \in \mathbb{C}^{M-m+1}$ with mean $\sqrt{\mathbf{I} - \Xi_t^{(c)}}\mathbf{x}_{[m,M],t}^{(a)}/\sqrt{\alpha}$ and covariance $\sigma_a^2\mathbf{I}$, i.e.,

$$q_a(\underline{\mathbf{z}}|\mathbf{x}_{[m,M],t}^{(a)}, \Xi_t^{(c)}) = \frac{1}{(\pi\sigma_a^2)^{M-m+1}} \exp \left\{ -\frac{\|\underline{\mathbf{z}} - \sqrt{\mathbf{I} - \Xi_t^{(c)}}\mathbf{x}_{[m,M],t}^{(a)}/\sqrt{\alpha}\|^2}{\sigma_a^2} \right\}. \quad (169)$$

Finally, we evaluate the fixed-point equation (157). Substitution of (166) into (157) gives expressions of $a_d - b_d - b_d^* + c_d$ and $d_d - c_d$ well-defined for $n \in \mathbb{R}$. Taking $n \rightarrow +0$, we have

$$\begin{aligned} \lim_{n \rightarrow +0} (a_d - b_d - b_d^* + c_d) &= \lim_{M \rightarrow \infty} \frac{1}{M} \mathbb{E} \left\{ \int q_0(\underline{\mathbf{z}}|\mathbf{x}_{[m,M],t}^{(0)}, \Xi_t^{(c)}) \right. \\ &\quad \times \left. \left((\mathbf{x}_t^{(0)})^H \Xi_t \mathbf{x}_t^{(0)} + \left\| \sqrt{\mathbf{I} - \Xi_t^{(c)}}(\mathbf{x}_{[m,M],t}^{(0)} - \langle \mathbf{x}_{[m,M],t}^{(1)} \rangle) \right\|^2 \right) d\underline{\mathbf{z}} \middle| \Xi_t, \boldsymbol{\theta}_t \right\}, \quad (170) \end{aligned}$$

$$\begin{aligned} \lim_{n \rightarrow +0} (d_d - c_d) &= \lim_{M \rightarrow \infty} \frac{1}{M} \mathbb{E} \left\{ \int q_0(\underline{\mathbf{z}}|\mathbf{x}_{[m,M],t}^{(0)}, \Xi_t^{(c)}) \right. \\ &\quad \times \left. \left((\mathbf{x}_t^{(1)})^H \Xi_t \mathbf{x}_t^{(1)} + \left\| \sqrt{\mathbf{I} - \Xi_t^{(c)}}(\mathbf{x}_{[m,M],t}^{(1)} - \langle \mathbf{x}_{[m,M],t}^{(1)} \rangle) \right\|^2 \right) d\underline{\mathbf{z}} \middle| \Xi_t, \boldsymbol{\theta}_t \right\}, \quad (171) \end{aligned}$$

with

$$\langle \mathbf{x}_t^{(1)} \rangle = \frac{\int \mathbf{x}_t^{(1)} \tilde{q}_1(\underline{\mathbf{z}}|\mathbf{x}_t^{(1)}, \Xi_t) p(\mathbf{x}_t^{(1)}|\boldsymbol{\theta}_t) d\mathbf{x}_t^{(1)}}{\int \tilde{q}_1(\underline{\mathbf{z}}|\mathbf{x}_t^{(1)}, \Xi_t) p(\mathbf{x}_t^{(1)}|\boldsymbol{\theta}_t) d\mathbf{x}_t^{(1)}}. \quad (172)$$

Substituting these expressions into (161) or (162), we have the coupled fixed-point equations

$$\sigma_0^2 = N_0 + \lim_{M \rightarrow \infty} \frac{1}{M} \left\{ P \text{Tr}(\Xi_t) + \mathbb{E} \left[(\mathbf{x}_{[m,M],t}^{(0)} - \langle \mathbf{x}_{[m,M],t}^{(1)} \rangle)^H (\mathbf{I} - \Xi_t^{(c)}) (\mathbf{x}_{[m,M],t}^{(0)} - \langle \mathbf{x}_{[m,M],t}^{(1)} \rangle) \middle| \Xi_t^{(c)}, \boldsymbol{\theta}_t \right] \right\}, \quad (173)$$

$$\sigma^2 = N_0 + \lim_{M \rightarrow \infty} \frac{1}{M} \left\{ P \text{Tr}(\Xi_t) + \mathbb{E} \left[(\mathbf{x}_{[m,M],t}^{(1)} - \langle \mathbf{x}_{[m,M],t}^{(1)} \rangle)^H (\mathbf{I} - \Xi_t^{(c)}) (\mathbf{x}_{[m,M],t}^{(1)} - \langle \mathbf{x}_{[m,M],t}^{(1)} \rangle) \middle| \Xi_t^{(c)}, \boldsymbol{\theta}_t \right] \right\}, \quad (174)$$

where the average over $\underline{\mathbf{z}}$ is taken with respect to the measure $q_0(\underline{\mathbf{z}}|\mathbf{x}_{[m,M],t}^{(0)}, \Xi_t^{(c)})d\underline{\mathbf{z}}$.

The coupled fixed-point equations (173) and (174) have the solution $\sigma_0^2 = \sigma^2$. Nishimori's result [36] implies that $\sigma_0^2 = \sigma^2$ is the correct solution. Assuming $\sigma_0^2 = \sigma^2$, we have the single fixed-point equation

$$\sigma^2 = N_0 + \lim_{M \rightarrow \infty} \frac{P}{M} \text{Tr}(\Xi_t) + V(\sigma^2), \quad (175)$$

with

$$V(\sigma^2) = \lim_{M \rightarrow \infty} \frac{1}{M} \mathbb{E} \left[(\mathbf{x}_{[m,M],t}^{(1)} - \langle \mathbf{x}_{[m,M],t}^{(1)} \rangle)^H (\mathbf{I} - \Xi_t^{(c)}) (\mathbf{x}_{[m,M],t}^{(1)} - \langle \mathbf{x}_{[m,M],t}^{(1)} \rangle) \middle| \Xi_t^{(c)}, \boldsymbol{\theta}_{[m,M],t} \right]. \quad (176)$$

In (175), the average over $\underline{\mathbf{z}}$ is taken with respect to the measure $q_0(\underline{\mathbf{z}}|\mathbf{x}_{[m,M],t}^{(0)}, \Xi_t^{(c)})d\underline{\mathbf{z}}$ with $\sigma_0^2 = \sigma^2$. Furthermore, $\langle \mathbf{x}_{[m,M],t}^{(1)} \rangle$ denotes the expectation of $\mathbf{x}_{[m,M],t}^{(1)}$ with respect to the posterior measure $q_1(\mathbf{x}_{[m,M],t}^{(1)}|\underline{\mathbf{z}}, \Xi_t^{(c)})d\mathbf{x}_{[m,M],t}^{(1)}$ given by

$$q_1(\mathbf{x}_{[m,M],t}^{(1)}|\underline{\mathbf{z}}, \Xi_t^{(c)}, \boldsymbol{\theta}_{[m,M],t}) = \frac{q_1(\underline{\mathbf{z}}|\mathbf{x}_{[m,M],t}^{(1)}, \Xi_t^{(c)})p(\mathbf{x}_{[m,M],t}^{(1)}|\boldsymbol{\theta}_{[m,M],t})}{\int q_1(\underline{\mathbf{z}}|\mathbf{x}_{[m,M],t}^{(1)}, \Xi_t^{(c)})p(\mathbf{x}_{[m,M],t}^{(1)}|\boldsymbol{\theta}_{[m,M],t})d\mathbf{x}_{[m,M],t}^{(1)}}. \quad (177)$$

Note that the fixed-point equation (175) is equivalent to (66).

E. Replica Continuity

We evaluate (152) under the RS assumption (Assumption 6). The function $G(N_0^{-1}\mathbf{Q}_d^{(s)})$, given by (87), reduces to [17]

$$G(N_0^{-1}\mathbf{Q}_d^{(s)}) = -(n-1)\ln\sigma^2 - \ln(\sigma^2 + n\sigma_0^2) - n\ln\pi, \quad (178)$$

which is well defined for $n \in \mathbb{R}$ and tends to zero as $n \rightarrow +0$.

Applying (161), (162), and (163) to (151), we obtain

$$I_d(\mathbf{Q}_d^{(s)}, \tilde{\mathbf{Q}}_d^{(s)}) = -\frac{n}{\alpha} \left[1 - \frac{N_0}{\sigma^2 + n\sigma_0^2} - \frac{N_0}{\sigma^2} + \frac{N_0\sigma_0^2}{\sigma^2(\sigma^2 + n\sigma_0^2)} \right] - \frac{1}{M} \ln F_d(\tilde{\mathbf{Q}}_d^{(s)}). \quad (179)$$

Substituting (166) into the moment generating function (149), we have an expression of (179) well defined for $n \in \mathbb{R}$. Taking $n \rightarrow +0$, under the assumption of $\sigma_0^2 = \sigma^2$, we have

$$\begin{aligned} & \lim_{n \rightarrow +0} I_d(\mathbf{Q}_d^{(s)}, \tilde{\mathbf{Q}}_d^{(s)}) \\ &= -\frac{1}{M} \ln \int q_1(x_{m,t}^{(1)} | \mathbf{z}, \Xi_t^{(c)}, \boldsymbol{\theta}_{[m,M],t}) q_0(\mathbf{z} | \mathbf{x}_{[m,M],t}^{(0)}, \Xi_t^{(c)}) p(\mathbf{x}_{[m,M],t}^{(0)} | \boldsymbol{\theta}_{[m,M],t}) d\mathbf{x}_{[m,M],t}^{(0)} d\mathbf{z}, \end{aligned} \quad (180)$$

with the marginal $q_1(x_{m,t}^{(1)} | \mathbf{z}, \Xi_t^{(c)}, \boldsymbol{\theta}_{[m,M],t}) = \int q_1(\mathbf{x}_{[m,M],t}^{(1)} | \mathbf{z}, \Xi_t^{(c)}, \boldsymbol{\theta}_{[m,M],t}) d\mathbf{x}_{[m,M],t}^{(1)}$ of (177). Substituting (178) and (180) into (153) and assuming that the obtained expression is correct as $n \rightarrow +0$, from (135), we arrive at

$$\begin{aligned} \mathbb{E}_{\tilde{\mathbf{Y}}_{\setminus t}, \mathbf{x}_{[1,m],t}} \left[p(\tilde{x}_{m,t} | x_{m,t}, \tilde{\mathcal{I}}_t, \mathbf{x}_{[1,m],t}, \boldsymbol{\theta}_{[m,M],t}) \right] &= \lim_{n \rightarrow +0} C_n^{(d)}(\mathbf{Q}_d^{(s)}, \tilde{\mathbf{Q}}_d^{(s)}) \\ &\times \int q_1(x_{m,t}^{(1)} | \mathbf{z}, \Xi_t^{(c)}, \boldsymbol{\theta}_{[m,M],t}) q_0(\mathbf{z} | \mathbf{x}_{[m,M],t}^{(0)}, \Xi_t^{(c)}) p(\mathbf{x}_{[m,M],t}^{(0)} | \boldsymbol{\theta}_{[m,M],t}) d\mathbf{x}_{[m,M],t}^{(0)} d\mathbf{z}, \end{aligned} \quad (181)$$

where we have assumed that the large-system limit and the limit $n \rightarrow +0$ are commutative. Due to the normalization of pdfs, the quantity $C_n^{(d)}(\mathbf{Q}_d^{(s)}, \tilde{\mathbf{Q}}_d^{(s)})$ should tend to 1 as $n \rightarrow +0$. This observation implies that the RHS of (181) is equal to the equivalent channel (65) between $x_{m,t}$ and the associated decoder for the MIMO channel (64) with perfect CSI at the receiver.

F. Multiple Solutions

The fixed-point equation (175) may have multiple solutions. In that case, one has to choose the solution minimizing the quantity (155). Due to $\lim_{n \rightarrow +0} \tilde{\Phi}_d(\mathbf{Q}_d^{(s)}) = 0$, the quantity $\tilde{\Phi}_d(\mathbf{Q}_d^{(s)})$ is given by $\tilde{\Phi}_d(\mathbf{Q}_d^{(s)}) = nF + O(n^2)$ as $n \rightarrow +0$, with the so-called free energy $F = \lim_{n \rightarrow +0} \frac{\partial}{\partial n} \tilde{\Phi}_d(\mathbf{Q}_d^{(s)})$. Thus, one should choose the solution minimizing the free energy F .

In order to calculate the free energy F , in the same manner as in the derivation of (179), we evaluate (146) as

$$\begin{aligned} \tilde{I}_d(\mathbf{Q}_d^{(s)}, \tilde{\mathbf{Q}}_d^{(s)}) &= -\frac{n}{\alpha} \left[1 - \frac{N_0}{\sigma^2 + n\sigma_0^2} - \frac{N_0}{\sigma^2} + \frac{N_0\sigma_0^2}{\sigma^2(\sigma^2 + n\sigma_0^2)} \right] - \lim_{M \rightarrow \infty} \frac{1}{M} \ln D_n^{(d)} \\ &- \lim_{M \rightarrow \infty} \frac{1}{M} \ln \int \mathbb{E}_{\mathbf{x}_t^{(0)}} [\tilde{q}_0(\mathbf{z} | \mathbf{x}_t^{(0)}, \Xi_t)] \left\{ \mathbb{E}_{\mathbf{x}_t^{(1)}} [\tilde{q}_1(\mathbf{z} | \mathbf{x}_t^{(1)}, \Xi_t)] \right\}^n d\mathbf{z}. \end{aligned} \quad (182)$$

We differentiate (178) and (182) with respect to n at $n = 0$ to obtain

$$F = \lim_{M \rightarrow \infty} \frac{1}{M} I(\mathbf{x}_{[m,M],t}; \mathbf{z}) + \frac{1}{\alpha} \left[D_e(N_0 \| \sigma^2) + \lim_{M \rightarrow \infty} \frac{1}{M\sigma^2} \text{Tr}(\Xi_t) + \ln(\pi e N_0) \right], \quad (183)$$

with

$$\begin{aligned}
 I(\mathbf{x}_{[m,M],t}; \mathbf{z}) &= \int q_0(\mathbf{z}|\mathbf{x}_{[m,M],t}^{(0)}, \Xi_t^{(c)}) p(\mathbf{x}_{[m,M],t}^{(0)}|\boldsymbol{\theta}_{[m,M],t}) \\
 &\quad \times \ln \frac{q_1(\mathbf{z}|\mathbf{x}_{[m,M],t}^{(0)}, \Xi_t^{(c)})}{\int q_1(\mathbf{z}|\mathbf{x}_{[m,M],t}^{(1)}, \Xi_t^{(c)}) p(\mathbf{x}_{[m,M],t}^{(1)}|\boldsymbol{\theta}_{[m,M],t}) d\mathbf{x}_{[m,M],t}^{(1)}} d\mathbf{x}_{[m,M],t}^{(0)} d\mathbf{z}. \quad (184)
 \end{aligned}$$

Minimizing (183) is equivalent to minimizing (68).

APPENDIX D

REDUCTION OF PROPOSITION 6 TO PROPOSITION 1

Let us prove that the fixed-point equation (66) coincides with the fixed-point equation (46). We first show that the last term in (46) is a lower bound on the last term in (66), by considering the MIMO channel (64) with additional side information. Let a genie inform the receiver about the correct values of the data symbols $\mathbf{x}_{(m,M),t}$. The MSE (67) for the genie-aided receiver should provide a lower bound on the original one. In order to eliminate the inter-stream interference from the MF output vector (69), the genie-aided receiver calculates $\mathbf{r}_s = \mathbf{r} - \sum_{m'=m+1}^M \xi_{t,m'} x_{m',t} / \alpha$, given by

$$\mathbf{r}_s = \frac{1}{\alpha} \boldsymbol{\xi}_{t,m} x_{m,t} + \boldsymbol{\eta}. \quad (185)$$

The performance of the interference-free channel (185), such as the MSE and the constrained capacity, is determined by the SNR

$$\overline{\text{snr}} = \frac{P \|\boldsymbol{\xi}_{t,m}\|^4}{\alpha \sigma^2 \boldsymbol{\xi}_{t,m}^H (\mathbf{I} - \Xi_t^{(c)}) \boldsymbol{\xi}_{t,m}}. \quad (186)$$

Proposition 5 and Lemma 1 imply that the numerator and denominator in (186) are given by $P \|\boldsymbol{\xi}_{t,m}\|^4 = P(1 - \xi^2(\tau))^4 + O(M^{-1/4})$ and $\alpha \sigma^2 \boldsymbol{\xi}_{t,m}^H (\mathbf{I} - \Xi_t^{(c)}) \boldsymbol{\xi}_{t,m} = \alpha \sigma^2 (1 - \xi^2(\tau))^3 + O(M^{-1/4})$ in the large-system limit, respectively. Thus, the SNR (186) converges in probability to $\overline{\text{snr}} = (1 - \xi^2(\tau))P / (\alpha \sigma^2)$ in the large-system limit, which coincides with the SNR for the AWGN channel (40) with $\sigma^2(\tau, \mu) = \sigma^2$. This expression implies that the last term (67) in the fixed-point equation (66) is bounded from below by $(1 - \mu)(1 - \xi^2(\tau))\mathbb{E}[\text{MSE}(\sigma^2, \theta_{m,t})]$ in the large-system limit.

We next prove that the last term in (46) is an upper bound on the last term in (66). Let us consider a suboptimal receiver, which estimates $x_{m,t}$ only from the first element r_m of the MF output vector (69), given by

$$r_m = \frac{1 - (\Xi_t^{(c)})_{m,m}}{\alpha} x_{m,t} + \sum_{m'=m+1}^M \frac{(\Xi_t^{(c)})_{m,m'}}{\alpha} x_{m',t} + \eta_m, \quad (187)$$

with η_m denoting the first element of $\boldsymbol{\eta}$. In order to evaluate an upper bound on the MSE (67) for this suboptimal receiver, we replace the inter-stream interference in (187) by the AWGN with the same variance. The MSE (67) for the obtained channel provides an upper bound on the original one, and is determined by the SNR

$$\overline{\text{snr}} = \frac{P(1 - (\Xi_t^{(c)})_{m,m})^2}{P \sum_{m'=m+1}^M |(\Xi_t^{(c)})_{m,m'}|^2 + \alpha \sigma^2 (1 - (\Xi_t^{(c)})_{m,m})}, \quad (188)$$

which converges in probability to $\underline{\text{snr}} = (1 - \xi^2(\tau))P/(\alpha\sigma^2)$ in the large-system limit, due to Proposition 5 and Lemma 1. This result implies that the last term (67) in the fixed-point equation (66) is bounded from above by $(1 - \mu)(1 - \xi^2(\tau))\mathbb{E}[\text{MSE}(\sigma^2, \theta_{m,t})]$ in the large-system limit. Combining the two bounds, we find that the fixed-point equation (66) is equal to the fixed-point equation (46).

The argument described above implies that the inter-stream interference is negligible in the large-system limit. It is straightforward to confirm that the mutual information $I(x_{m,t}; \tilde{x}_{m,t} | \Xi_t^{(c)}, \boldsymbol{\theta}_{[m,M],t})$ converges to the constrained capacity of the AWGN channel (40), i.e., the integrand in (43), by repeating the same argument. Similarly, it is straightforward to find that (68) is equal to (47). Combining these results and the argument described in Appendix A-A, we find that Proposition 1 holds.

REFERENCES

- [1] G. J. Foschini and M. J. Gans, "On limits of wireless communications in a fading environment when using multiple antennas," *Wireless Pers. Commun.*, vol. 6, pp. 311–335, 1998.
- [2] E. Telatar, "Capacity of multi-antenna Gaussian channels," *Euro. Trans. Telecommun.*, vol. 10, no. 6, pp. 585–595, Nov.–Dec. 1999.
- [3] A. M. Tulino, A. Lozano, and S. Verdú, "Impact of antenna correlation on the capacity of multiantenna channels," *IEEE Trans. Inf. Theory*, vol. 51, no. 7, pp. 2491–2509, Jul. 2005.
- [4] T. L. Marzetta and B. M. Hochwald, "Capacity of a mobile multiple-antenna communication link in Rayleigh flat fading," *IEEE Trans. Inf. Theory*, vol. 45, no. 1, pp. 139–157, Jan. 1999.
- [5] A. Lapidath and S. M. Moser, "Capacity bounds via duality with applications to multiple-antenna systems on flat-fading channels," *IEEE Trans. Inf. Theory*, vol. 49, no. 10, pp. 2426–2467, Oct. 2003.
- [6] S. M. Moser, "The fading number of multiple-input multiple-output fading channels with memory," *IEEE Trans. Inf. Theory*, vol. 55, no. 6, pp. 2716–2755, Jun. 2009.
- [7] B. M. Hochwald and T. L. Marzetta, "Unitary space-time modulation for multiple-antenna communications in rayleigh flat fading," *IEEE Trans. Inf. Theory*, vol. 46, no. 2, pp. 543–564, Mar. 2000.
- [8] B. Hassibi and T. L. Marzetta, "Multiple-antennas and isotropically random unitary inputs: The received signal density in closed form," *IEEE Trans. Inf. Theory*, vol. 48, no. 6, pp. 1473–1484, Jun. 2002.
- [9] A. L. Moustakas, S. H. Simon, and T. L. Marzetta, "Capacity of differential versus nondifferential unitary space-time modulation for MIMO channels," *IEEE Trans. Inf. Theory*, vol. 52, no. 8, pp. 3622–3634, Aug. 2006.
- [10] L. Zheng and D. N. C. Tse, "Communication on the Grassmann manifold: A geometric approach to the noncoherent multiple-antenna channel," *IEEE Trans. Inf. Theory*, vol. 48, no. 2, pp. 359–383, Feb. 2002.
- [11] W. Yang, G. Durisi, and E. Riegler, "On the capacity of large-MIMO block-fading channels," *IEEE J. Sel. Areas Commun.*, vol. 31, no. 2, pp. 117–132, Feb. 2013.
- [12] S. Verdú, "Spectral efficiency in the wideband regime," *IEEE Trans. Inf. Theory*, vol. 48, no. 6, pp. 1319–1343, Jun. 2002.
- [13] L. Zheng, D. N. C. Tse, and M. Médard, "Channel coherence in the low-SNR regime," *IEEE Trans. Inf. Theory*, vol. 53, no. 3, pp. 976–997, Mar. 2007.
- [14] S. Ray, M. Médard, and L. Zheng, "On noncoherent MIMO channels in the wideband regime: Capacity and reliability," *IEEE Trans. Inf. Theory*, vol. 53, no. 6, pp. 1983–2009, Jun. 2007.
- [15] B. Hassibi and B. M. Hochwald, "How much training is needed in multiple-antenna wireless link?" *IEEE Trans. Inf. Theory*, vol. 49, no. 4, pp. 951–963, Apr. 2003.
- [16] M. Médard, "The effect upon channel capacity in wireless communications of perfect and imperfect knowledge of the channel," *IEEE Trans. Inf. Theory*, vol. 46, no. 3, pp. 933–946, May 2000.
- [17] K. Takeuchi, M. Vehkaperä, T. Tanaka, and R. R. Müller, "Large-system analysis of joint channel and data estimation for MIMO DS-CDMA systems," *IEEE Trans. Inf. Theory*, vol. 58, no. 3, pp. 1385–1412, Mar. 2012.

- [18] T. Li and O. M. Collins, "A successive decoding strategy for channels with memory," *IEEE Trans. Inf. Theory*, vol. 53, no. 2, pp. 628–646, Feb. 2007.
- [19] K. Padmanabhan, S. Venkatraman, and O. M. Collins, "Tight upper and lower bounds on the constrained capacity of non-coherent multi-antenna channels," in *Proc. 2008 IEEE Int. Symp. Inf. Theory*, Toronto, Canada, Jul. 2008, pp. 2588–2592.
- [20] K. Takeuchi, R. R. Müller, M. Vehkaperä, and T. Tanaka, "Practical signaling with vanishing pilot-energy for large noncoherent block-fading MIMO channels," in *Proc. 2009 IEEE Int. Symp. Inf. Theory*, Seoul, Korea, Jun. 2009, pp. 759–763.
- [21] K. Takeuchi, R. R. Müller, and M. Vehkaperä, "Bias-based training for iterative channel estimation and data decoding in fast fading channels," *IEICE Trans. Commun.*, vol. E94-B, no. 7, pp. 2161–2165, Jul. 2011.
- [22] —, "A construction of turbo-like codes for iterative channel estimation based on probabilistic bias," in *Proc. IEEE Global Commun. Conf. (GLOBECOM 2011)*, Houston, Texas, USA, Dec. 2011.
- [23] —, "Iterative LMMSE channel estimation and decoding based on probabilistic bias," submitted to *IEEE Trans. Commun.*, 2012.
- [24] D. N. C. Tse and S. V. Hanly, "Linear multiuser receivers: effective interference, effective bandwidth and user capacity," *IEEE Trans. Inf. Theory*, vol. 45, no. 2, pp. 641–657, Mar. 1999.
- [25] S. Verdú and S. Shamai (Shitz), "Spectral efficiency of CDMA with random spreading," *IEEE Trans. Inf. Theory*, vol. 45, no. 2, pp. 622–640, Mar. 1999.
- [26] J. Evans and D. N. C. Tse, "Large system performance of linear multiuser receivers in multipath fading channels," *IEEE Trans. Inf. Theory*, vol. 46, no. 6, pp. 2059–2078, Sep. 2000.
- [27] S. Shamai (Shitz) and S. Verdú, "The impact of frequency-flat fading on the spectral efficiency of CDMA," *IEEE Trans. Inf. Theory*, vol. 47, no. 4, pp. 1302–1327, May 2001.
- [28] T. Tanaka, "A statistical-mechanics approach to large-system analysis of CDMA multiuser detectors," *IEEE Trans. Inf. Theory*, vol. 48, no. 11, pp. 2888–2910, Nov. 2002.
- [29] A. L. Moustakas, S. H. Simon, and A. M. Sengupta, "MIMO capacity through correlated channels in the presence of correlated interferers and noise: A (not so) large N analysis," *IEEE Trans. Inf. Theory*, vol. 49, no. 10, pp. 2545–2561, Oct. 2003.
- [30] R. R. Müller and W. H. Gerstacker, "On the capacity loss due to separation of detection and decoding," *IEEE Trans. Inf. Theory*, vol. 50, no. 8, pp. 1769–1778, Aug. 2004.
- [31] D. Guo and S. Verdú, "Randomly spread CDMA: Asymptotics via statistical physics," *IEEE Trans. Inf. Theory*, vol. 51, no. 6, pp. 1983–2010, Jun. 2005.
- [32] K. Takeda, S. Uda, and Y. Kabashima, "Analysis of CDMA systems that are characterized by eigenvalue spectrum," *Europhys. Lett.*, vol. 76, no. 6, pp. 1193–1199, 2006.
- [33] C. K. Wen and K. K. Wong, "Asymptotic analysis of spatially correlated MIMO multiple-access channels with arbitrary signaling inputs for joint and separate decoding," *IEEE Trans. Inf. Theory*, vol. 53, no. 1, pp. 252–268, Jan. 2007.
- [34] K. Takeuchi, T. Tanaka, and T. Yano, "Asymptotic analysis of general multiuser detectors in MIMO DS-SS channels," *IEEE J. Sel. Areas Commun.*, vol. 26, no. 3, pp. 486–496, Apr. 2008.
- [35] D. Sherrington and S. Kirkpatrick, "Solvable model of a spin-glass," *Phys. Rev. Lett.*, vol. 35, no. 26, pp. 1792–1796, Dec. 1975.
- [36] H. Nishimori, *Statistical Physics of Spin Glasses and Information Processing*. New York: Oxford University Press, 2001.
- [37] Mézard, G. Parisi, and M. A. Virasoro, *Spin Glass Theory and Beyond*. Singapore: World Scientific, 1987.
- [38] K. H. Fischer and J. A. Hertz, *Spin Glasses*. Cambridge, UK: Cambridge University Press, 1991.
- [39] F. Guerra, "Broken replica symmetry bounds in the mean field spin glass model," *Commun. Math. Phys.*, vol. 233, pp. 1–12, 2003.
- [40] M. Talagrand, "The Parisi formula," *Annals of Mathematics*, vol. 163, pp. 221–263, 2006.
- [41] F. D. Neeser and J. L. Massey, "Proper complex random processes with applications to information theory," *IEEE Trans. Inf. Theory*, vol. 39, no. 4, pp. 1293–1302, Jul. 1993.
- [42] G. D. Forney, Jr., "Trellis shaping," *IEEE Trans. Inf. Theory*, vol. 38, no. 2, pp. 281–300, Mar. 1992.
- [43] K. Takeuchi, R. R. Müller, M. Vehkaperä, and T. Tanaka, "An achievable rate of large block-fading MIMO systems with no CSI via successive decoding," in *Proc. 2010 Int. Symp. Inf. Theory and its Appl. & Int. Symp. Spread Spectrum Tech. and Appl.*, Taichung, Taiwan, Oct. 2010, pp. 519–524.
- [44] T. M. Cover and J. A. Thomas, *Elements of Information Theory*, 2nd ed. New Jersey: Wiley, 2006.
- [45] M. Ledoux, *The Concentration of Measure Phenomenon*. Providence, RI: American Mathematical Society, 2001.

- [46] F. Guerra and F. L. Toninelli, "The thermodynamic limit in mean field spin glass models," *Commun. Math. Phys.*, vol. 230, pp. 71–79, 2002.
- [47] —, "The infinite volume limit in generalized mean field disordered models," *Markov. Proc. Rel. Fields*, vol. 9, pp. 195–207, 2003.
- [48] L. Cottatellucci and R. R. Müller, "A systematic approach to multistage detectors in multipath fading channels," *IEEE Trans. Inf. Theory*, vol. 51, no. 9, pp. 3146–3158, Sep. 2005.
- [49] H. Nishimori, "Comment on "statistical mechanics of CDMA multiuser demodulation" by Tanaka," *Europhys. Lett.*, vol. 57, no. 2, pp. 302–303, Jan. 2002.
- [50] S. Verdú, *Multiuser Detection*. New York: Cambridge University Press, 1998.
- [51] S. B. Korada and A. Montanari, "Applications of the Lindeberg principle in communications and statistical learning," *IEEE Trans. Inf. Theory*, vol. 57, no. 4, pp. 2440–2450, Apr. 2011.
- [52] L. A. Pastur and M. V. Shcherbina, "Absence of self-averaging of the order parameter in the Sherrington-Kirkpatrick model," *J. Stat. Phys.*, vol. 62, no. 1/2, pp. 1–19, 1991.
- [53] D. N. C. Tse and P. Viswanath, *Fundamentals of Wireless Communication*. Cambridge, UK: Cambridge University Press, 2005.
- [54] M. Vehkaperä, K. Takeuchi, R. R. Müller, and T. Tanaka, "How much training is needed for iterative multiuser detection and decoding?" in *Proc. IEEE Global Communications Conference (GLOBECOM 2009)*, Honolulu, USA, Nov. 2009.
- [55] K. Kitagawa and T. Tanaka, "Optimization of sequences in CDMA systems: A statistical-mechanics approach," *Computer Networks*, vol. 54, pp. 917–924, 2010.
- [56] M. C. Gursoy, "On the capacity and energy efficiency of training-based transmissions over fading channels," *IEEE Trans. Inf. Theory*, vol. 55, no. 10, pp. 4543–4567, Oct. 2009.
- [57] K. Nakamura and T. Tanaka, "Microscopic analysis for decoupling principle of linear vector channel," in *Proc. 2008 IEEE Int. Symp. Inf. Theory*, Toronto, Canada, Jul. 2008, pp. 519–523.